Distribution Agreement

In presenting this thesis or dissertation as a partial fulfillment of the requirements for an advanced degree from Emory University, I hereby grant to Emory University and its agents the non-exclusive license to archive, make accessible, and display my thesis or dissertation in whole or in part in all forms of media, now or hereafter known, including display on the world wide web. I understand that I may select some access restrictions as part of the online submission of this thesis or dissertation. I retain all ownership rights to the copyright of the thesis or dissertation. I also retain the right to use in future works (such as articles or books) all or part of this thesis or dissertation.

Signature:

_____ _____

Angele Bruce Date

Synthetic Platforms for Accessing Tag-Free Macrocyclic Peptide Libraries

By:

Angèle Bruce

Doctor of Philosophy

Chemistry

Monika Raj, PhD

Advisor

Christine Dunham, PhD

Committee Member

Katherine M. Davis, PhD

Committee Member

Accepted:

Kimberly Jacob Arriola, Ph.D., MPH

Dean of the James T. Laney School of Graduate Studies

Date

Synthetic Platforms for Accessing Tag-Free Macrocyclic Peptide Libraries

By

Angèle Bruce

B.Sc., University of Portland, 2017

Advisor: Monika Raj, PhD

An abstract of

A dissertation submitted to the Faculty of the James T. Laney of Graduate Studies of Emory University in partial fulfillment of the requirements for the degree of Doctor of Philosophy in Chemistry

2025

Abstract

Synthetic Platforms for Accessing Tag-Free Macrocyclic Peptide Libraries

Macrocyclic peptides are an increasingly important modality within the pharmaceutical industry. Methods for their discovery are currently limited to platforms that require large encoding tags and few are versatile enough to include a large variety of non-canonical amino acids. In this work, we successfully developed synthetic platforms to access pooled macrocyclic libraries that lack these limitations. First, we utilized CyClick cyclization chemistry in a multi-step pooled library synthesis. We optimized two scavenger-resin purifications steps for the linear and macrocyclization mixtures for selective enrichment of our pooled library. Additionally, we demonstrated the ability to linearize, derivatize, and sequence library members through direct mass spectrometric analysis of each peptide species, allowing us to avoid the use of an encoding tag. As a follow-up, we also explored the use of hydrazone-based cyclization chemistry as a method that sees quantitative peptide conversion and bypasses the purification steps required for CyClick library generation. This strategy was also amenable to a facile linearization and derivatization protocol. Both strategies were employed in affinity selections against protein targets and pooled *in vitro* permeability assays to demonstrate their potential applications. We discovered a CyClick peptide that perturbs the HIV capsid protein assembly and are in the process of characterizing hydrazone macrocycle binders for the gamma aminobutyric acid type A receptor-associated protein (GABARAP).

By: Angèle Bruce

Synthetic Platforms for Accessing Tag-Free Macrocyclic Peptide Libraries

By

Angèle Bruce

B.Sc., University of Portland, 2017

Advisor: Monika Raj, PhD

An abstract of

A dissertation submitted to the Faculty of the James T. Laney of Graduate Studies of Emory University in partial fulfillment of the requirements for the degree of Doctor of Philosophy in Chemistry

2025

Table of Contents

Figure List

1.1 Introduction to Macrocyclic Peptides as Therapeutics

Small molecules have traditionally dominated the field of drug discovery and have been the primary focus of development efforts by the pharmaceutical industry for the past century.[1] Drugs of this class primarily exploit target proteins that display a defined binding pocket, a feature which it is estimated only 15% of the proteome possess.[2] In recent decades, more complicated and larger biologic drugs have seen a substantial uptick in the resources dedicated to their research and development, with biologics comprising 50% of FDA drug approvals in 2022.[3] Monoclonal antibodies in particular have become a huge component of the pharmaceutical industry, able to bind with high selectivity to targets lacking a defined binding pocket.[4] Among pharmaceutical modalities, peptides inhabit a unique chemical space that bridges the gap between small organic entities and larger, biologically derived protein/antibody drugs. Peptide drug candidates tend to exist in the 0.5-1.5 kDa size range, allowing for extended interactions with shallow protein surfaces. This feature, similar to antibody-type interactions, confers access to a broader range of potential protein targets and greater target selectivity than smaller molecules.[5] Additionally, unlike cell-derived antibodies, peptides are synthetically accessible to organic chemists and compatible with traditional medicinal chemistry optimization strategies.[6]

Macrocyclization is a widely used strategy that has been employed to improve the pharmacological properties of peptide therapeutics. These intramolecular ring-forming reactions restrict the conformational flexibility of peptides and have been shown to lead to a preorganization of backbone structure and geometry that is preferential for target binding.[5,7] Additionally, macrocyclization often reduces the susceptibility of peptides to exopeptidases, significantly improving their half-life in biological systems.[8] Several macrocyclic peptide drugs are in use in the clinic today. The advantages of peptide macrocyclization have prompted investigation into a wide variety of cyclization chemistries that covalently link head-to-tail, head/tail-to-side chain, or side chain-to-side chain (Figure 1).

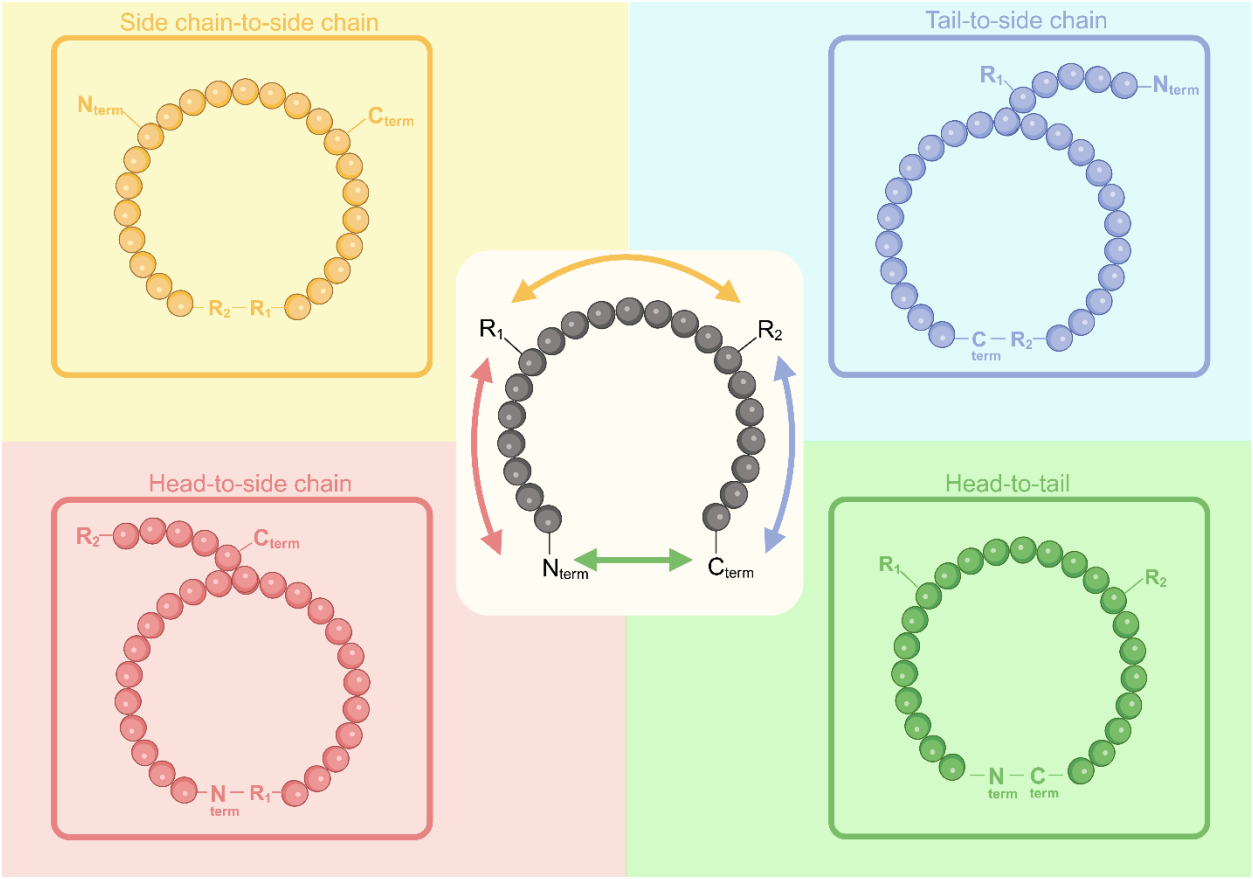

Figure 1: Types of peptide macrocyclization linkages

1.2 Peptide Macrocyclization Strategies

A significant challenge in the development of any macrocyclization chemistry is selectivity. Reactive amino acids (lysine, cysteine, serine, threonine, aspartate, glutamate, histidine, and tyrosine) can often interfere with a desired cyclization pathway if left unprotected. Chemoselective macrocyclizations are therefore highly desirable to avoid additional deprotection and purification steps in macrocycle synthesis. Methods for head-to-tail or head/tail-to-side chain macrocyclizations include those that result in a native lactam backbone and those that generate unnatural linkages.

1.2.1 Chemoselective Amide-Forming Macrocyclizations

Several ligation strategies have been applied to peptides for generating lactam macrocycles. Many achieve high chemoselectivity when employed on fully unprotected substrates. Native chemical ligation (NCL) is a

strategy initially developed for the manual synthesis of proteins, linking larger peptide fragments through a newly generated amide bond. An N-terminal cysteine (Cys) undergoes a thiol-thioester exchange with a C-terminal thioester. Subsequently, a spontaneous S-to-N intramolecular acyl transfer results in a new amide bond (Figure 2).[9] While highly selective, this method for cyclization requires the presence of a cysteine or the implementation of a desulfurization protocol. Ketoacid-hydroxylamine (KAHA) is another ligation used for cyclization that uses the selective reaction between a C-terminal ketoacid and an N-terminal hydroxylamine under mild conditions. In a similar fashion to NCL, the initial reaction is followed by an O-to-N acyl shift that results in a new amide bond (Figure 2).[10] Unfortunately, this reaction suffers from a slow cyclization rate, a high degree of residue epimerization, and oxidation of the terminal hydroxylamine. Staudinger ligation can also be applied to unprotected peptides through installation of an N-terminal azide that reacts with a C-terminal phosphino-thioester (Figure 2).[11] While highly chemoselective, the reaction only generates high yields when a Gly residue is at the ligation site, limiting sequence diversity.[12] Additionally, the phosphinothiols used to modify the C-terminus have poor aqueous solubility.[13]

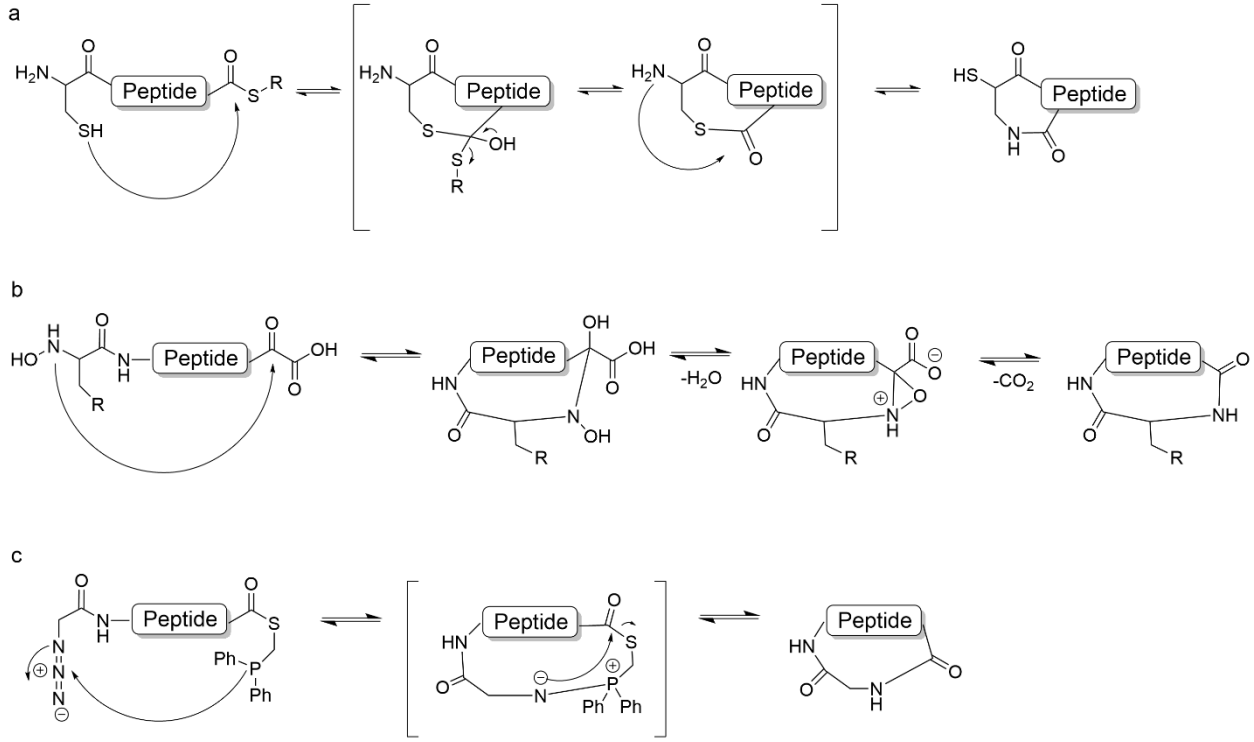

Figure 2: Schemes for chemoselective amide-forming cyclization reactions (a) Native chemical ligation (b) Ketoacid-hydroxylamine ligation (c) Staudinger ligation

1.2.2 Chemoselective Non-Amidic Macrocyclizations

Apart from these amide-forming ligation reactions, there are a number of strategies that utilize the native N-terminal amine, lysine, and cysteine residues to achieve chemoselectivity. Imine mediated macrocyclization between the N-terminus and an installed aldehyde has been demonstrated to be a reliable macrocyclization pathway. The cyclic imine can readily be trapped by intermolecular or intramolecular reactions with nucleophiles or reduced to an amine with sodium cyanoborohydride (Figure 3).[14] Lysine (Lys) residues have also been employed for imine-mediated, chemoselective macrocyclizations. With the addition of formaldehyde, it has been demonstrated that lysine can undergo selective crosslinking with nearby tyrosine or arginine residues (Figure 3).[15]

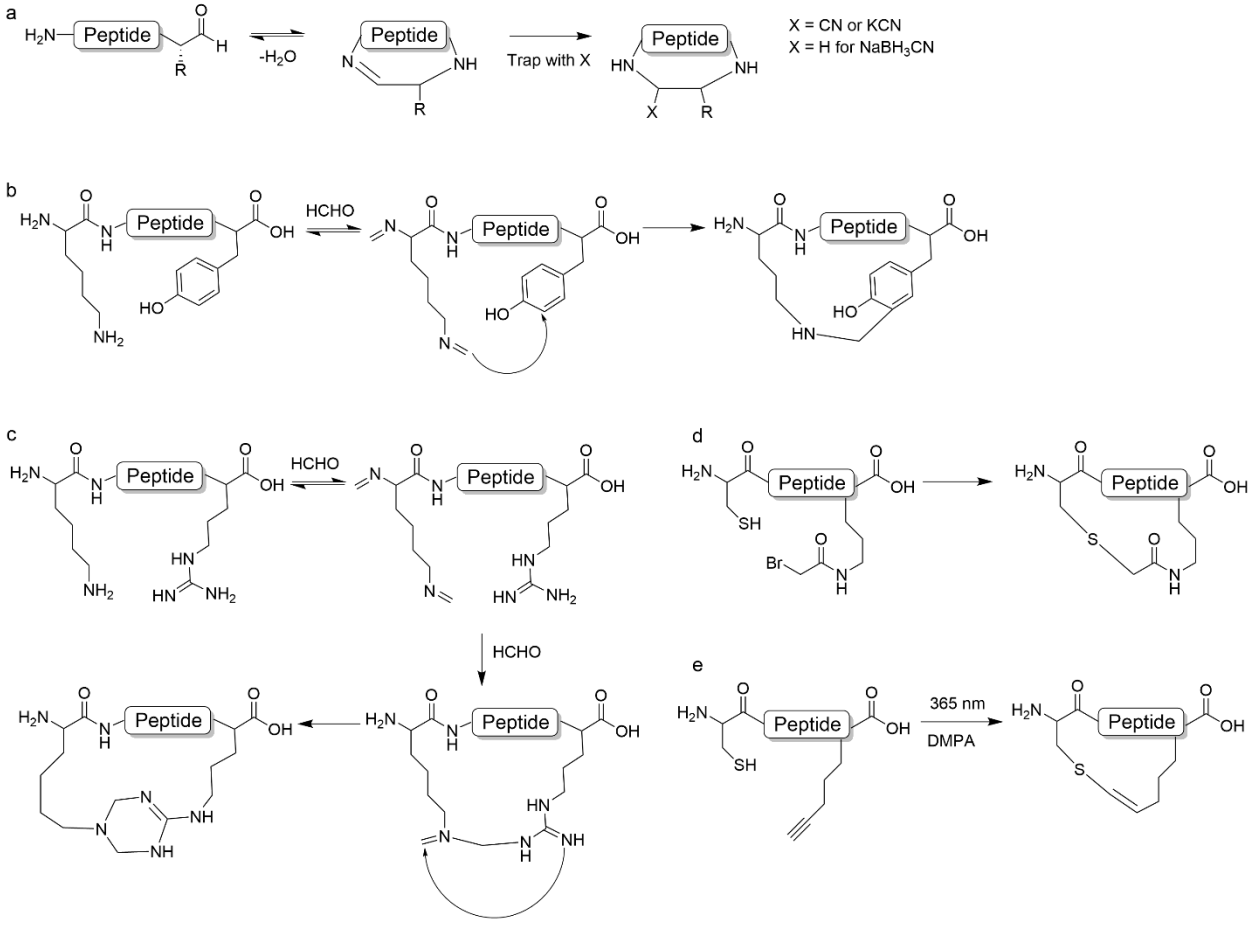

Figure 3: Schemes for chemoselective cyclizations reactions that form unnatural peptide linkages (a) Imine-mediated cyclization and capture (b) Lysine-Tyrosine stapling reaction (c) Lysine-Arginine stapling reaciont (d) Thioether formation through cysteine mediated nucleophilic substitution reaction (e) Thioether formation through thiol-yne reaction

Disulfide formation between two Cys side chains has been a staple to execute and chemoselective cyclization strategy between canonical amino acid residues.[16] The nucleophilicity of the cysteine residue has also been exploited for macrocyclizations with alkenes/alkynes, chloro- or bromoacetate groups, and aryl halides (Figure 3).[17-19] These cyclization strategies have afforded access to new conformational scaffolds in peptide discovery but have not ameliorated other limitations of peptide cyclization.

In addition to the challenge of chemoselectivity, there is the difficulty of achieving intramolecular over intermolecular bond formation during a cyclization reaction. Due to the overlap in reactivity between moieties on the same peptide and those on another molecule of the same sequence, oligomeric peptide species are often significant byproducts of cyclization (Figure 4). This can be avoided through the implementation of a pseudo-dilute environment. This is traditionally achieved through cyclization while the peptide is attached to a solid-phase resin and often requires various orthogonal deprotection strategies. In other instances, solution phase cyclization reactions are performed with large solvent volumes.[20-23] All of the cyclization reactions described above required pseudo-dilute conditions to achieve high yields of the desired monocycle. Dilution to this extent is inefficient and a less sustainable synthetic practice.[24]

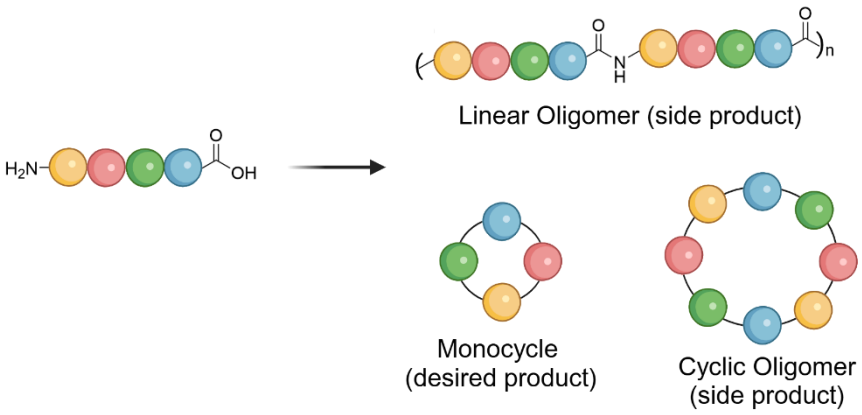

Figure 4: Limitations of peptide macrocyclization chemistries without intramolecular selectivity

1.3 High-Throughput Screening Platforms for Peptide Drug Discovery

Significant research effort has been dedicated to the discovery and investigation of cyclic peptide ligands, with citations and publications related to the topic increasing annually, and substantially, since the early 1990s.[25] This work has yielded a total 18 FDA approved macrocyclic peptide drugs between 2001 and 2021, many of which are either natural products or their optimized analogues/derivatives.[26] The reliance on natural product scaffolds artificially limits the target scope and application of this drug class, yet *de novo* discovered or designed macrocyclic peptide drugs represent make up far fewer of clinical trial candidates and only 1 has been approved by the FDA.[27] This is in part due to the greater difficulty in both the generation of macrocyclic peptide libraries and the elucidation of hit compound structure when compared to small molecule libraries.

High-throughput screening (HTS) of libraries is the most commonly employed strategy for discovering drug candidates.[28] Screenings can take place in a "one-well, one-compound" context, where library members are assessed individually for binding affinity to the target, or in a pooled context, where a library mixture is incubated with the target and binding molecules are separated/identified from non-binding molecules. For preclinical peptide discovery efforts, pooled screening strategies have been favored.[29] The vast chemical space of peptide structures and significant influence of single amino acids on target binding requires the exploration of millions to billions of compounds, an intractable number for one-compound one-well screenings.

Large-scale, solution-phase library synthesis is hindered by the fact that most macrocyclization chemistries generate numerous oligomeric byproducts when employed above pseudo-dilute concentrations,[23] making the synthesis and purification of large libraries cost- and labor-intensive. Additionally, traditional tandem mass spectrometry techniques for peptide sequencing are not easily applied to macrocyclic peptide species. Because these compounds lack a terminal end, the fragments generated from a macrocycle are not sufficient information for reconstructing connectivity. Over the years various technologies have been developed to bypass these obstacles to accessing macrocyclic peptide libraries, each featuring a unique set of advantages and disadvantages.

1.3.1 Biologically Synthesized Technologies

Phage display is technology originally developed in the 1980s that genetically encodes peptide sequences that are "displayed" on the surface coat of a bacteriophage (Figure 5). This technology leverages the internal viral machinery to synthesize peptide sequences and historically relied upon disulfide formation between two cysteine residues for cyclization.[30] Cyclization techniques in phage display have expanded to include a variety of cysteine selection linkers or the incorporation of a single cysteine reactive non-canonical residue in the peptide sequence.[31,32] The bacteriophage acts as a solid support that provides pseudo-dilution for intramolecularly selective cyclization. After pooled screening of the phage library, selected phage can be eluted and genetic material amplified for facile DNA sequencing. While this technology is incredibly efficient, it is limited to the incorporation of a single non-canonical residue, which reduces the ability to incorporate residues with differing pharmacophores.[33] Additionally, the required attachment of library members to the large bacteriophage coat is suspected to play a role in the prevalence of false positive hit identification.[34]

mRNA display is another display technology that produces libraries of peptides covalently liked to mRNA strands that encode them (Figure 5). Purified ribosomes, tRNAs, and translation factors are utilized *in vitro* to generate a peptide library from an initial mRNA library.[35] This technology has been further expanded by the Suga lab in two important ways. The first was using genetic code reprogramming was used to replace an N-terminal formyl-Met with an N-chloroacetylated amino acid, a group which can undergo spontaneous cyclization with cysteine to form a thioether tether. The second involved the evolution of flexible tRNA synthetases that can be charged with a range of non-canonical amino acids.[36-38] Similar to phage display, post-screening PCR amplification allows for straightforward sequence deconvolution with well-established DNA sequencing technologies. mRNA display has become one of the most ubiquitous tools for peptide drug discovery in the pharmaceutical industry but still suffers some specific disadvantages. The mRNA tag is significantly larger than the peptide, densely charged, and capable of influencing the binding interaction between peptide and target. The tag is also highly susceptible to RNAses and can be damaged during sample handling, skewing sequencing results.[39]

Split-intein circular ligation of peptides and proteins (SICLOPPS) is a unique strategy that employs plasmid encoded peptide sequences flanked by fragments of a self-excising intein protein. The plasmid library is transformed into E. Coli and peptide sequences are generated intracellularly. The intein fragments expressed on both termini of the peptide dimerize and splice the intact intein out of the sequence while joining both ends with an amide bond (Figure 5).[40] To date this is the only pooled library generation strategy the allows for screening of the peptide without an attached tag and is compatible with intracellular screening. Despite these advantages it is the most limited in regards to library diversity, allowing for the incorporation of only 1 to 2 non-canonical residues per library.[40]

1.3.2 Organic Synthesis Strategies

A fully synthetic strategy, one-bead-two-compound (OBTC), displays cyclized peptides on the outer layer of solid-phase resin with linear peptide decoding tags featured on the interior (Figure 5). After selection, beads bound to the target can be eluted and the internal linear decoding sequence can be selectively cleaved for MS/MS sequencing.[41,42] While this method benefits from the full range of solid-phase peptide synthetic techniques, imperfect cyclization efficiency can generate libraries with inseparable mixtures of cyclized vs. linear peptide and the presence of multiple copies of library members can enable multidentate interactions in affinity selections that lead to false positives.[42,43]

Lastly, DNA-encoded libraries are a promising strategy that powerfully combines the advantages of fully synthetic chemistry with the ease of nucleic acid-based sequence deconvolution. Amino acid building blocks are added sequentially and encoded by ligation of a short DNA sequence with each coupling step (Figure 5).[44] This allows for a high degree of chemical diversity while preserving quick and efficient decoding through DNA sequencing. While promising, this strategy still relies on large decoding tags linked to the peptide. Additionally, building blocks are somewhat limited in comparison to standard solid-phase peptide synthesis due to the constraints of aqueous reactions conditions and preservation of the growing DNA tag.[44]

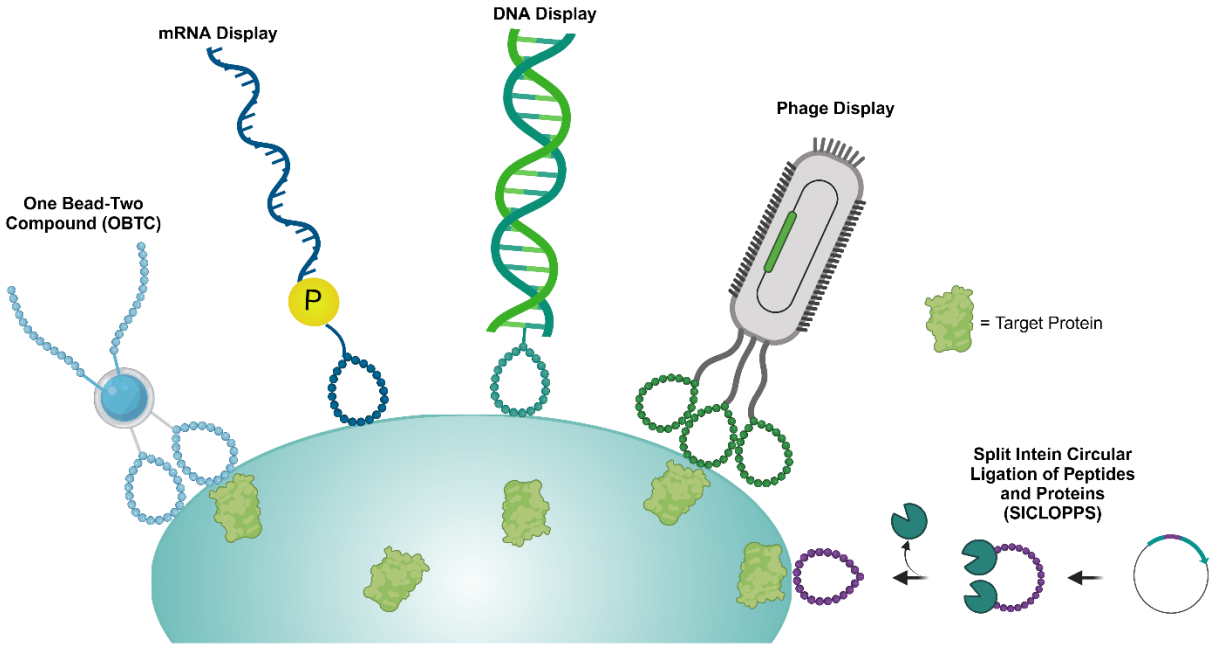

Figure 5: Current macrocyclic peptide library generation technologies

1.4 Novel Cyclization Chemistries for Tag-Free Peptide Library Generation

Across the variety of published macrocyclic library synthesis techniques, there is none that simultaneously allows for unlimited incorporation of non-canonical residues, screens library members without an appended encoding tag, and allows for unambiguous sequencing in pooled selections. The development of such a method requires a peptide cyclization strategy that can reliably generate the intramolecular cyclization product and a means to sequence the native peptide structure. In our work, we pursued this with two novel aldehyde-based cyclization strategies.

In 2019, our group published on a uniquely chemoselective and exclusively intramolecular cyclization reaction coined "CyClick" chemistry. The reaction proceeds through an intramolecular imine formed between the N-terminal amine and a C-terminal or side chain installed aldehyde. This condensation brings the amide nitrogen that is adjacent to the imine close to the electrophilic C-terminal carbon, allowing for a nucleophilic attack and the formation of fused 4-imidazolidinone ring.[45] While the initial imine formation

can occur in an intermolecular fashion, the secondary ring closure was not observed even at high cyclization concentrations.

In reviewing the literature, we identified a number of publications where intermolecular imidazolidinone formation between aldehydes and polyamides had been demonstrated.[46-48] This led us to investigate the intramolecular selectivity of our CyClick cyclization reaction in collaboration with the Houk group at UCLA. The group performed DFT calculations that suggest the ring contraction from the cyclic imine proceeds through a zwitterionic intermediate. In the intramolecular pathway, optimized bond geometries revealed that transannular intramolecular hydrogen bonding was responsible for significant stabilization of the transition states between the imine, zwitterion, and the 4-imidazolidinone containing "CyClick" product. Such stabilization was not observed in the competing intermolecular reaction, as only one of the transition states featured a much weaker intramolecular hydrogen bond. The higher kinetic energy barrier of intermolecular product formation supports the observation that our CyClick chemistry does not generate any intermolecular oligomers.[49]

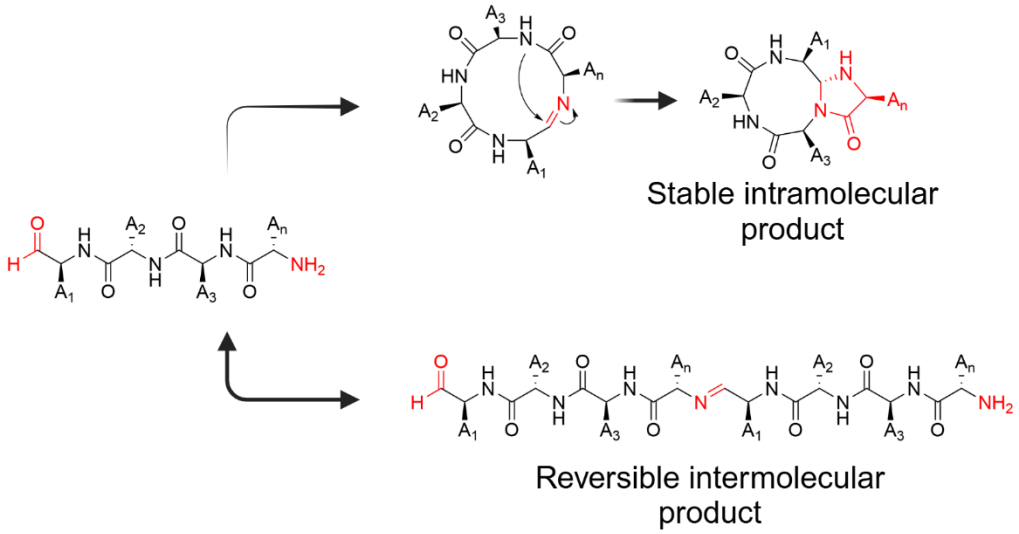

Figure 6: CyClick cyclization scheme demonstrating intramolecular vs. intermolecular product formation

Expanding on our work with aldehyde-based peptide macrocyclizations, we explored the use of methylhydrazines as a nucleophilic moiety for the formation of head-to-tail linkages. We hypothesized that the thermodynamic favorability of hydrazone formation would allow for facile cyclization of peptides similar to the use of imine-driven macrocyclizations.[14] A similar strategy had been used previously on recombinant synthetic peptide sequences that were installed with hydrazide and aldehyde groups for head-to-tail linkages.[50] Unlike our CyClick chemistry, nothing about the mechanism confers selectivity for intramolecular macrocyclization; however, we observed a significant preference for the monocycle and near quantitative conversion from linear to macrocycle products. We were also able to subject the reaction mixture to conditions that converted the cyclodimers back to the monocyclic product, yielding yet another macrocyclization strategy with control over the formation of oligomers.

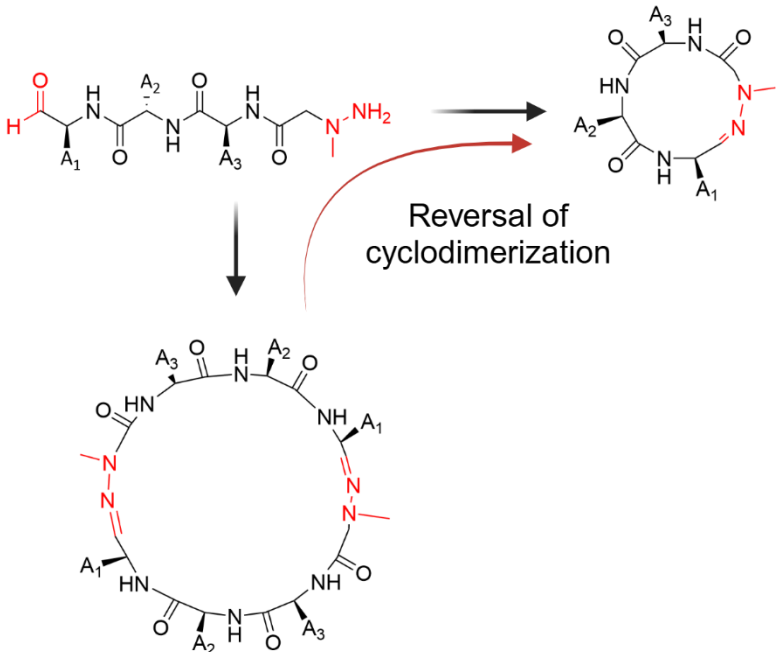

Figure 7: Scheme of hydrazone peptide cyclization and oligomerization

In addition to the ability to avoid products of intermolecular reaction with these two macrocyclization chemistries, we have developed simple strategies for peptide linearization. Very few peptide macrocyclization chemistries have facile, sequence methods for their reversal.[51,52] This feature provides access to direct mass spectrometric peptide sequencing as an alternative to the use of encoding tags and

delivers access to peptide libraries that can be screened as their native structure. The development of this library technology presents a currently unmatched opportunity for probing peptide macrocycle binding and permeability in a high-throughput manner.

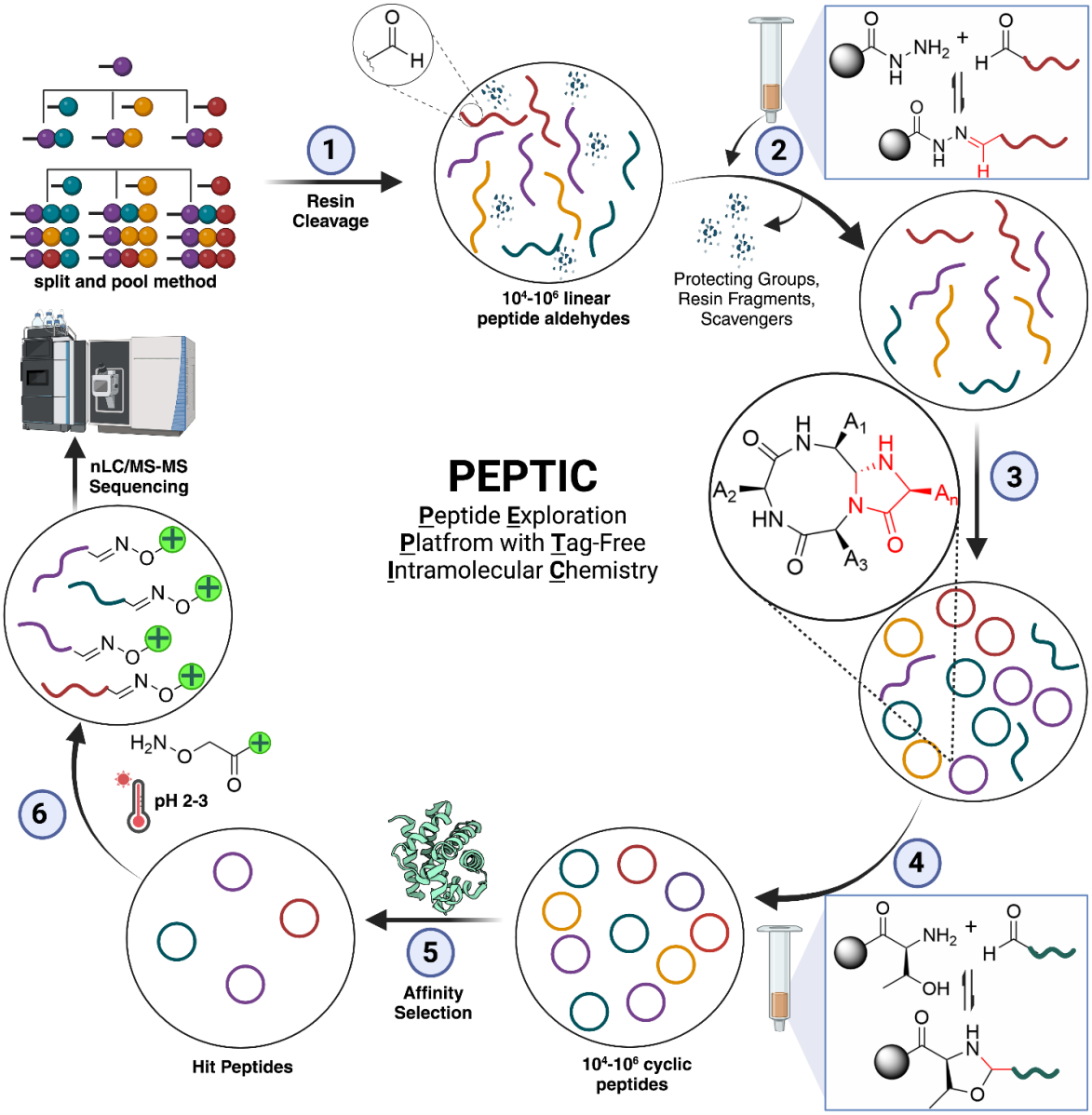

Chapter 2: Development of the Peptide Exploration Platform with Tag-Free Intramolecular Chemistry (PEPTIC) with CyClick Cyclization

Bruce, A.; Adebomi, V.; Czabala, P.; Palmer, J.; McFadden, W. M.; Lorson, Z. C.; Slack, R. L.; Bhardwaj, G.; Sarafianos, S. G.; Raj, M. A Tag-Free Platform for Synthesis and Screening of Cyclic Peptide Libraries. *Angew Chem Int Ed* **2024**, *63* (21), e202320045.

2.1 Filling the Gap in Macrocyclic Peptide Library Technologies with CyClick Chemistry

In reviewing the existing strategies for macrocyclic peptide library generation and screening, we believed our CyClick cyclization chemistry could be used to provide a means to fill the existing gaps in their capabilities. Current strategies all rely upon either the biological synthesis of peptide library members and/or the use of large, appended structures to encode peptide sequences. [31,36,40,41,44] The former reduces the ability to incorporate non-canonical amino acids that improve cell permeability or have desirable bioactivity, requiring further optimization after hits are identified. The latter can influence the way a peptide binds in affinity selections, leading to false positive hits, and limits the scope of library applications.

The main obstacles to moving to a fully synthetic and tag-free method is achieving chemo- and intramolecular selective cyclization chemistry and determining a high confidence strategy for sequencing the native peptide. Based on our knowledge of the intramolecular selectivity of CyClick cyclization, we knew we could generate individual macrocycles in one-pot without oligomeric byproducts. Additionally, we suspected the aminal of the CyClick peptide could be susceptible to hydrolysis and allow for peptide linearization when subjected to the right conditions. These two aspects made CyClick cyclization an appealing strategy for developing a tag-free, solution-phase macrocyclic library generation platform.

2.2 Development of the Peptide Exploration of Platform with Tag-Free Intramolecular Chemistry (PEPTIC)

2.2.1 Linear Library Synthesis and Purification

To synthesize a diverse library of solution phase macrocyclic peptides, we initiated our investigation by accessing a library of C-terminal linear peptide aldehydes amenable to CyClick cyclization. Our strategy involved, first, the resin loading of an unprotected threonine residue followed by coupling with a fluorenylmethyloxycarbonyl (FMOC) protected amino aldehyde residue. This generated a stable oxazolidine linker that allowed for the iterative addition of amino acids on solid support through a split and pool method. For each variable position of the peptide sequence, the resin was "split" into differing vessels for loading with a different amino acid building block. After coupling, the resin was once again "pooled" before deprotection.[53] This method allowed for easy diversification of peptide sequences with each synthesis step. Subsequent

detachment from the solid support under acidic conditions yielded a library of C-terminal linear peptide aldehydes.

To purify the library of linear peptide aldehydes, we leveraged the orthogonal aldehyde handle for reversible, selective enrichment with an aldehyde scavenging resin. We hypothesized that by reversibly attaching peptide aldehydes to a new solid support, we could wash away other impurities generated during synthesis and resin cleavage and subsequently release the peptides back into solution. We screened various aldehyde-scavenger resins previously described in literature, this included hydrazide-[54,55], sulfonyl hydrazide-[56], and threonyl-(TG)/cysteinyl- (CG)[57] functionalized resins. These resins form stable hydrazone, sulfonyl hydrazone, and oxazolidine/thiazolidine linkages, respectively, upon condensation with an aldehyde (Figure 8, Supplementary Table 1).

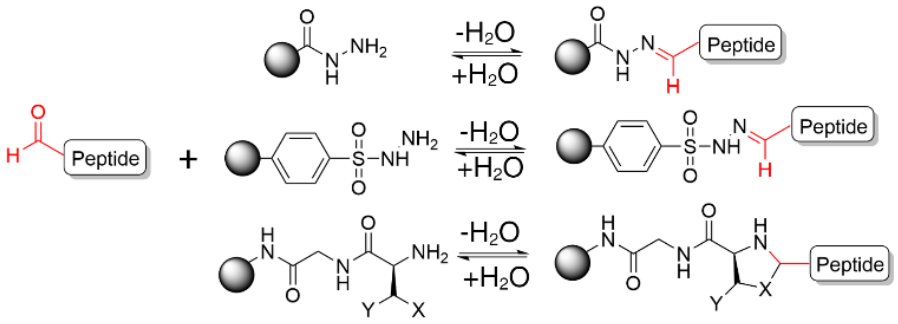

Figure 8: Screened strategies for resin-based aldehyde scavenging

When applied to our model peptide H_2N-AVGPFEYA-CHO the hydrazide resin yielded the most promising outcomes. We found that the scavenging of our model peptide was optimal when incubating the crude peptide with our resin in acetonitrile with 2% acetic acid at 60 ℃. Hydrolysis of the hydrazone to release the linear peptide aldehyde into solution was achieved simply by changing the reaction solvent to 50:50 ACN:H_2O with 2% acetic acid at 60℃ (Figure 9a). With these established conditions, we successfully demonstrated the efficient scavenging, washing, and hydrolysis of the individual model peptide aldehyde **1a,** H_2N-AVGPFEYA-CHO directly from a crude mixture, resulting in a solution of pure linear peptide aldehyde **1a** (Figure 9b)**.** Consistent recoveries between 75-90% were achieved with known quantities of pure starting peptide.

In an effort to demonstrate our strategy on a more realistic sample mixture, we generated a small-scale split-and-pool library. The library was designed with a 10 amino acid sequence and 4 variable positions, with each variable position containing one of two amino acid building blocks. After synthesis and cleavage, the crude mixture of 16 peptide aldehydes was subjected to our hydrazone-based purification protocol, showcasing efficient recovery and enrichment of all 16 peptide aldehydes by LC-MS (Figure 9c).

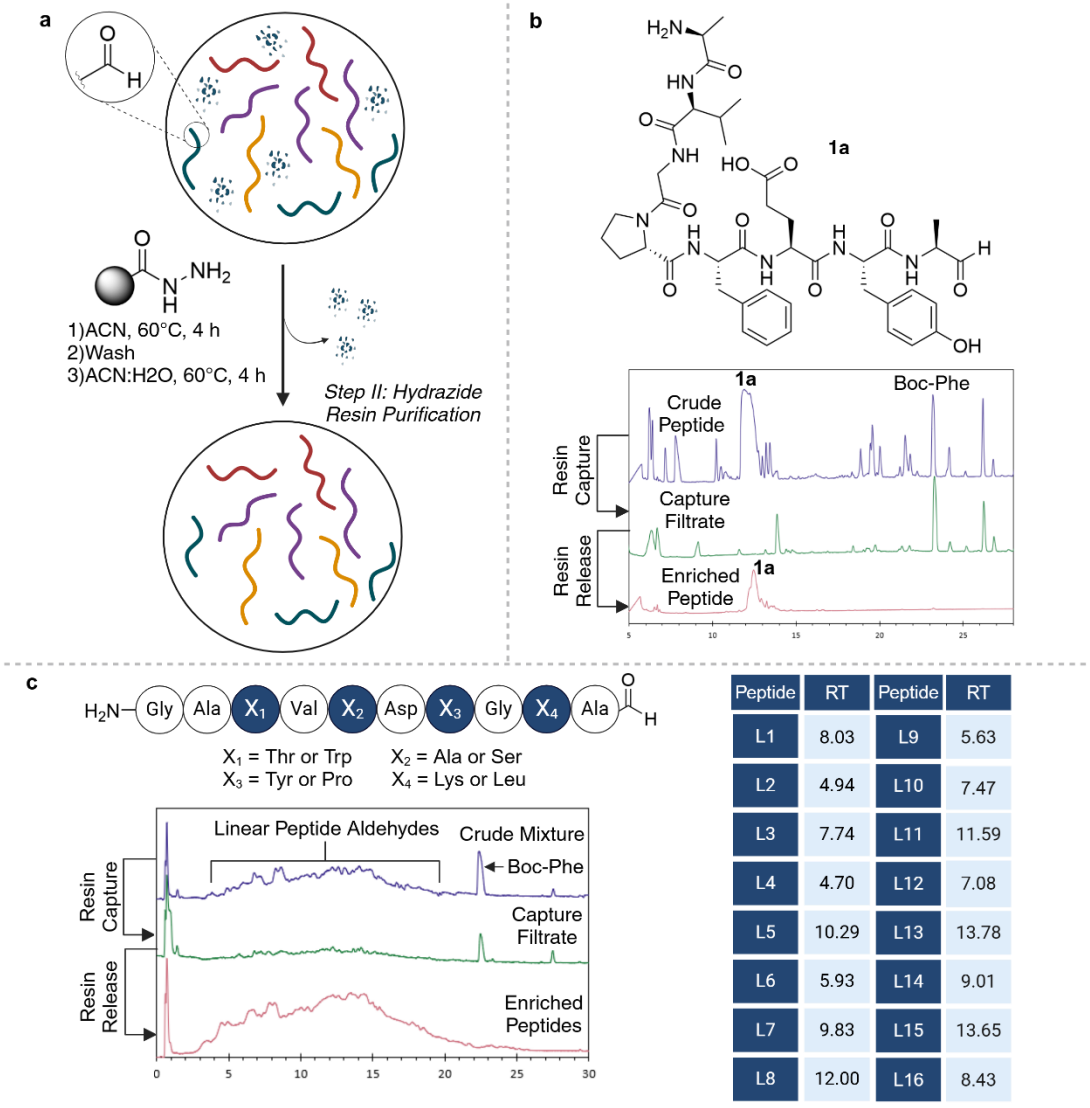

Peptide	RT	Peptide	RT
L1	8.03	L9	5.63
L2	4.94	L10	7.47
L3	7.74	L11	11.59
L4	4.70	L12	7.08
L5	10.29	L13	13.78
L6	5.93	L14	9.01
L7	9.83	L15	13.65
L8	12.00	L16	8.43

Figure 9: Hydrazide resin purification of linear peptide aldehydes (a) General scheme for the reversible capture of linear peptide aldehydes with hydrazide resin(b) Structure of model peptide **1a** with stacked chromatograms (DAD) of the crude model peptide **1a**, the filtrate collected after hydrazide resin scavenging, and the filtrate after hydrolysis from resin/regeneration of peptide **1a**. (c) Purification of peptide aldehyde small-scale library containing 16 sequences, stacked chromatograms (DAD) from hydrazide purification steps, and table displaying the retention time of each linear peptide aldehydes (L1-L16) from the purified small-scale library

2.2.2 One-pot Cyclization and Purification

With purified linear peptides in hand, we endeavored to apply our exclusively intramolecular CyClick cyclization in a one-pot macrocyclization. We adjusted conditions from the initial CyClick study, switching from dimethylaminopyridine (DMAP) to diisopropylethylamine (DIEA) as our base. This allowed for facile evaporation of the reagent along with the reaction solvent after cyclization. We subjected our small-scale library of 16 unprotected linear peptide aldehydes to CyClick reaction conditions, using 1% DIEA in DMF at 60℃. The resulting reaction mixture was analyzed by LC-HRMS before and after the cyclization to investigate the formation of any crosslinked byproducts, for which we found no evidence. Notably, we observed the formation of all the 16 cyclic peptides under the reaction conditions, further confirming the potential of CyClick to generate tag-free cyclic peptide libraries in solution without crosslinked by products (Figure 10b).

While CyClick cyclization is highly selective, the conversion to the macrocyclic product is highly varied across peptide sequences, resulting in a mixture of linear and macrocyclic species.[45] To improve the composition of our libraries, we once again leveraged the aldehyde handle on the linear peptides as a means of removing the unwanted starting materials from the library mixture. We initially implemented the optimized hydrazide resin conditions due to its previously demonstrated success in scavenging linear peptide aldehydes. Unfortunately, the results were inconsistent when applied to the cyclization reaction mixture of our model peptide. While the hydrazide resin did significantly reduce the absolute amount of linear peptide in solution, a concomitant reduction in CyClick product was observed. This reduction was attributed to the acidic conditions facilitating both hydrazone formation and the linearization of our cyclic peptides.

To circumvent the undesired linearization associated with acidic scavenging conditions, we employed threonine functionalized resin that reacts with aldehydes under basic conditions. This strategy traps aldehydes through oxazolidine formation. Fortunately, the optimized conditions for threonine-based capture mirrored those utilized for our CyClick cyclization. This allows for both steps, macrocyclization and resin purification, to happen in quick succession and in one-pot. By incubating the cyclization mixture from a model peptide **1a**

with 5 equivalents of threonine-glycine (TG) functionalized resin, 5 equivalents of sodium sulfate, in 1% DIEA in DMF at 50-60℃, we efficiently removed linear peptide aldehydes without concurrent linearization of cyclic product **2a** (Figure 10a, Supplementary Table 2, Supplementary Figure 1). Sodium sulfate addition was critical for achieving oxazolidine crosslinking and complete removal of linear peptide aldehydes from the cyclization mixture. We hypothesize that this was due to the water generated from imine formation with the N-terminal amine hydrolyzing the imine before the oxazolidine ring closure. After optimization on our model peptide **1a**, we successfully applied TG-resin for purifying the small-scale library of 16 cyclic peptides from the one-pot cyclization mixture following two rounds of TG resin purification (Figure 10b, Supplementary Figure 2).

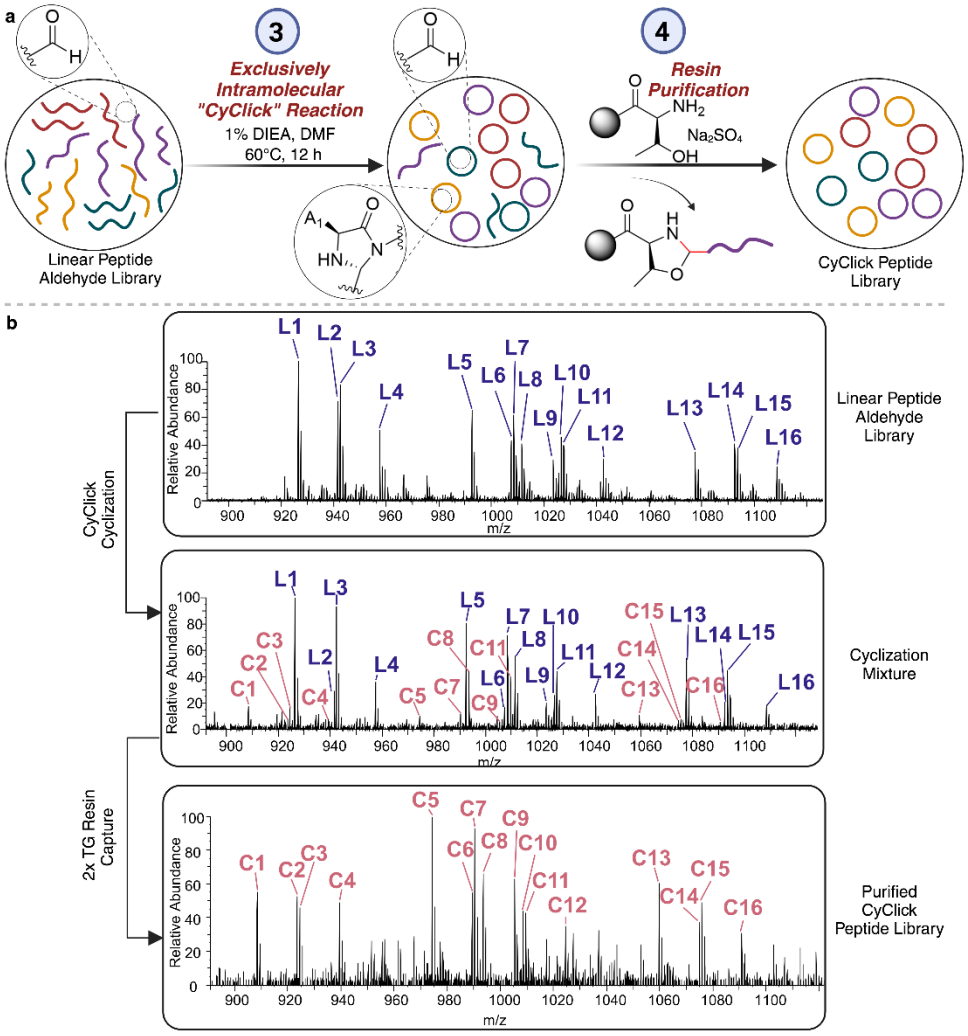

Figure 10: Cyclization and purification of a mixture peptide aldehydes. (a) Scheme for the cyclization and resin-based purification of small-scale peptide aldehyde library. (b) Spectra of direct infusion analysis of 16 peptide small-scale library, including the linear mixture (top), cyclization mixture (middle) and pure cyclic peptide mixture after two successive incubations with TG functionalized scavenger resin under optimized conditions (bottom).

2.2.3 CyClick Peptide Linearization, Derivatization, and Stability Studies

Following the optimization of our library synthesis and purification steps, we focused on devising a method to linearize our peptides, facilitating a tag-free sequencing strategy. Direct sequencing of macrocyclic peptides by tandem mass spectrometry, relative to linear peptides, is particularly challenging due to the complexity of the resulting MS2 spectra. Methods that utilize MS^3 level fragmentation and corresponding data analysis workflows for deconvolution of cyclic peptide sequences are effective but difficult to implement with larger library sizes that contain more redundant peptide masses.[58] Linearization strategies for cyclic peptide sequencing have been implemented previously by leveraging site-specific cleavage at Tyr,[59] Met,[60,61] or Ser[62] residues. Additionally, a unique method was developed utilizing a photocleavable tetrazine linker as a macrocyclization strategy in OBOC libraries, allowing for facile linearization under 350 nM irradiation[63]. For this work, we did not want to be limited by the requirement of including a specific amino acid, which is necessary for the site-selective linearization methods. We additionally sought a method that was compatible with CyClick cyclization due to its unique intramolecular selectivity. An investigation into the intermolecular condensation of aldehydes with α-aminoamides revealed literature precedents for the hydrolysis of 4-imidazolidinones, which could be applied to CyClick cyclized peptides.[48] Initial attempts involved incubating peptide macrocycle 2a in water under acidic conditions, resulting in limited ring opening. However, elevating the temperature to 80°C prompted full conversion of peptide macrocycle 2a to linear peptide aldehyde 1a within 8 hours, as confirmed by HPLC and MS analysis (Supplementary Figure 3).

The full reversibility of CyClick cyclization not only aids in the predictability of peptide fragmentation but also reveals an aldehyde handle that can easily be targeted for ionization-boosting derivatization. Previous studies have demonstrated that the addition of guanidinium groups to linear peptides improves their limit of detection and yields unambiguous y-ion fragmentation ladders. To achieve these ends, we synthesized a simple arginine-containing tetrapeptide linked with N-terminal hydroxylamine, H_2N-O-GGRG for the derivatization of peptide aldehyde 1a to generate oxime 3a (Figure 11a). The derivatization of peptide aldehyde 3a significantly enhanced signal intensity of both the precursor and fragment ions by an order of magnitude. The MS^2 spectrum of the derivatized peptide also featured a prominent y-ion ladder from y_1 to y_{n-2}, where n is the number of

residues in the peptide (Figure 11b). While this precludes unambiguous sequencing of the N-terminal dipeptide sequence, fixing the identity of the amino acid at either of the two positions or ensuring no isobaric sequences are included in the library design at the two positions are easily implemented solutions.

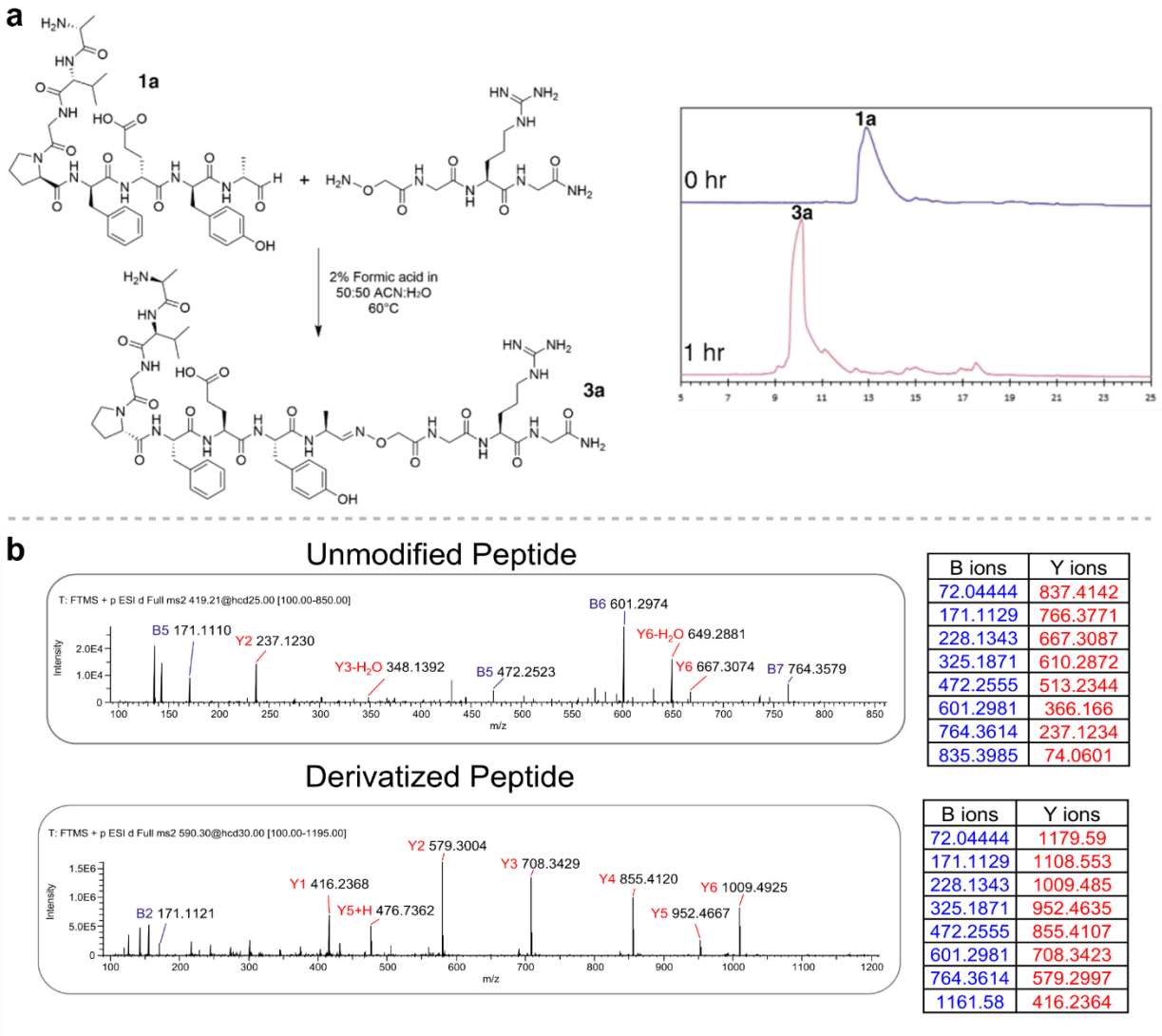

B ions	Y ions
72.04444	837.4142
171.1129	766.3771
228.1343	667.3087
325.1871	610.2872
472.2555	513.2344
601.2981	366.166
764.3614	237.1234
835.3985	74.0601

B ions	Y ions
72.04444	1179.59
171.1129	1108.553
228.1343	1009.485
325.1871	952.4635
472.2555	855.4107
601.2981	708.3423
764.3614	579.2997
1161.58	416.2364

Figure 11: Derivatization of peptide aldehyde with hydroxylamine reagent (a) Model peptide **1a** derivatization scheme and stacked chromatograms of reaction progress. (b) MS2 spectra of unmodified peptide **1a** vs. derivatized linear peptide **3a**

To determine the limit-of-detection for sequencing, serial dilutions of peptide 3a were performed followed by analysis using nanoLC/MS-MS. A clear y-ion ladder with signal intensity above $1x10^4$ was achieved down to 0.169 femtomoles of peptide 3a (Figure 12, Supplementary Figure 4). This detection limit was an order of magnitude lower than that achieved with a standard linear peptide library of 1×10^8 members utilized for affinity-selection mass spectrometry (AS-MS).[64] We expect this improved detection at low concentrations will both improve confidence of peptide hits and allow equally large macrocycle libraries to be implemented for AS-MS workflows.

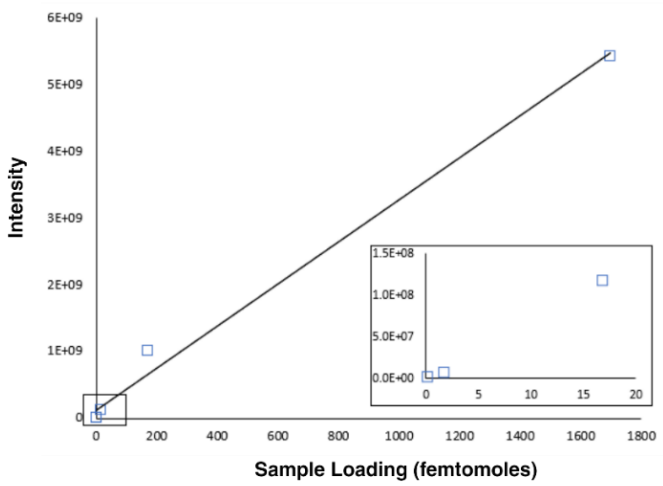

Femtomoles	Intensity
1,696	5.44E9
169.6	1.01E9
16.96	1.17E8
1.69	7.69E6
0.169	8.94E5

Figure 12: Limit of detection of derivatized model peptide **3a**. Chart for sample loading (femtomoles) vs signal intensity of precursor ion

Noting the significant overlap in reaction conditions for linearization and derivatization, we attempted to perform both steps simultaneously in a one-pot process on macrocyclic peptide 2a (Figure 13a). We were delighted to observe the quantitative conversion of macrocycle 2a to the linear oxime product 3a in the one-pot reaction with no unwanted byproducts (Figure 13b). We sought to demonstrate the strength of this one-pot linearization/derivatization by applying the optimized conditions to a small-scale library of 16 cyclic peptides. We observed successful derivatization of all 16 peptides in a mixture and achieved high sequencing confidence afforded by the near complete y-ion ladder for all identified peptides (Figure 13d). During LC-MS/MS analysis of the mixture, we successfully detected and sequenced peptides with overlapping retention times by enabling dynamic exclusion in our data-dependent acquisition settings. This feature prevents a

precursor ion from being selected for MS2 fragmentation repeatedly within a set time frame. This is an important capability as identified hits from affinity selections are likely to have similar polarity and chemical

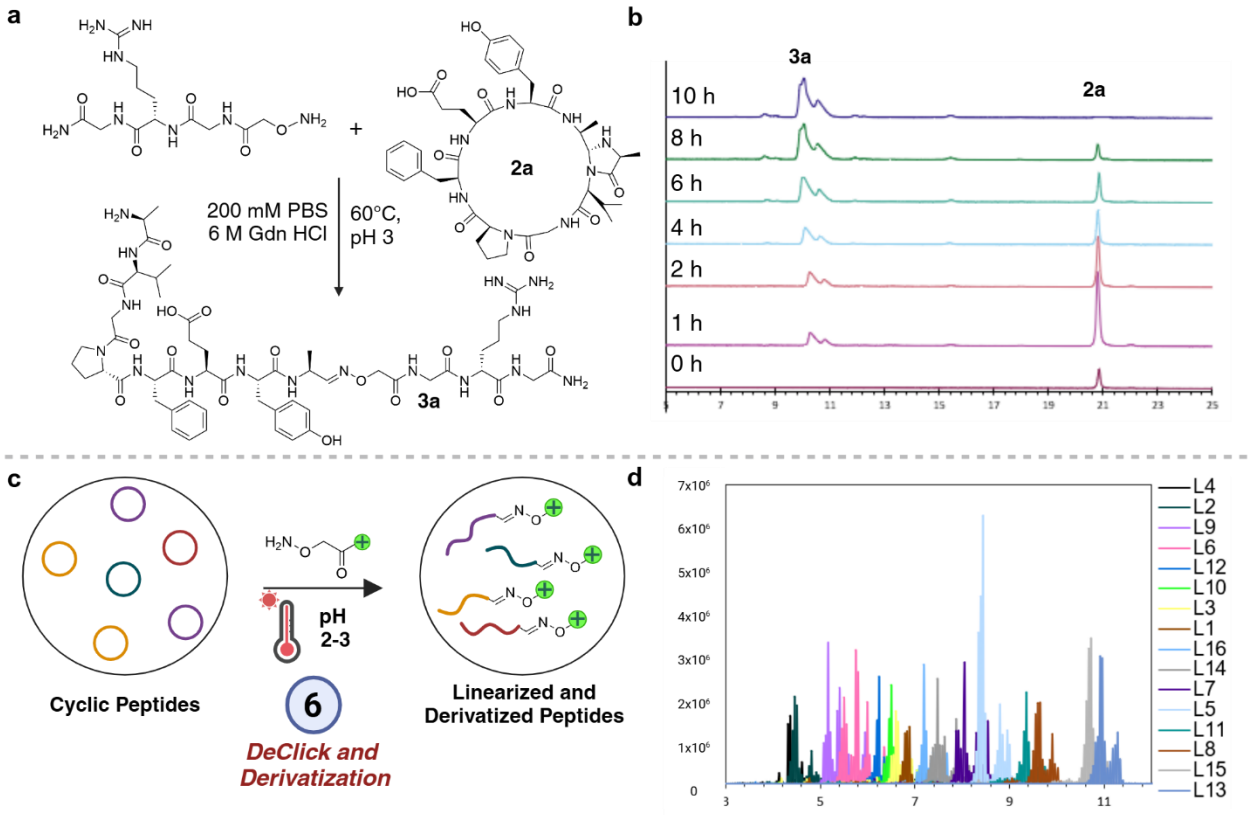

Figure 13: Linearization and derivatization of cyclic peptides. a) One-pot linearization and derivatization of cyclic model peptide **2a** to derivatized linear peptide **3a.** b) Stacked chromatograms displaying time-point analysis of one-pot linearization and derivatization of cyclic model peptide **2a** to derivatized linear peptide **3a**. c) Linearization and derivatization of the resulting linear peptide aldehyde library with sensitivity enhancers. d) Extracted ion chromatograms of the derivatized small-scale cyclic peptide library.

characteristics.

Recognizing that our peptides were susceptible to linearization, we explored their stability in the presence of other nucleophiles that would be present on protein targets. We wanted to confirm our library members would not be linearized unwantedly during the pooled affinity selection process. We subjected our model peptide 2a to our screening conditions, pH 7.4, 1M PBS buffer at room temperature, as well as those conditions in the presence of relevant nucleophiles (Lys, Cys, glutathione, and benzyl hydroxylamine). The solutions were monitored by HPLC for 3 hours and no linearization of the peptide was observed, supporting our optimized conditions as being necessary for the reversal of the cyclization reaction (Figure 14c).

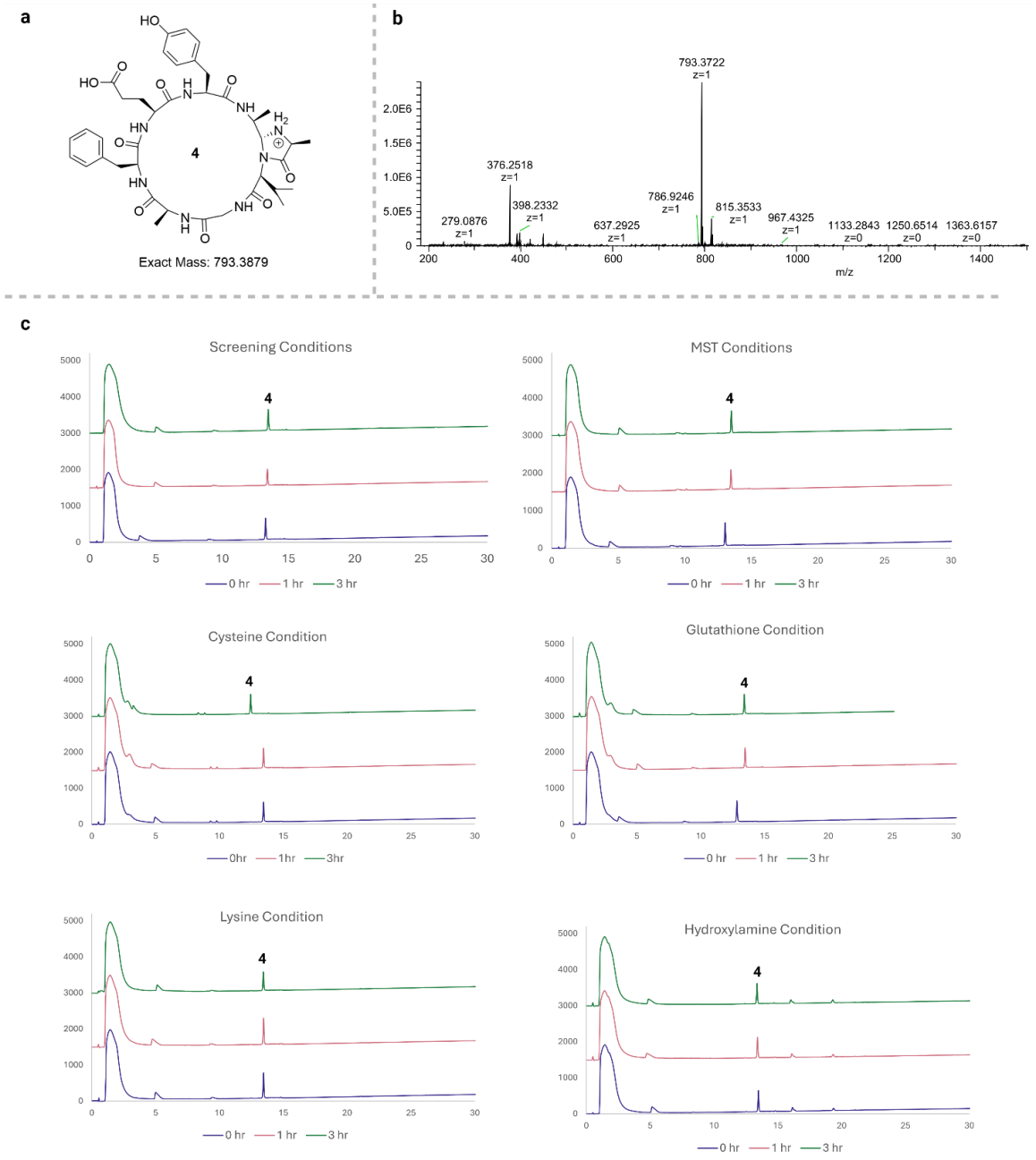

Figure 14: CyClick peptide stability studies (a) Model cyclic peptide 4 structure (b) Spectrum of purified model peptide 4 (c) Stacked chromatograms for time course analysis of peptide susceptibility to screening conditions and various nucleophiles (Cys, Lys, glutathione, and benzylhydroxylamine)

2.3 PEPTIC Application in Ligand Discovery

As a proof-of-concept experiment to validate the application of PEPTIC technology for identifying cyclic peptide binders against protein targets, we performed an affinity selection against the well characterized anti-HA mAb clone 12ca5. This antibody has been utilized for the development of linear peptide-based affinity selection-mass spectrometry (AS-MS) methods due to its high affinity for the well-defined DXXDY antigen-binding motif.[64,65]

To test our libraries against 12ca5, we employed both magnetic bead-based affinity capture and high-performance size exclusion chromatography (HPSEC) affinity selection methods.[64,66] These methods have been demonstrated to enrich high-affinity peptide binders at nano- to picomolar concentrations from complex library mixtures. When performed with our CyClick libraries, the linearization/derivatization step is easily performed immediately after selection.

For the magnetic bead-based assay, we immobilized 0.13 nmoles of biotinylated 12ca5 on streptavidin magnetic beads and incubated with a $1x10^6$ member CyClick peptide library with 0.5% DMF in PBS at an estimated 200 pM per member concentration. We simultaneously performed a positive control selection with the antigen sequence YPYDVPDYA at the same concentration. After elution, peptides were subjected to our one-pot linearization/derivatization conditions, desalted, and submitted for nLC/MS-MS analysis. The positive control peptide was clearly detected with high signal intensity, confirming that the selection as performed would enrich high affinity binders. Analysis of the library selection experiments yielded several peptide precursors, however, there was significant plastic contamination that complicated resulting MS^2 spectra.

We utilized the Comet search tool within the open-source Trans-Proteomic Pipeline software package to identify peptide sequences from our collected spectra. This tool generates *in silico* spectra predictions from a selected database and searches acquired mass spectral data to determine matches based on specified confidence criteria and parameters. For our search parameters, we included the C-terminal derivatization as a fixed PTM (+326.1814) and limited our identifications to those with an expect score. Unfortunately, the confidence in sequence hits was too low to confirm their presence in the eluate. It is suspected that material from the microcentrifuge tubes used for the selection and subsequent linearization/derivatization reaction leached into

solution. Future attempts at this assay will exclusively employ glass reaction vials to avoid extensive sample contamination.

For the HPSEC assay, we incubated 12ca5 with a $1x10^4$ member CyClick peptide library with 5% DMSO in PBS at ~450 nM per member concentration. Due to the inherent separation capability of size exclusion, the breakthrough fraction containing protein and bound peptide was free of significant contamination. The fraction was acidified to separate peptide binders from 12ca5 and subjected to our one-pot linearization/derivatization conditions prior to analysis by nLC-MS/MS (Figure 15a) . We were excited to see clear MS^2 spectra with the characteristic y-ion ladder associated with our derivatized peptides. From the theoretical database search, we narrowed down 25 sequences for which we had high confidence in the sequencing results (Supplementary Table 3). We chose two sequences, H_2N-GDVGPDAYDYA-CHO and H_2N-GDAGPYDADYA-CHO (Supplementary Figure 6) to resynthesize and test their qualitative binding by microscale thermophoresis (MST) (Figure 15b). Additionally, we chose a sequence H_2N-GDVWALYASYA-CHO, from the library that was not enriched in the selection as a negative control. For each peptide, the N-terminal Gly was replaced with Lys and the side chain was labeled with the fluorophore fluorescein isothiocyanate (FITC) (Supplementary Figure 7). To qualitatively assess binding, 40 nM solutions of each peptide were incubated with 3 μM of 12ca5 antibody. Thermophoretic time traces were collected in quadruplicate with peptide only and peptide-antibody solutions. For both enriched peptide sequences (H_2N-GDVGPDAYDYA-CHO and H_2N-GDAGPYDADYA-CHO) there was a significant shift in the thermophoretic time traces when incubated with the antibody while none was observed for the negative control (H_2N-GDVWALYASYA-CHO) (Figure 15c). This confirmed that the enriched sequences were indeed binding to 12ca5 and were preferentially selected due to this binding interaction.

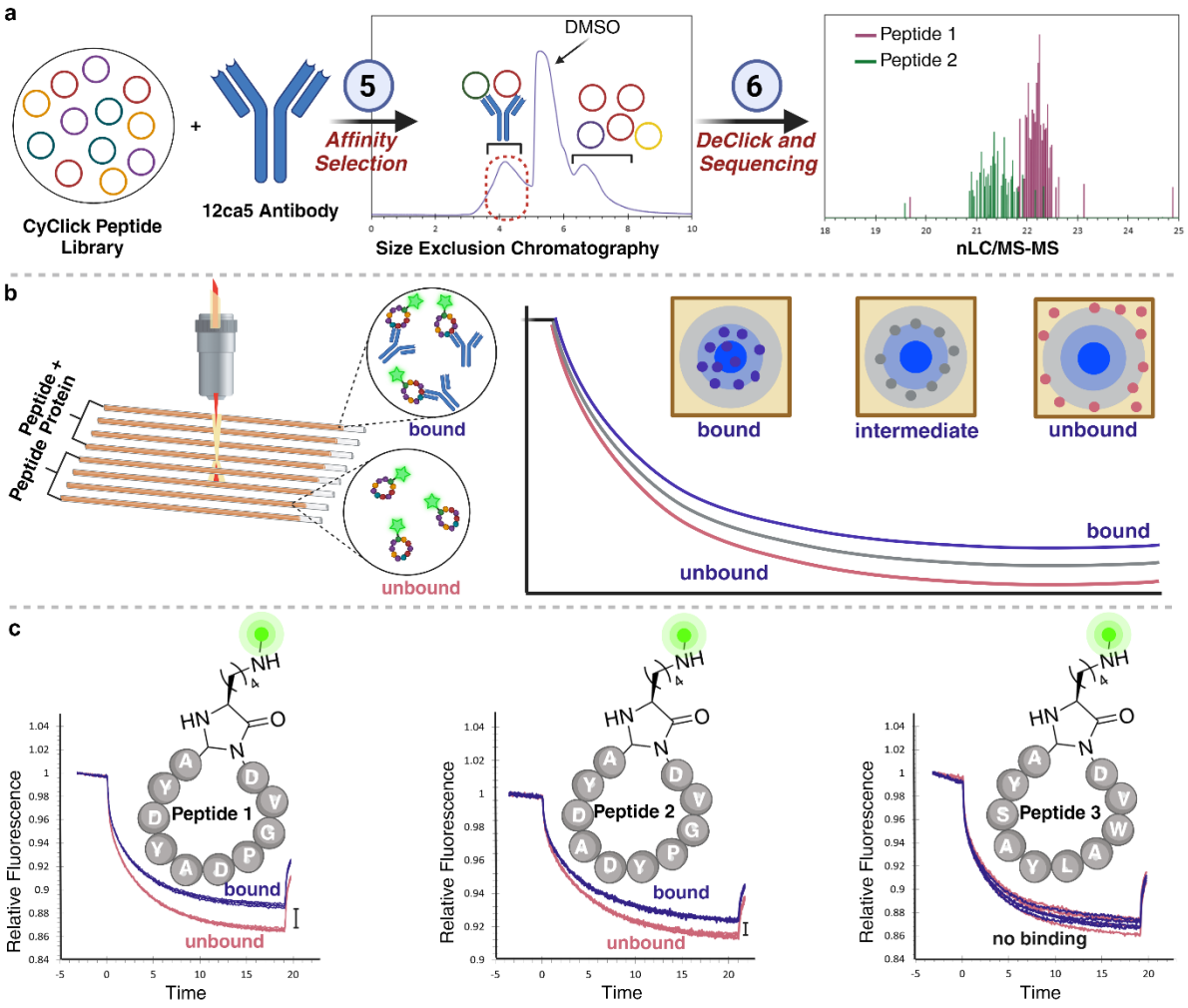

Figure 15: Affinity selection experiments with mixture of cyclic peptides. (a) General workflow for HPSEC affinity selection and identification of cyclic peptide binders of 12ca5 antibody from a cyclic peptide library by PEPTIC workflow using linearization of cyclic peptide binders, derivatization of linear peptide aldehydes followed by analysis using nano LC-MS/MS. (b) Representation of microscale thermophoretic assay and analysis of bound from unbound. (c) Individual cyclic peptides based on enriched peptide sequences using HPSEC affinity selection against 12ca5 antibody showed qualitative binding to 12ca5 antibody as analyzed by microscale thermophoretic assay, pink: peptide only; blue: peptide + protein. Microscale thermophoretic assay with random sequence not enriched by PEPTIC workflow did not show any binding with 12ca5 antibody.

2.3.1 Identifying a Macrocyclic Peptide Ligand for the HIV-1 Capsid Protein

We further applied our PEPTIC method to identify a cyclic peptide that interacts with the HIV-1 capsid protein (CA). The binding site in the HIV-1 capsid core is a frequently targeted cavity in CA hexamers and natively interacts with multiple host proteins during viral infection.[67,80] The protein-protein interactions in this binding

pocket are driven by a common phenylalanine-glycine (FG) dipeptide motif found in several host proteins, including nucleoporin 153 (Nup153), which is an essential factor for HIV-1 nuclear entry and viral replication.[67-69] Based on the efficiency of small molecule inhibitors that target this binding site of the HIV-1 capsid core, we applied our PEPTIC method to generate variations of the reported binding FG sequence of Nup153 (PDB: 6AYA[70]).[71,72] First, we determined the optimal position of cyclizing the Nup153 FG sequence; either immediately C-terminal to the FG-motif ("FG-SIDE") or several resides downstream ("FG-END") with two, 54-member CyClick peptide libraries (Figure 16a and 16b). To assess their effectiveness at perturbing the capsid core, we applied a thermal shift assay (TSA). This technique determines if protein-ligand interactions occur by measuring changes to the thermal stability of purified proteins from additional intramolecular interactions if ligand-binding occurs. An environmentally sensitive fluorophore, SYPRO™ Orange dye, is used for signal readout. The dye is quenched in water but fluoresces when in contact with the hydrophobic core of proteins, which are exposed after protein denaturation. The shift in denaturation temperature during the assay provides insight into the stabilizing or destabilizing effect of a ligand on the protein of interest.

We found that the C-terminal position increased the thermal stability of disulfide-stabilized CA hexamers (CA_{HEX})[73] *in vitro*, and thus was the best to work from this scaffold (Figure 16d). Notably, similar results were observed with "FG-SIDE" cyclic peptide library for point mutated HIV capsid protein (CAN74D and CAM66I) (Supplemental Figure 8). The observed change in melting temperatures for FG-SIDE is relatively small but statistically significant ($p = 0.038$). We then selected a representative peptide from the library, "cyFG-3", to investigate binding affinity using TSA and characterize binding (Figure 16d). Biolayer Interferometry (BLI) was used to determine the binding constants of cyFG-3 to a modified CA_{HEX} construct that includes a C-terminal 6xHis Tag ($CA_{HEX:6HIS}$). After immobilizing $CA121_{HEX:6HIS}$ to the HIS-affinity probes, we report the biochemical constants for cyFG-3 are $K_D = 0.963 \pm 0.06$ μM, $k_{on} = 8.90 \pm 0.53 \times 10^3$ $M^{-1}s^{-1}$, $k_{off} = 8.58 \pm 0.136 \times 10^{-3}$ s^{-1} (Figure 16e). We confirmed our result with a cyclic peptide by carrying out a BLI assay with a positive control, a small molecule antiviral Lenacapavir (LEN) that was recently approved for use in highly treatment-experienced individuals who are HIV-1–positive and on a failing antiretroviral therapy (ART) regimen.[67,73,74] The biochemical constants for LEN to $CA_{HEX:6HIS}$ are $K_D = 28.6 \pm 0.2$ nM, $k_{on} = 1.040 \pm 0.007$

$x10^4$ $M^{-1}s^{-1}$, k_{off} = 2.978 ± 0.015 $x10^{-4}$ s^{-1} (Supplemental Figure S9b). It is reported that LEN increases the assembly rate of CA *in vitro*, as determined using a plate-based assay measuring absorbance at 350 nm (A_{350}) over time as a proxy of CA protein association.[67,75] Using this functional A_{350} assay, we found that cyFG-3 also binds to the same site as the cyclic peptide and increases the rate of CA assembly, similar to but less drastic than LEN (Figure 15e and 15f Supplemental Figure 9c). This is important to note, as compounds and

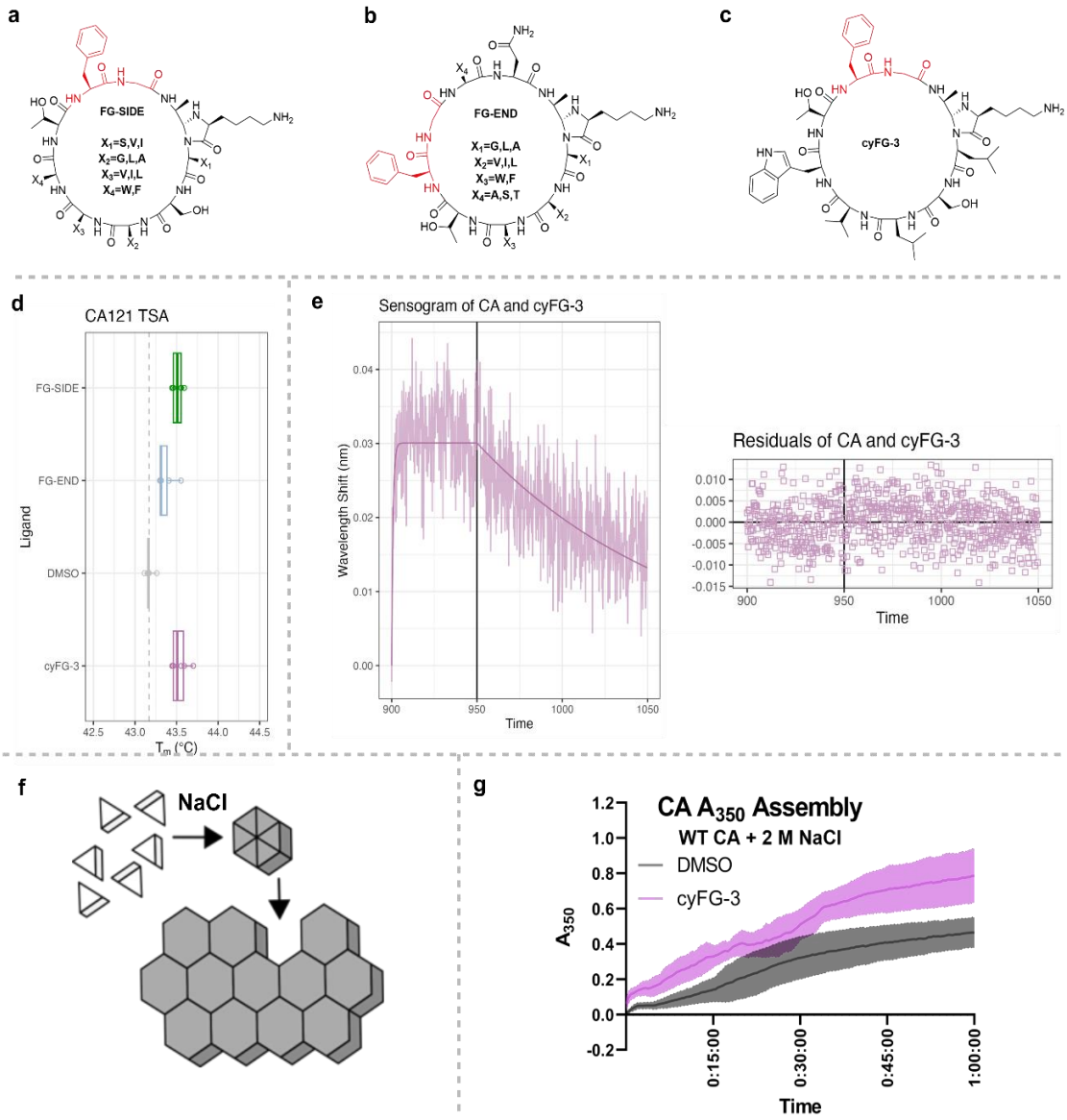

Figure 16: Example of library screening for cyclic peptides with phenylalanine-glycine (FG) motifs that bind the HIV-1 capsid protein (CA). Structures of a) FG-SIDE, b) FG-END, c) cyFG-3. d) Average melting temperature (Tm) values as determined by thermal shift assay (TSA) of CA hexamers incubated with the libraries of peptides containing the FG motif on the side (FG-SIDE) or end (FG-END), and the purified cyFG-3 from the FG-SIDE library. e) Representative biolayer interferometry (BLI) sensograms of double background subtracted data and modeled fit for CA hexamers with cyFG-3 at 75 μM (blue). Global KD = 0.963 ± 0.06 μM, k_{on} = 8.90 ± 0.53×103 M Residuals of the model are shown below the plot as a difference between the modeled line and observed data. f) Schematic of in vitro CA assembly. Purified CA monomers are clear in solution, but when a high concentration of NaCl increases the ionic strength of the solution, CA multimerizes into hexamers and large assemblies that turn the solution cloudy, which can be tracked with A350 nm as a proxy of assembly. g) Kinetics of in vitro CA assembly increase with pretreatment with cyFG-3 (pink), as CA assembles faster than the control DMSO (gray). Average of 6 technical replicates (N = 3) with standard deviation shown.

mutations that increase or decrease the stability of CA often impair viral fitness.[70,76,77] A second representative

peptide cyFG-5 was also characterized for binding. This peptide differs from cyFG-3 by only Leu to Ser substitution adjacent to the N-terminus, yet the measured binding affinity by BLI was significantly weaker with values of K_D = 65.9 ± 0.08 μM, k_{on} = 8.93 ± 0.41 x10^2 $M^{-1}s^{-1}$, k_{off} = 4.44 ± 0.11x10^2 s^{-1}. Despite this fact, co-crystallization of this peptide with the CA assembly was more successful than with cyFG-3 (Figure 17b). The solved structure demonstrates significant overlap of the "FG" binding motif with both the small molecule PF74 and the Nup153 peptide mimic (Figure 17a, Figure 17c). With this additional structural information on CyClick peptide conformation at the FG binding site of CA, we plan to design focused libraries to further increase interactions at the binding site and improve binding affinity to the assembly.

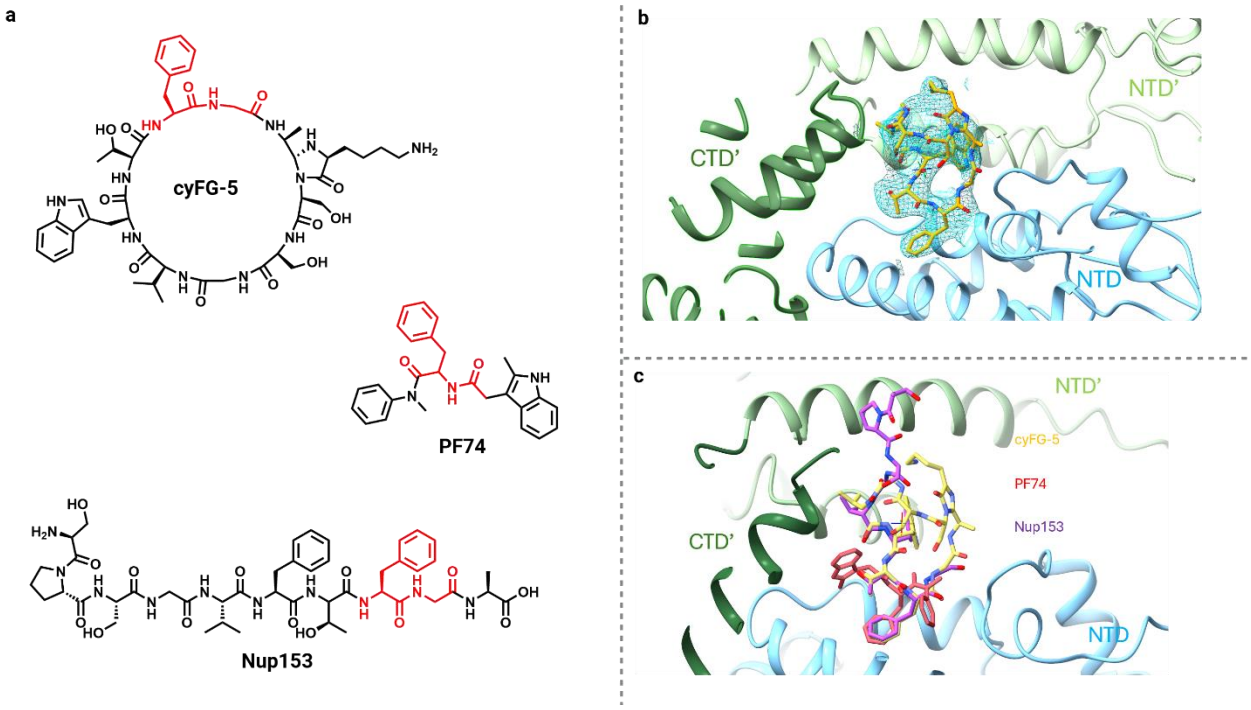

Figure 17: Ligands for FG binding site of HIV capsid assembly protein (a) Chemical structures of cyFG-5, small molecule PF74, and Nup153 peptide mimic (b)cyFg-5 peptide co-crystallized with HIV-1 CA hexamers (c) Overlay of crystal structures of cyFG-5, small molecule PF74, and Nup153 peptide mimic in complex with HIV-1 CA hexamers

2.4 PEPTIC Application for Pooled *In Vitro* Membrane Permeability Assay

In addition to affinity selections, we aimed to expand the scope of application of CyClick peptide libraries. The parallel artificial membrane permeability assay is an *in vitro* experimental technique that mimics the passive permeation of a substance across a cell's lipid bilayer.[78] The assay involves the incubation of the test compound in a donor well and measures its permeation across a lipid-coated artificial membrane into an acceptor

compartment, with permeability quantified by analyzing compound concentration in the acceptor well. This assay is often performed in a one-compound one-well format, however, we hypothesized that we could employ our libraries to perform a high-throughput, pooled version of the assay. This type of study has previously been attempted using lactam macrocycles in a small, mass-encoded peptide library.[79] While it did yield useful information, the need to avoid redundant masses limited the sequence diversity of what could be explored in that work. The facile linearization and derivatization of our CyClick libraries we suspect will allow for further expansion of pooled permeability screening as peptides can be directly sequenced and quantified relatively between the acceptor and donor wells.

The first step in developing this application of our CyClick libraries was to assess our ability to assess the range of our ability to accurately sequence and quantify peptides in a complex mixture. Most reported peptide analysis methods have been developed towards the analysis of digested protein samples, which contain a complex mixture of peptide with different sequence length and amino acid composition. In the context of our libraries the peptides are of the same length and have high sequence similarity, posing a unique challenge in regard to peak overlap during chromatographic separations. To address these challenges, we utilized the capabilities of a trapped ion mobility-time of flight (timsTOF) mass spectrometer paired with reverse phase liquid chromatography separation to resolve the closely related peptide sequences.

Trapped ion mobility spectrometry is a technique that separates ions according to their size and shape. Ions are carried by a moving gas stream and an electric field is applied to "trap" them along different positions in the gas flow. This provides a completely orthogonal dimension of separation to standard reverse phase chromatography.[80] We hypothesized that the addition of the ion mobility dimension and the speed of the TOF mass analyzer would yield high sequence coverage across the peptide library.

We initiated this study by synthesizing a CyClick peptide library (C1) designed with a 9 amino acid sequence with 4 variable positions (Figure 18a). Each variable position was made with 8 different building blocks, resulting in a 4,096-member library with 419 unique peptide masses. This design was chosen to ensure a baseline of sequence diversity that would yield peptides with a range of permeation rates. To begin developing our

analysis method, we linearized and derivatized a portion of our CyClick library. We initially applied a data independent acquisition (DIA) strategy, a method that fragments every precursor ion detected in the MS1 spectrum. This strategy has yielded higher sequence coverage when applied to proteolytic digests because unlike data dependent acquisition, it does not discriminate which peptides will be fragmented based on their signal intensity upon elution. Peptide identification is commonly performed using *in silico* generated spectral libraries, however, this provided minimal sequence identifications when applied to our peptide library. We hypothesized that this was due to the significant sequence and fragment ion overlap between peptide species in the library. As an alternative strategy, we generated a sample specific spectral library through collection of data-dependent acquisition (DDA) MS run. Additionally, adjustments to the sample loading, ion accumulation time, and fragmentation energy afforded further improvement to sequence coverage (Supplementary Table 4).

With our analytical strategy in hand, we performed three replicates of a pooled PAMPA assay with our library C1. We identified 124 peptide sequences that were detected in our acceptor well compartment across all 3 replicate assays. These peptides were primarily enriched with valine, leucine, alanine, and phenylalanine residues in each of the variable positions. This result was consistent with established trends of hydrophobicity and passive membrane permeability. Additionally, the fact that only a small percentage of the library was found to be passively permeable reflects the overarching low permeability of most peptide sequences.

We also sought to generate a quantitative measure that could be used to compare the relative permeability of individual peptide species. When the PAMPA assay is performed on individual compounds, the absolute concentration in the donor and acceptor well is used to calculate an apparent permeability (Papp) value. While absolute concentration of each peptide cannot be measured in the pooled library context, we expected we could use ion signal intensity as a crude measure for relative concentration. The ionization efficiency of peptides can vary significantly across different sequences; however, ionization remains fairly constant for a single peptide structure when analyzing that peptide across different samples within the same sample matrix. This allows for a relative determination of concentration between assay compartments. We decided to use the ratio of the normalized signal intensity in the acceptor well (A) over that of the donor well (D), resulting in an intensity

ratio (A/D) where the increase is directly related to peptide permeation. This value is also unbiased to the initial concentrations of each macrocycle in the library.

We expanded our investigation to 5 additional peptide libraries (C2, A1, A2, E1, and E2) moving the position of fixed and variable amino acids and adding an additional set of building blocks. Including our initial library, we would theoretically access permeability information on 24,576 peptides with just 6 assay wells. We assayed each library in triplicate and identified a total of 15,681 peptides, of which 591 were found in the acceptor well of all three replicates. The A/D ratio for each peptide hit was calculated and averaged for all three replicates, with that majority falling between 0.8-1.2. Additionally, we once again found an enrichment of primarily hydrophobic leucine, valine, phenylalanine, and proline residues across the variable positions in the library. We are now performing ongoing experiments to validate a representative sample of these peptide hits for their individual permeability measurements.

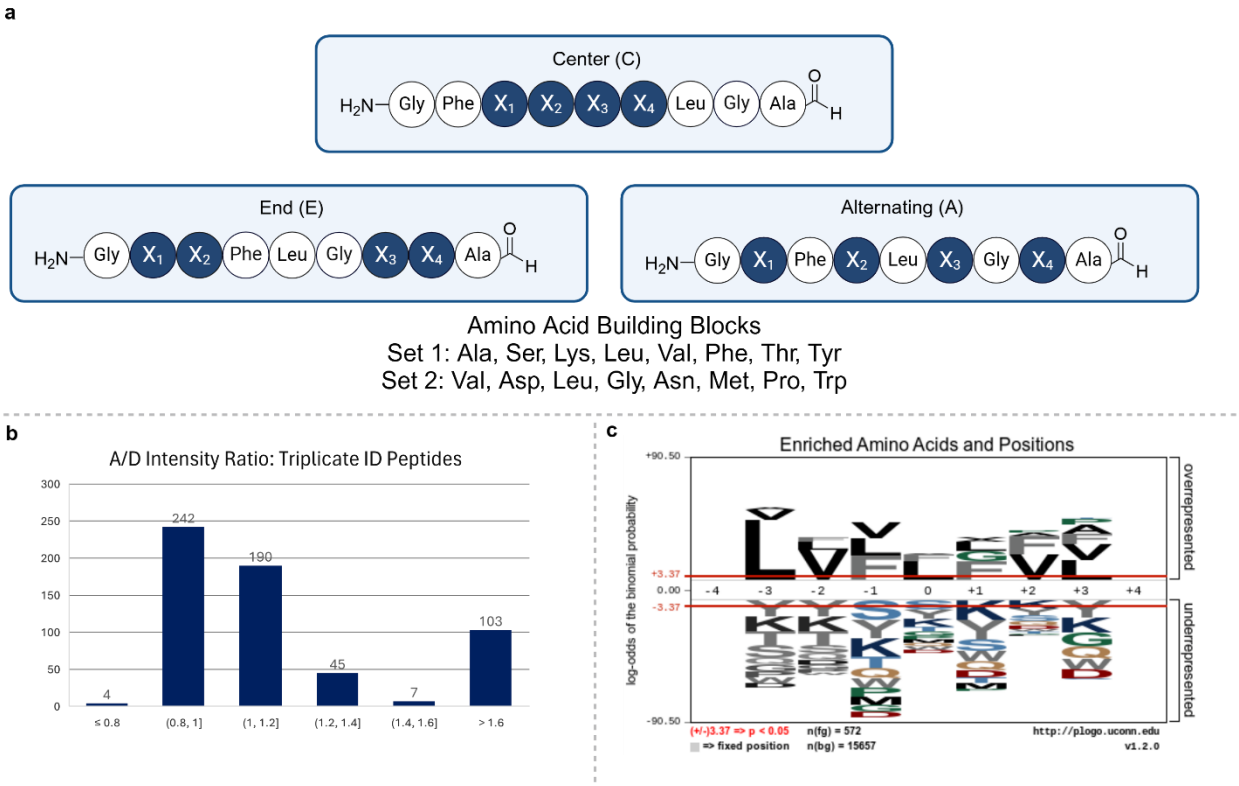

Figure 18: CyClick libraries employed in high throughput PAMPA assays (a) Design and building blocks used for positionally varied libraries (b) Histogram representing A/D ratios for hit peptides from all three replicates of assayed libraries (c) Probability of residue identity in each position of permeable peptide sequences

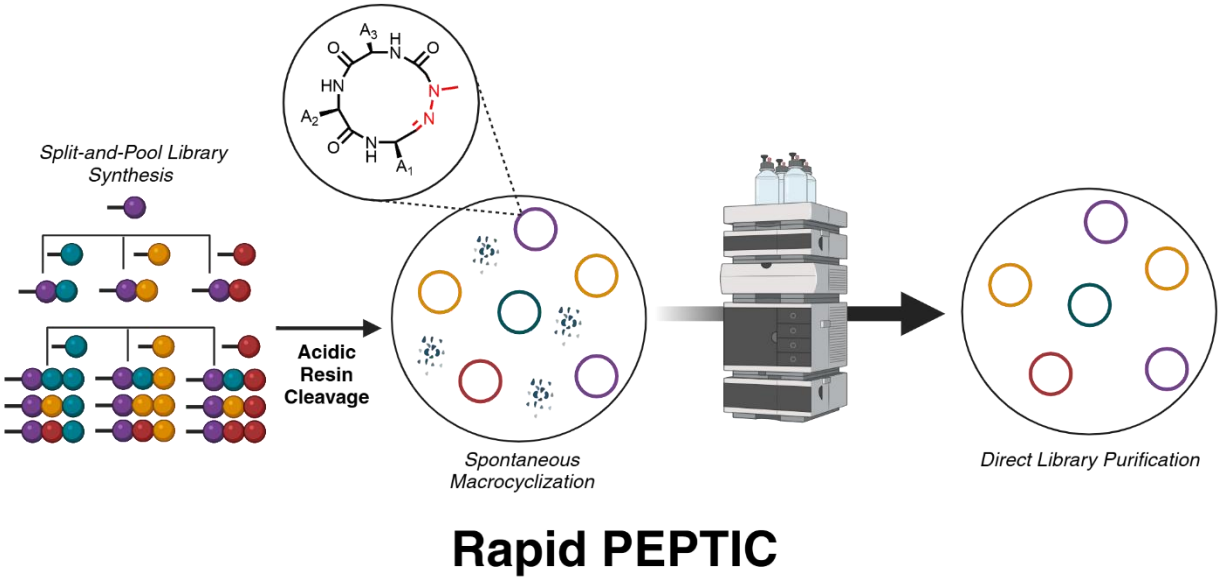

Chapter 3: Hydrazone Macrocyclization for Rapid PEPTIC Workflow

Contributing Authors:

Angèle Bruce, Dr. Victor Adebomi, Dr. Jonathan Palmer, , Dr. Gaurav Bhardwaj, Dr. Monika Raj

3.1 Expanding PEPTIC Library Technologies

Our initial investigation into utilizing CyClick chemistry for synthetic macrocycle generation proved successful; however, the workflow continues to face limitations regarding the speed and efficiency of library synthesis. After resin preparation and manual split-and-pool synthesis, the library must still be subject to multiple capture and release purification steps as well as a 12 hour macrocyclization reaction. Additionally, one of the main drawbacks of CyClick cyclization is the significant differences in conversion across differing peptide sequences. The original published study demonstrated significant variation in yield between peptide sequences when substituting the identity of the amino acid directly adjacent to the N-teminus.[45] In the context of a pooled library of macrocycles, this results in a significantly uneven distribution of peptide concentration and biases the library against certain sequences. While it is ideal to select peptides with good synthetic accessibility, this variation inherently reduces the chemical diversity of our libraries and the chemical space that could be explored through them. To generate a complementary strategy that addresses these limitations of CyClick libraries, we sought to use another aldehyde-based reaction that might result in more evenly distributed macrocyclization yields while still being amenable to linearization for direct sequencing.

To identify an appropriate reaction for our desired goals, we explored publications that previously utilized spontaneous aldehyde condensation reactions like imine, hydrazone, and oxime formation. These condensation chemistries are thermodynamically favorable and likely to be rapid in an intramolecular context. We ruled out the use of imine chemistry due to the higher susceptibility of the linkage to hydrolysis and nucleophilic attack.[14] Hydrazone and oxime macrocyclizations have been demonstrated to have high rates of conversion[81,82] and the linkages are known to be more stable to hydrolysis in comparison to imines[83]. Hydrazone chemistry has been used extensively for dynamic covalent libraries and has been applied successfully to peptide macrocyclization.[50,84,85] Oxime chemistry has been employed for the efficient synthesis of side chain-to-tail macrocyclization of peptides, with all attempted sequences resulting in >80% yield of the macrocyclic product.[82]

The evidence from published work supported that both strategies could be applicable to our goals, however, we believed hydrazone chemistry would provide the ideal mix of macrocycle conversion along with facile

linearization and derivatization. This hypothesis was supported by the various studies employing hydrazone/oxime exchange for bioconjugation and glycan enrichment in glycoproteomics.[54] Additionally, we wanted to avoid possible competition between our macrocyclization moiety and our derivatization reagent.

3.2 Development of Second-Generation PEPTIC Workflow

3.2.1 Accessing N-terminal Hydrazine Residue

To initiate our investigation into utilizing hydrazone condensation in our PEPTIC workflow, we explored strategies for accessing the nucleophilic hydrazine or hydrazide moiety at the N-terminus of our peptides. We explored both solution phase preformation of a protected hydrazine monomer residue that could be introduced in one step during solid-phase peptide synthesis (SPPS) as well as options to generate the residue directly on resin through multi-step reactions.

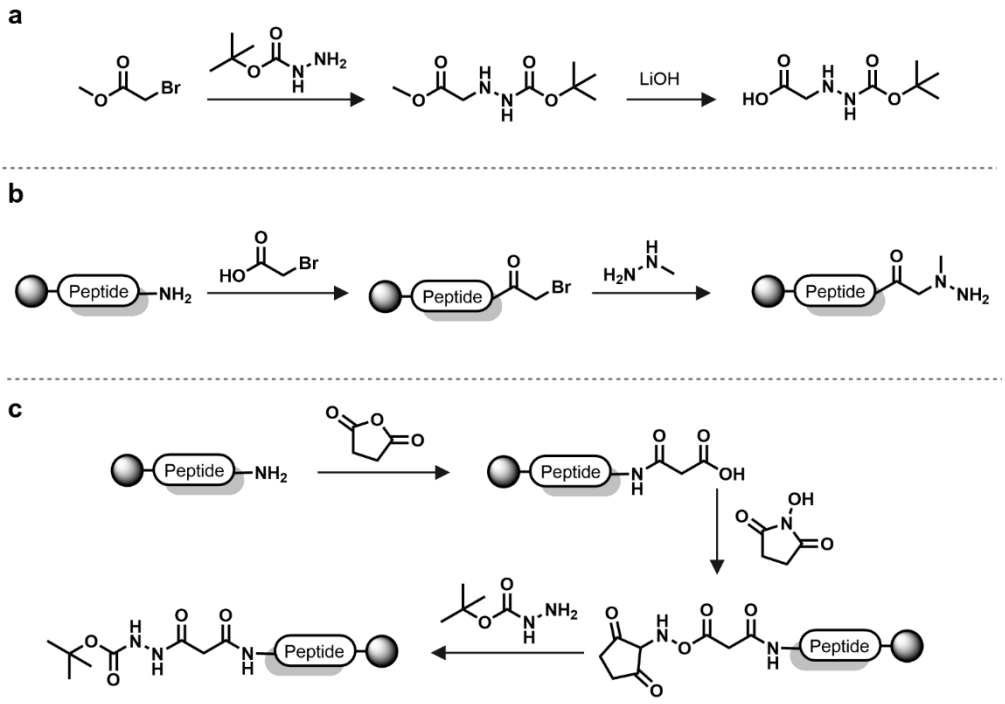

Figure 19: Reaction schemes for accessing N-terminal (a),(b) hydrazine and (c) hydrazide moieties for peptide hydrazone synthesis

To synthesize our protected monomer, we pursued a simple two step scheme. In the first step, we used *tert*-butyl carbazate for a displacement reaction with ethyl bromoacetate, generating the N-protected residue in ester form. In a second step, the ethyl ester was removed through base hydrolysis to afford the carboxylic acid product that could be employed in SPPS. To generate a hydrazine group directly on solid support, we borrowed conditions for peptoid construction through submonomer addition. A bromoacetic acid unit was coupled to the N-terminal residue and subsequent displacement was performed with methylhydrazine. We also attempted to use hydrazine HCl, however, we could not find a suitable solvent system that solubilized the polar hydrazine molecule while maintaining the swelling of the hydrophobic resin polymer. Lastly, we attempted to generate an N-terminal hydrazide moiety on resin using a three-step strategy. We first capped the N-terminus with succinic anhydride, generated an activated ester on the free carboxylate, and attempted hydrazinolysis with *tert*-butyl carbazate (Figure 19). Of the three methods explored, we found success with two hydrazine strategies but failed to produce the desired hydrazide on resin. Given the high equivalents of monomer necessary for peptide synthesis, we determined that on resin methylhydrazine displacement was the most efficient and effective for ongoing studies.

3.2.2 Exploring Hydrazone Macrocyclization

With our hydrazine displacement reaction in hand, we moved to assess if the macrocyclization with a C-terminal aldehyde would proceed with the high conversion that we hypothesized. We synthesized linear peptide aldehydes with varying number of residues (7-11) all bearing an N-terminal alkylated hydrazine. Upon liquid chromatography- high resolution mass spectrometry (LC-HRMS) analysis, we were pleased to observe no linear starting material remained. All peptides had converted to primarily the monocyclic product and varying amounts of the cyclic dimer (Figure 20, Supplementary Figure 11).

a

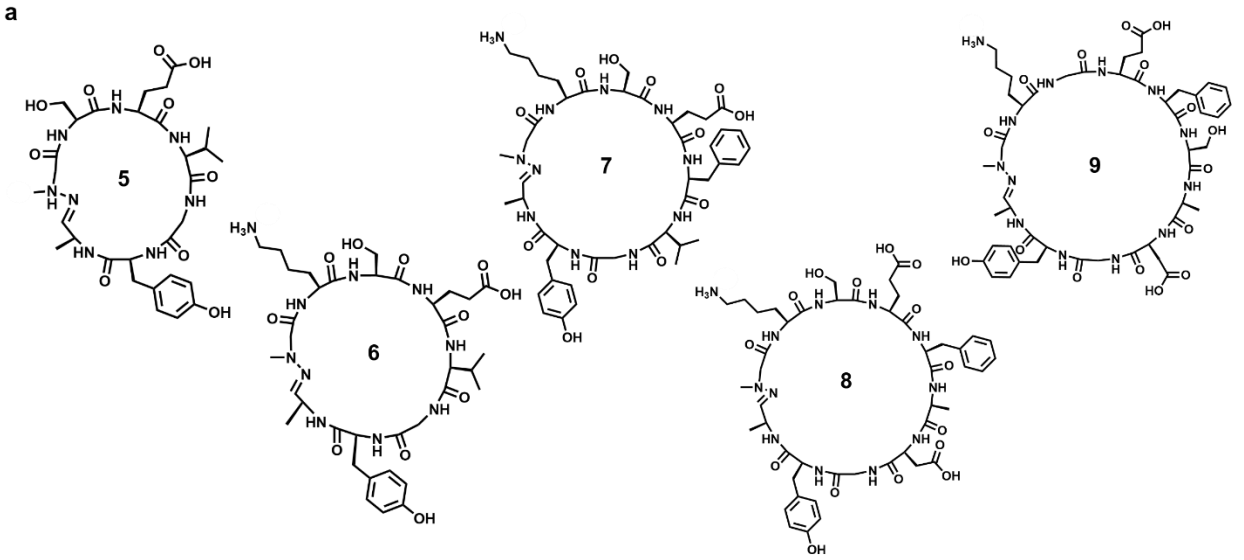

b

Peptide	Linear %	Monocycle %	Cyclic dimer %
5	<1%	85%	15%
6	<1%	89%	11%
7	<1%	95%	5%
8	<1%	97%	3%
9	<1%	95%	5%

Figure 20: Generation of hydrazone macrocycles (a) Chemical structures of model hydrazone peptides **5-9** (b) Table outlining the percent conversion of each peptide to the monocycle or cyclic dimer as determined by LC-HRMS analysis

From this initial observation, we wanted to determine if cyclization was occurring immediately during peptide cleavage or proceeding on the column during reverse phase separation. Hydrazone condensation is an acid catalyzed reaction; both the peptide cleavage and high-performance liquid chromatography (HPLC) separation of peptides occur at low pH. To investigate this phenomenon, we cleaved example peptides **5**, **6**, and **9** with a TFA cleavage cocktail and removed the remaining acid with cold ether. The peptides were split into two dissolution conditions, dissolved in just water/acetonitrile and or in water/acetonitrile modified with diisopropylethylamine to neutralize any remaining acid. Prior to peptide analysis, the LC pumps were purged with LC grade water and acetonitrile containing no modifiers.

Upon direct infusion of the crude peptide mixture, the predominant product mass observed was of the monocyclic peptide species (Figure 21). This confirmed that the macrocyclization of the peptide was primarily occurring directly during peptide cleavage and competed with the formation of the oxazolidine. Additionally, for peptide **5** we noted the presence of oxazolidine adduct formed between the peptide and the Thr-Gly peptide fragment used as a linker for amino aldehyde loading. This is a commonly observed minor side product when generating linear peptide aldehydes using this strategy. Direct infusion of the base modified peptide mixture yielded no peak for the desired mass and a predominant peak that represented a loss of 71.0371 amu from the linear peptide species. The basic solvent system appeared to catalyze a cleavage reaction that resulted in the loss of the desired product entirely. We suspect this cleavage is occurring at the C-terminal aldehyde residue through hydrazinolysis of the amide bond and results in macrocyclization at the same site (Supplementary Figure 12). The product was not amenable to our linearization protocol and could not be fragmented for sequencing. In addition, the lack of any Thr-Gly adduct related to this product suggests the loss of the aldehyde handle. Given our results without the presence of base, however, we felt confident that peptides generated on resin could be immediately purified as the macrocyclic product after resin cleavage.

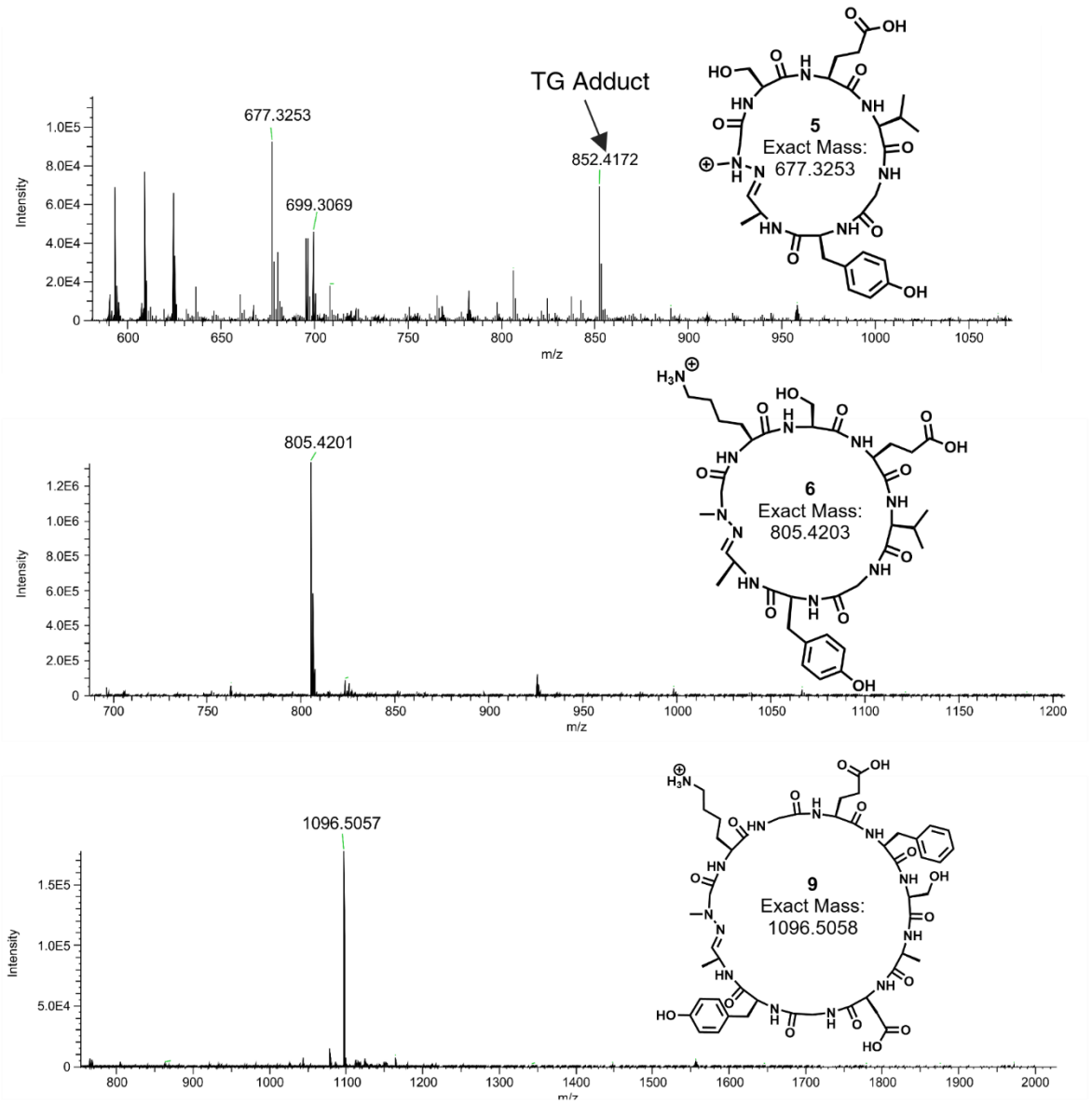

Figure 21: Spectra collected from direct MS injection of crude model peptide **5** (top), **6** (middle), and **9** (bottom)

We sought to demonstrate the efficiency of our hydrazone peptide macrocyclization with each of our example peptides. The crude peptides were each subject to preparatory scale HPLC purification. Upon analysis of the peak fractions, the main chromatographic peaks only contained the monocyclic peptide product (Supplementary Figure 13). To demonstrate the feasibility of this strategy for making macrocycle mixtures, we generated a small-scale library of 16 hydrazone peptides through split-and-pool synthesis (Figure 22a,

Supplementary Figure 14). After TFA cleavage and ether workup, the peptides were analyzed by LC-HRMS before and after preparatory HPLC purification. A gradient of 5-60% acetonitrile in water was used for preparatory chromatography and all peaks that eluted within that gradient, excluding the injection peak, were collected for library analysis. In the chromatograms for both the crude and purified mixture the masses for all 16 hydrazone library peptide macrocycles (HL1-16) were detected and no linear starting material remained (Figure 22b). Additionally, all peptides were detected when the mixture was analyzed with no acidic modifiers in the mobile phase (Supplementary Figure 15). Both the crude and purified mixture contained some amount of the linear Thr-Gly oxazolidine adduct of each peptide, ranging between 1.5-7% in the crude and 0.5-2.6% of each in the purified (Figure 22c). We believe the reduction in relative amount of oxazolidine adduct can be attributed to the separation of free TG fragments and interconversion between the adduct and the hydrazone macrocycle under the acidic conditions of the mobile phase used for chromatography.

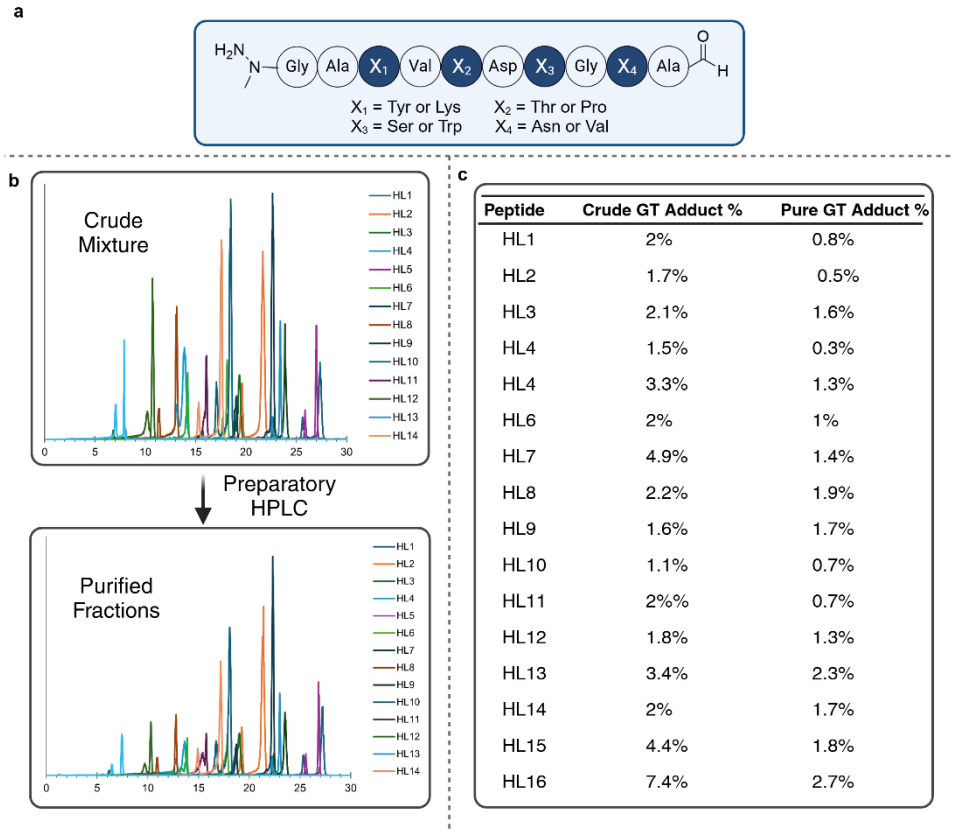

Peptide	Crude GT Adduct %	Pure GT Adduct %
HL1	2%	0.8%
HL2	1.7%	0.5%
HL3	2.1%	1.6%
HL4	1.5%	0.3%
HL4	3.3%	1.3%
HL6	2%	1%
HL7	4.9%	1.4%
HL8	2.2%	1.9%
HL9	1.6%	1.7%
HL10	1.1%	0.7%
HL11	2%%	0.7%
HL12	1.8%	1.3%
HL13	3.4%	2.3%
HL14	2%	1.7%
HL15	4.4%	1.8%
HL16	7.4%	2.7%

Figure 22: Purification of small-scale 16 hydrazone peptide library (a) Design of small-scale hydrazone library and building blocks (b) Combined extracted ion chromatograms for the 16 HL macrocyclic peptides from the crude cleaved peptide mixture (top) and the mixed purified fractions (bottom) (b) Table outlining the percent of Thr-Gly oxazolidine adduct for each of the HL peptides from LC-HRMS analysis.

3.2.3 Hydrazone Linearization, Derivatization, and Dimer Reversal

A key step in our devised PEPTIC workflow is the linearization of our macrocycles to allow for direct peptide sequencing. We hypothesized that our hydrazone macrocycles would be amenable to linearization through hydrolysis in a similar fashion to our CyClick peptides. This would reform the aldehyde C-terminus and give access to oxime-based tagging with our arginine-containing hydroxylamine probe.

Our initial attempt directly mimicked out previous linearization conditions, subjecting model peptide **5** to one pot linearization and derivatization using 2 equivalents of the derivatization probe at pH 2.0 and 60 degrees. While we did observe rapid disappearance of the macrocycle mass, we unexpectedly did not detect any of the hydroxylamine tagged peptide. We suspected the heating of the reaction was influencing the formation of undesired products. The linearization/derivatization reaction was then attempted at room temperature, keeping other conditions constant. This afforded near full conversion to the desired tagged peptide within 4 hours, with minor reversal to macrocycle within 8 hours (Figure 23a). When the derivatized product was subjected to MS dissociation, we once again achieved a complete y-ion ladder (Figure 23b).

We additionally sought to demonstrate the one-pot linearization and derivatization of our small-scale hydrazone library. The purified small-scale library was incubated with the probe in acidic conditions for 4 hours and subsequently analyzed by LC-MS/MS. The derivatized linear products for all 16 peptides were detected and the MS2 spectra provided a complete y-ion ladder for each of the peptide species (Supplementary Figure 16). With this result, we felt confident our strategy could be employed efficiently on complex macrocycle mixtures.

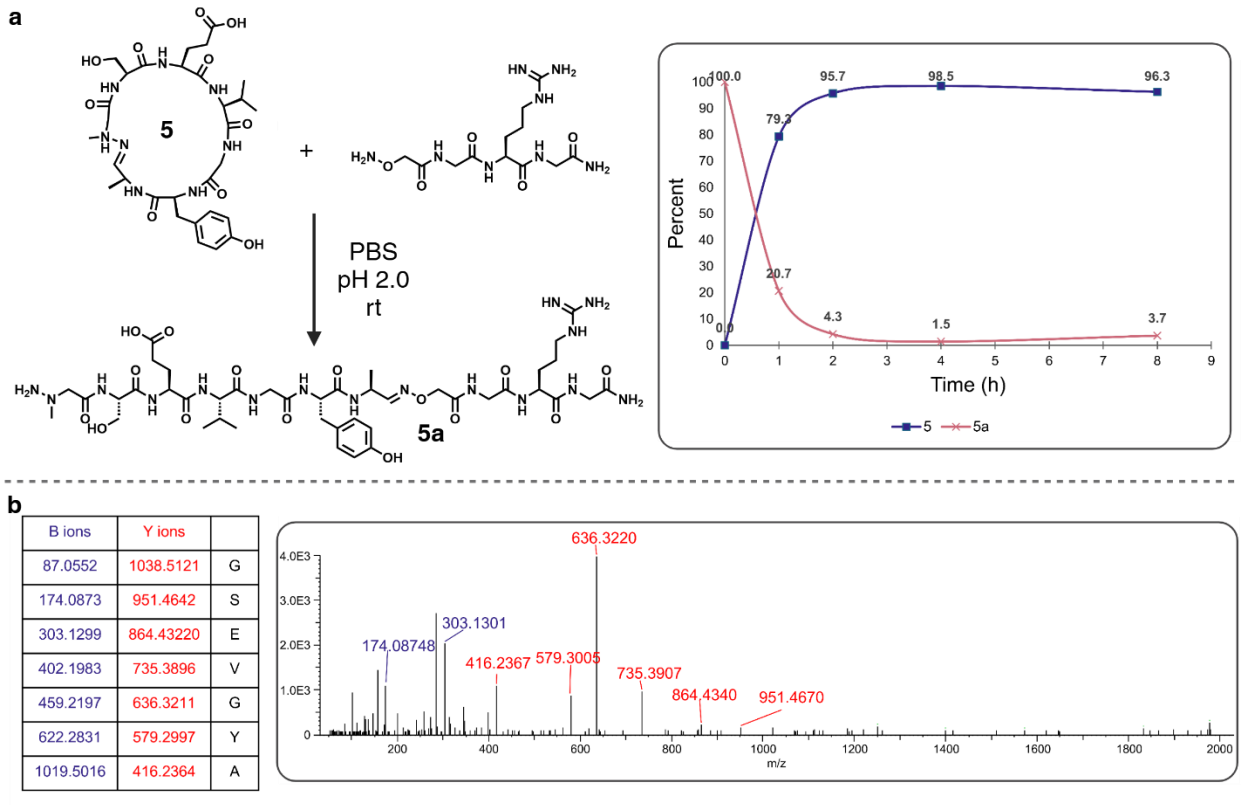

B ions	Y ions	
87.0552	1038.5121	G
174.0873	951.4642	S
303.1299	864.43220	E
402.1983	735.3896	V
459.2197	636.3211	G
622.2831	579.2997	Y
1019.5016	416.2364	A

Figure 23: Derivatization and linearization of model peptide **5** (a) Scheme for linearization/derivatization and plot of the rate of conversion from macrocycle **5** to derivatized linear peptide **5a** (b) Table of predicted fragments and MS2 spectrum of derivatized peptide **5a.**

In addition to achieving linearization, we wanted to investigate if we could employ a method to reduce the degree of macrocyclic dimerization of our peptides. Based on previous reports as well as our own linearization conditions, we know the hydrazone linkage is dynamic in acidic conditions. We hypothesized that subjecting a cyclodimer to acidic conditions at high dilution would result in dynamic hydrazone exchange and bias the monocyclic species (Figure 24a). This hypothesis was given some preliminary merit upon purification of the 6-residue macrocyclic dimer for this study. The fraction initially identified as the cyclodimer remained on the instrument for a period of time before lyophilization. Once dried and reconstituted, analysis showed that about 30% of the cyclodimer had reverted the monocycle. This cyclodimer/monocycle mixture was incubated at pH 2.0 and 40°C and saw steady conversion from the cyclodimer to the monocyclic peptide over 8 hours (Figure 23b). We detected no cyclic dimer after the solution was neutralized and maintained at room temperature. We

moved to apply this strategy to our small-scale 16 hydrazone peptide library, however, analysis of the crude and purified library showed no trace of cyclodimer products. There was no change in the mixture content before and after dimer reversal was implemented. We are aiming to generate a mixture with dimers to determine the feasibility of this strategy in the context of a mixture.

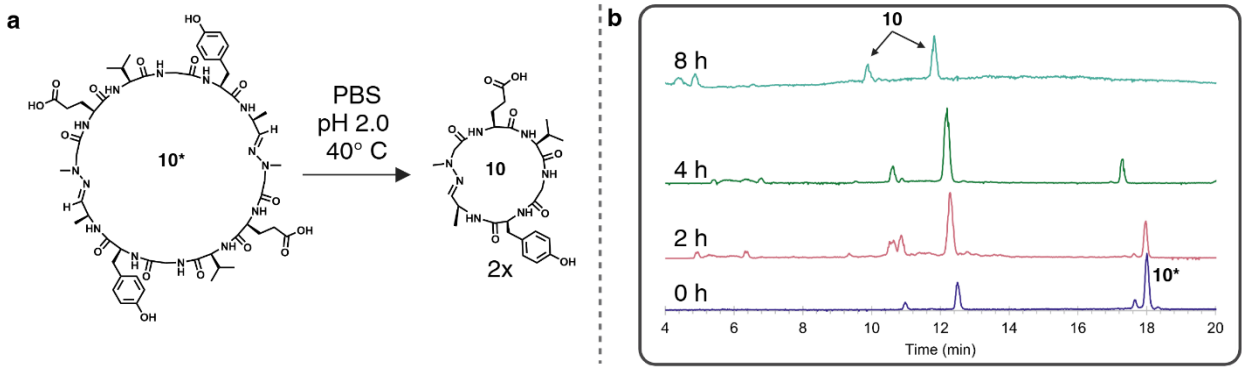

Figure 24: Peptide **10** cyclic dimer interconversion (a) Scheme for cyclic dimer reversal (b) Stacked chromatograms of reaction progress

3.2.4 Hydrazone Macrocycle Stability

In a similar vein to our work conducted with CyClick macrocyclizations, we wanted to investigate the stability of these hydrazone macrocycles against various nucleophiles. We wanted to determine if the presence of nucleophilic residues, both among library members and on the face of protein targets, would result in the destruction of our macrocycles within the time frame of their deployment in affinity selections. Our model hydrazone peptides with 6, 7, and 9 residues were utilized in this exploration. Each peptide was incubated in pH 7.0 PBS with 10 equivalents of L-lysine, N-acetyl cysteine methyl ester, or DL-cysteine (Figure 25a). These small molecules were used to simulate an environment with these reactive residues within a peptide/protein as

well as at the N-terminus. The peptides were analyzed by LC-MS without modifier at 1.5, 3, and 24 hour increments to determine macrocycle stability.

Across all three macrocycle sizes, the free cysteine was the only nucleophile to induce significant degradation.

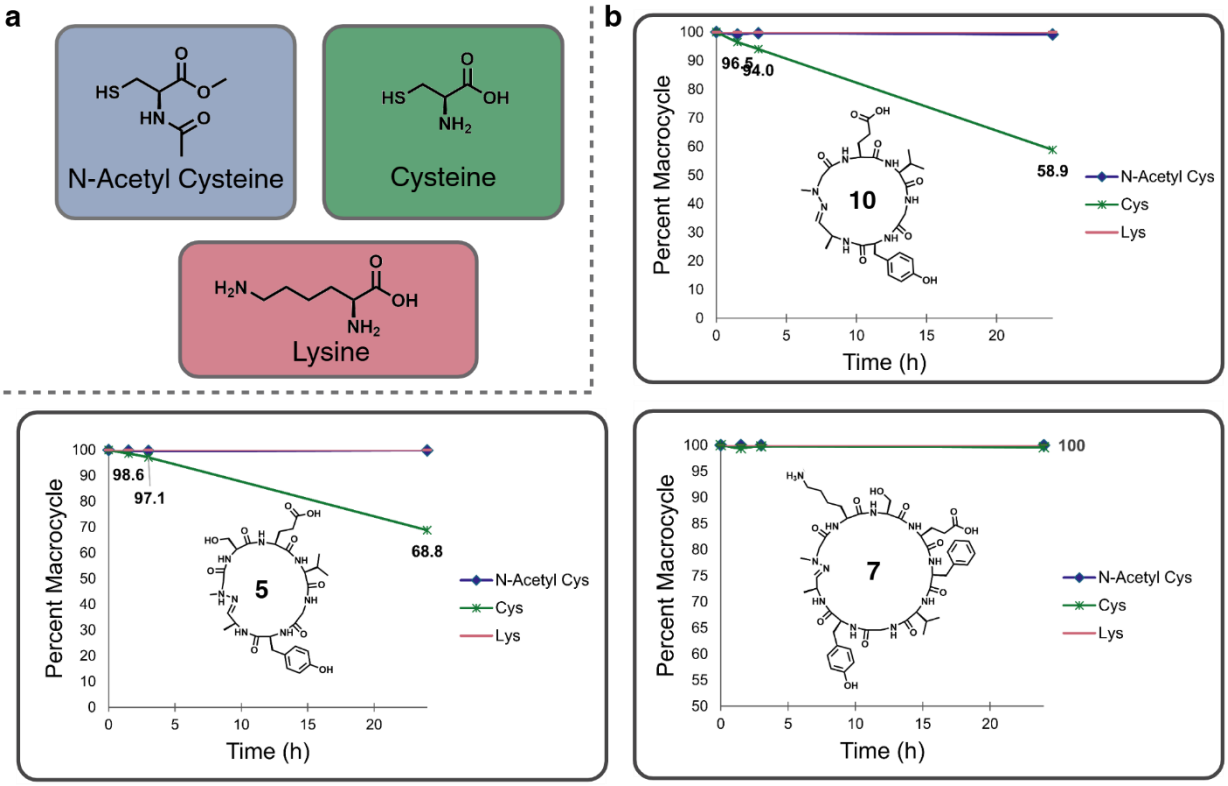

Figure 25: Hydrazone peptide stability studies (a) Structure of nucleophilic residues investigated with hydrazone macrocycles (b) Plots for the relative degradation of a model peptides **10** (top right), **5** (bottom left, and **7** (bottom right) in the presence of 10 equivalents of each nucleophile in neutral buffer

The 6-residue peptide was shown to be the most susceptible to this nucleophilic cleavage, with 58% remaining intact after 24 hours of incubation with cysteine. Approximately 68% of the 7-residue macrocycle and 99% of the 9-residue macrocycle remained intact during this time frame. Based on this trend, we hypothesize that with increasing ring size there is reduced strain and improved overall macrocycle stability. Additionally, both the N-acetylated cysteine and lysine residues had minimal effect on macrocycle stability. All three ring sizes remained 99% intact over the 24 hours of incubation (Figure 25b). This result suggests that our hydrazone macrocycles will maintain their structure when exposed to the most concerning nucleophilic residues. Additionally, even though they are susceptible to destruction by N-terminal cysteine, the macrocycle does remain intact for the time frame of affinity selections and analysis (1-3 hours).

3.3 Applications of Hydrazone PEPTIC

3.3.1 Affinity Selection Against Gamma aminobutyric acid type A receptor-associated protein (GABARAP)

To demonstrate the application of the hydrazone macrocycle platform for ligand discovery, we pursued a target of therapeutic relevance with designed and validated peptide ligands. While primarily known for its role in inhibitory neurotransmission, emerging research has shown the Gamma aminobutyric acid type A receptor-associated protein (GABARAP) also participates in crucial protein-protein interactions (PPIs) involved in the process of autophagy.[86] Evidence suggests the direct inhibition of the GABARAP PPIs could be a promising strategy for sensitizing cancer cells to chemotherapy treatments, as established tumors rely heavily on the autophagy pathway for retaining nutrients.[87]

Employing important binding residues identified in previous studies, we targeted the natural binding site for the LC3-interacting region and Atg8-interacting motif. Tryptophan, leucine, and isoleucine residues were found to be particularly important for binding as well as interspersed glutamate residues (Figure 26a).[88] We designed a 12-residue macrocycle library with 6 variable positions, theoretically generating 17,150 unique peptide sequences (Figure 25b). The library was incubated with a 50 μL aliquot of a 20 μM GABARAP solution for 30 minutes before separation by high performance size exclusion chromatography (HPSEC). The breakthrough fraction containing the protein was collected, acidified, and incubated with 2 equivalents (relative to the initial library concentration) of the derivatization probe.

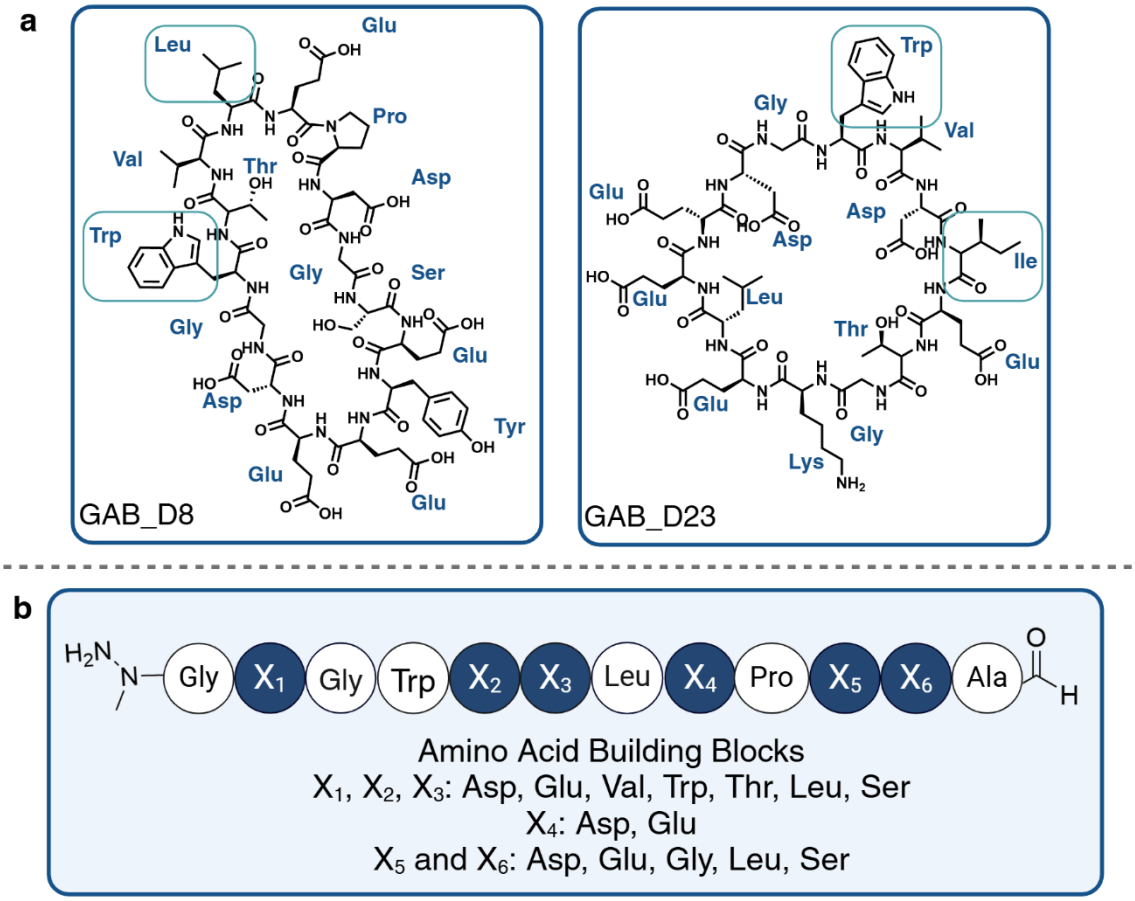

Figure 26: GABARAP hydrazone library (a) Structures for reported macrocycle peptide ligands GAB_D8 and GAB_D23. Important binding residues outlined in boxes. (b) Design of hydrazone peptide library with 6 variable positions and varied building blocks

The eluate from the affinity selection was desalted and analyzed by nLC-MS/MS. We again utilized the Comet search tool within the open-source Trans-Proteomic Pipeline software package to analyze the MS2 spectra for matching hits to our theoretical library sequence database. In the open search parameters, the derivatization was accounted for as a +326.1814 modification at C-terminal alanine residues and the methylhydrazine moiety as a +29.0266 modification to N-terminal glycine We confidently identified 10 peptide sequences in our database search and confirmed through direct analysis of the annotated MS2 spectra (Figure 27, Supplementary Figure 17). Of these sequences, we chose three for resynthesis and evaluation of binding affinity through surface plasmon resonance (Figure 27).

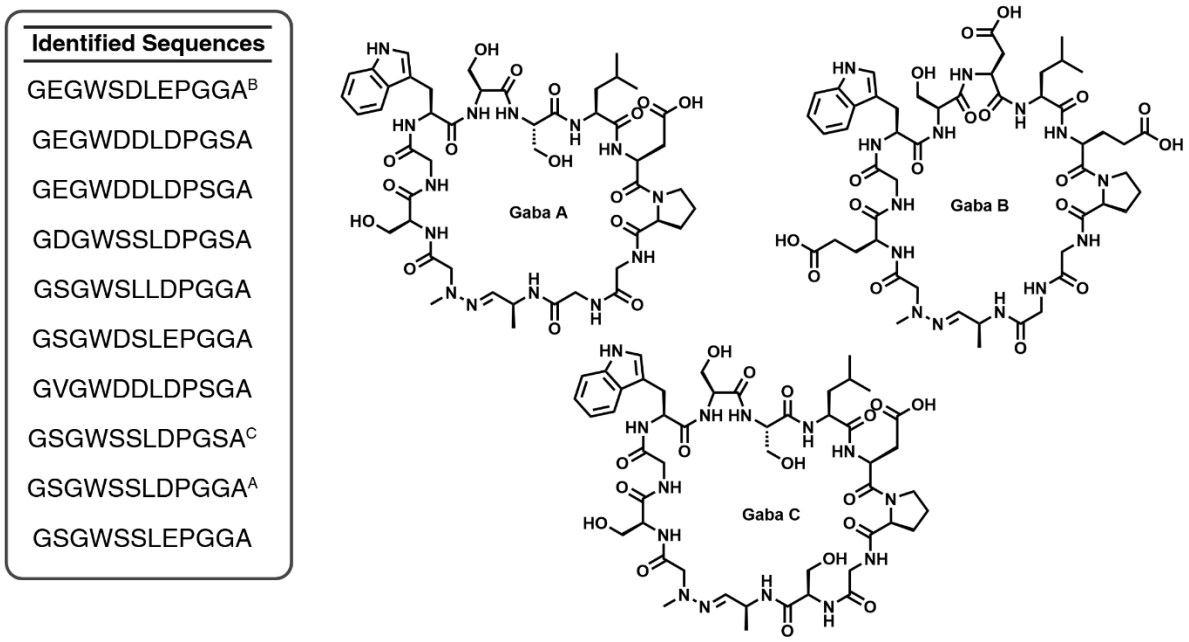

Figure 27: Sequences identified from HPSEC affinity selection with GABARAP protein target and structures of peptides resynthesized for validation.

3.3.2 Parallel Artificial Membrane Permeability Assay (PAMPA)

In addition to affinity selection-mass spectrometry, we explored the use of our hydrazone macrocycle libraries for a pooled PAMPA workflow. We had two main aims in our investigation. The first was to establish this library generation strategy as viable for this application. The second was to compare the enriched sequences between the hydrazone and CyClick libraries to determine the effect of macrocyclization linker on sequence permeability. The designs for CyClick libraries A1, A2, E1, and E2 were used for generating complimentary hydrazone libraries, replacing the N-terminal glycine with the methylated hydrazine residue.

We first assessed if our previously developed method on the timsTOF would be suitable for the analysis of our linearized hydrazone peptides. We expected the minor difference in overall structure should have minimal effect on the elution times and collisional cross section of the sequences. Fortunately, the previously established analysis method for CyClick peptide library analysis also provided significant coverage for the hydrazone libraries as well. We performed three replicates of the assay with each library and subjected the peptides to our

linearization and derivatization protocol. Upon analysis we identified far fewer peptide species than in the context of the CyClick libraries and in total identified only six sequences that were detected in triplicate (Figure 28). We hypothesize that this significant reduction in permeable sequences is due to two main factors. The first is the positive influence on permeability of the turn induced by the fused imidazolidinone structure in CyClick peptides. Based on a modeled CyClick peptide structure from the initial investigation, we believe this turn allows for more intramolecular hydrogen bonding across the peptide backbone. This interaction in peptides is known to improve the passive permeability through the lipid membrane. The second factor we believe is the introduction of the two nitrogen atoms at the point of cyclization. These atoms are more polar and capable of forming hydrogen bonds with surrounding water molecules, conferring a higher entropic cost to entering the hydrophobic artificial lipid membrane.

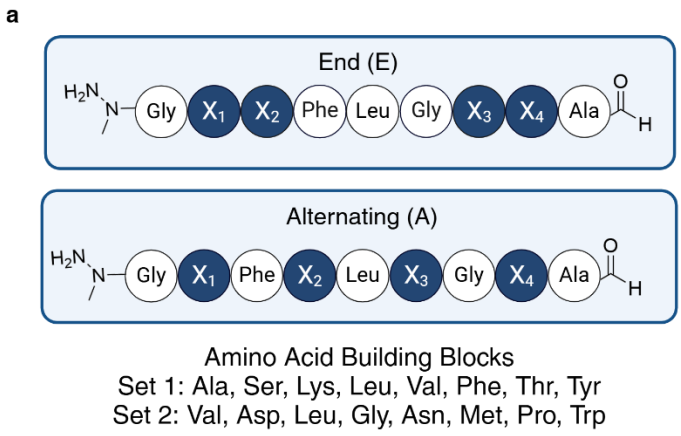

b

Triplicate Sequences	A/D Ratio
GGFMLVGGA	1.3
GVSFLGAVA	5.6
GVSFLGVAA	5.8
GTAFLGVAA	15.3
GTAFLGAVA	15.7
GGFMLGGVA	19.7

Figure 28: Hydrazone libraries utilized for high throughput PAMPA assays (a) Design and building blocks used for positionally varied libraries

4.1 Discussion

The most popular macrocyclic peptide library generation and screening techniques in use today are responsible for the discovery of thousands of novel cyclic peptide ligands to important biological targets; however, they still face a few particular limitations. The major obstacles to the success of cyclic peptide drugs are their low bioavailability and cellular penetration. High affinity peptide ligands discovered during *in vitro* screens generally see decreased performance when faced with a lipid bilayer, requiring extensive optimization to improve permeability while maintaining potency and selectivity. Additionally, these screens can yield a large number of false positive hits and select peptides that exhibit low stability within the cellular environment. With the development of PEPTIC technology, we have provided a unique cyclic peptide library generation scheme that allows for simultaneous application in pooled affinity selections and *in vitro* permeability assays. Acquiring data on both target binding and passive permeability on the same set of molecules would provide useful information for lead development in a time and resource efficient manner. Additionally, this fully synthetic technique allows for the incorporation of non-canonical residues. We envision PEPTIC libraries being utilized for the incorporation of more penetration and stability enhancing features at the beginning of the cyclic peptide discovery process. Our tag-free approach to peptide screening also permits library members to interact with targets without the interference of large, appended structures, leading to the reduction of false positive hits. Given these advantages, we believe this technology has the potential to provide a high-quality pipeline of lead cyclic peptide compounds with improved absorption properties.

Given the simplicity of the workflow, we also envision PEPTIC libraries to allow for the expanded implementation of pooled macrocyclic library ligand discovery efforts. While mRNA and phage display are popular technologies, they can require significant monetary investment and be technically difficult to implement for a variety of labs that perform primarily synthetic work. In contrast, PEPTIC libraries can be easily generated without significant expertise in cell and molecular biology techniques and at a cost similar to standard combinatorial syntheses. Institutions with mass spectrometry facilities equipped for proteomics workflows can implement a variety of affinity selection strategies with these libraries.

While it has many advantages, this novel technology is not without limitations. The variable cyclization efficiency of individual peptide sequences is assumed to result in a non-uniform concentration across individual library members. This can lead to some degree of bias in a pooled screen that is not currently predictable. While this issue cannot be fully ameliorated without a fuller understanding of the nuanced influences on cyclization yield, simple concepts employed in library design can be used to minimize variation in cyclization efficiency. The introduction of turn-inducing elements, like proline or N-methylated amides, are known to significantly improve peptide conversion to the CyClick product and can be incorporated in the synthesis of all library members. In addition, the identity of the N-terminal residues has been observed to alter cyclization efficiency of otherwise identical sequences, a feature that can also be controlled by library design. Another limitation is the relatively smaller library sizes that can be screened by AS-MS workflows (~10^6-10^8) compared to genetically encoded techniques (~10^8-10^{13}). Because hit compounds cannot be amplified post-selection and the direct sequencing of hits relies on the ability to generate good quality fragmentation spectra, the size of PEPTIC libraries for screening is limited by the enrichment capabilities of the screening method employed. At higher library size the number of target-binding sequences present in the library grows; to the extent that screening eluate becomes too complex for full sequence coverage of hit peptides. Additionally, at larger library sizes the concentration of each library member is reduced, resulting in a lower absolute amount of material available for sequencing.

4.2 Future Directions

4.2.1 Improving Peptide Limit of Detection

The current limit of the detection for our derivatized linear peptide aldehydes is based on the use of an arginine residue in the derivatization reagent. While the guanidine on arginine provides a high level of ionization efficiency, it is only one of a variety of functional groups that could be used to improve detection and sequencing. We expect the use of a derivatization reagent that contains a permanent positive charge would further lower our limit of detection. Previous studies utilizing pyrylium salts[89] and a substituted guanidinium group[90] demonstrated detection of peptide species at attomolar concentrations. With our current detection and

sequencing limit is at picomolar concentrations, the use of a permanently charged group could improve it by many orders of magnitude. The incorporation of these groups into a new aldehyde reactive derivatization reagent, coupled to nanoLC-MS/MS analysis, could result in access to larger library analysis while maintaining high quality sequencing spectra.

4.2.2 Focused Libraries Targeting the HIV Capsid FG Binding Site

To expand upon our preliminary studies with CyClick peptide ligands to the HIV-1 capsid assembly, ongoing work will utilize the insights from binding and structural studies to design new libraries targeting the FG site. Based on the affinity data collected on cyFG-3 and cyFG-5, the identity of residue adjacent to the N-terminus seems significant for binding interaction. The polar Ser of cyFG-5 significantly reduces binding affinity relative to Leu in this position. Future libraries could substitute various aliphatic, hydrophobic residues like Ile, Val, or Ala or unnatural analogs like *tert*-Leu, norleucine, or 4-pentenylalanine.

Additionally, future work should include optimizing the use of the sensor tip applied in biolayer interferometry measurements as a tool for selecting peptide binders out of pooled mixtures. A previous study by the Pentelute group was able to employ this method with linear peptide libraries and explore the incorporation of a variety of non-natural residues.[65] In this study one of the main limitations was the confidence in sequencing peptide hits from the low enrichment capacity of the BLI sensor tip. We would expect that the generally higher binding affinity of cyclic peptides over linear peptides and improved detection with our derivatization reagent would allow for more peptide identifications compared to their work. This strategy would also benefit from the ability to monitor association and dissociation of peptides in real time. Differing libraries could be directly compared to determine which pools produced higher affinity binding interactions prior to analysis.

4.2.3 Structural Substitutions for Reversable Linkers

While the reversable nature of the CyClick and hydrazone peptide macrocycles is ideal for our library applications, the lability of the cyclization linker is a point of concern for their application directly as therapeutic molecules. Ongoing work should investigate the replacement of these linkages with stable groups that are likely to provide the same conformational effects on peptide structure. Previous studies by the Yudin group have

demonstrated the ability of an oxadiazole-proline motif to induce a beta turn in peptides and increase the number of intramolecular hydrogen bonds.[91] This is similar to the effect of the 4-imidazolidinone moiety in CyClick peptides. Replacement of the N-and C-terminal residues with this motif could be explored as a stable alternative to CyClick peptides. Direct sequence grafting and structural investigations would need to be performed to assess how closely the linker allows for mimicking side chain orientation and backbone rigidity. For hydrazone macrocycles, use of an N-terminal beta-alanine residue that could be cyclized with a C-terminal carboxylic acid would provide an additional atom to the ring backbone similarly to the N-terminal hydrazine residue. Substituted oximes are also known to be much more resistant to hydrolysis and would mimic the double bond structure of the hydrazone macrocycles in our libraries. These modifications would again need to be studied for their conformational effects and the relative stability of the macrocyclic oxime.

Supplementary Information

I. General All commercial materials without further purification. All solvents were reagent or HPLC (Fisher) grade. All reactions were performed under air in glass vials or round bottom flasks. HPLC and MS were used for the analysis of each reaction.

Materials Fmoc-Ala-OH, Fmoc-Arg(Pbf)-OH, Fmoc-Asp(tBu)-OH, Fmoc-Cys(Trt)-OH, (Fmoc-Gln(Trt)-OH, Fmoc-Glu(tBu)-OH, Fmoc-Gly-OH, Fmoc-His(Trt)-OH, Fmoc-Ile-OH, Fmoc-Leu-OH, Fmoc-Lys(Boc)-OH, Fmoc-Phe-OH, Fmoc-Pro-OH, Fmoc-Ser(tBu)-OH, Fmoc-Thr(tBu)-OH, Fmoc-Trp(Boc)-OH, Fmoc-Tyr(tBu)-OH, and Fmoc-Val-OH, Fmoc-aminooxy acetic acid, Rink Amide resin 100-200 mesh (0.59 mmole/g loading), and Merrifield Resin were purchased from Advanced ChemTech (Louisville, KY). Fmoc-Thr-OH was purchased from AAPPtec (Louisville, KY). Fmoc-Ala-CHO was purchased from Combi-Blocks (San Diego, CA). 1-hydroxy-7-azabenzotriazole (HOAt), N,N'-diisopropylcarbodiimide (DIC), and N,N-diisopropylethylamine (DIPEA) were obtained from Chem-Impex (Wood Dale, IL). Ultralink Hydrazide Resin and Anti-HA-Biotin (12ca5) were obtained from Thermo Fisher Scientific. Glacial acetic acid (AcOH), formic acid (FA), N,N-dimethylformamide (DMF), dichloromethane (DCM), methanol (MeOH), acetonitrile (ACN), water (H_2O) were obtained from VWR International (Philadelphia, PA). Lenacapavir (LEN) was purchased from MedChemExpress (Monmouth Junction, NJ) and suspended in ≥99.9% DMSO (Sigma-Aldrich).

II. Instrumentation and Sample Analysis

Analytical HPLC Analysis of peptides was performed on an Agilent 1100 series HPLC equipped with either an Agilent Eclipse Plus C18 column (4.6x100 mm, 5 μm particle size) or an Ascentis Express C18 column (2.1x50 mm, 2.7 μm particle size). All separations were performed utilizing a gradient of 0.1% formic acid in water (solvent A) vs. 0.1% formic acid in acetonitrile (solvent B).

LC/MS High resolution LC/MS was performed on a Dionex 3000 Ultimate UPLC system connected to a ThermoFisherLTQ Orbitrap Velos mass spectrometer with a heated electrospray source. For direct infusion experiments, the solution was infused at a rate of 75 μl min^{-1} and the positive ion spray voltage was set to 3.0 kV. The instrument parameters were as follows: scan range = 200-2000 m/z; capillary temp = 320℃, RF lens = 60%. For LC/MS experiments, samples were run on an Ascentis Express C18 column (2.1x50 mm, 2.7 μm particle size. The standard method for analysis of peptide mixtures was run with a flow rate of 300 μL min^{-1} and ramped from 2% to 60% of solvent B over 45 minutes at ambient room temperature.

nanoLC/MS High resolution nanoLC/MS-MS analysis of affinity selection eluates was performed on a Waters Acquity nanoLC Orbitrap Ascend mass spectrometer. Custom packed fused silica C18 trapping and analytical columns were used for separation of peptide eluate.

Comet Peptide Search Searches of the LC/MS-MS data from affinity selections were conducted using theoretical sequence databases, in the form of FASTA files, generated from the initial design of each library. For both CyClick and Hydrazone libraries, the parameters file selected no enzyme for cleavage and a C-terminal variable modification of +326.1814 was used. For the hydrazone libraries, a fixed N-terminal modification of +29.0266 was used.

timsTOF Peptide Analysis Peptides were resuspended in Buffer A (0.1% formic acid in water) and quantified using the Pierce™ Quantitative Peptide Assay (Thermo Fisher Scientific) following the manufacturer's instructions. 100 ng of peptides, unless stated otherwise, were loaded onto pre-wetted EvoTips (EvoSep) and injected into an Evosep One system (EvoSep) coupled to a timsTOF Pro2 mass spectrometer (Bruker Daltonics). Samples were analyzed using the 20 SPD Zoom predefined gradient with a commercial analytical column (Aurora Elite, IonOpticks).

timsTOF Data analysis MS raw files were analyzed using FragPipe GUI (version 22) with MSFragger (version 4) as the search algorithm[1]. A custom FASTA file was generated, with each synthesized peptide included as a separate entry. Database searches were configured with methionine oxidation and N-terminal acetylation as variable modifications, while GRG with an additional aminooxy acetic acid was set as a fixed modification. No cleavage enzyme was specified, and cysteine carbamidomethylation was disabled. FDR was kept at 1 %. Label-free quantification (LFQ) was enabled, and all downstream analyses were performed in R, using LFQ values for quantitative assessments. Intensities were normalized by median centering and $\log_2$-scaling. Missing values were imputed by Random Forest imputation[2] and downshift sampling, for proteins missing at random or not at random, respectively[3]. All statistical comparisons between the two groups were performed based on two-tailed Student's t-tests.

III. Fmoc-Solid Phase Peptide Synthesis Model peptide H_2N-AVGPFEYA-CHO as well as all peptide libraries were manually synthesized on Rink Amide resin preloaded with Fmoc-Ala-CHO (preloading procedure described below) using standard protocols. Resin was swelled in 50:50 DMF:DCM cosolvent for 1 hour. To facilitate initial Fmoc deprotection, the swelling solution was replaced with 20% piperidine in DMF and the resin was placed on a wrist action shaker for 20 minutes at room temperature. After Fmoc deprotection, the resin was washed with twice with DMF, MeOH, and DCM. Subsequent amino acid couplings were performed using 5 equivalents of Fmoc-protected amino acid, HOAt, and DIC in DMF, shaking for 30 minutes at room temperature. Iterative deprotection and coupling steps were performed until the full sequence was achieved. Fmoc deprotection was reduced to 15 minutes for these subsequent steps.

Procedure for preloading of Rink Resin Fmoc-Gly-OH and Fmoc-Thr-OH (unprotected side chain) were coupled with the general peptide synthesis procedure to swollen Rink resin. Following terminal Fmoc deprotection, the resin was added to a round bottom flask and stirred slowly (60 rpm) while refluxing in a solution of Fmoc-Ala-CHO (5 equivalents) in 1% DIEA v/v in MeOH for 5 h at 60 °C. The resin was transferred to a SPPS tube and washed with MeOH (5 x 3 mL), DMF (5 x 3 mL), DCM (5 x 3 mL), and THF (5 x 3 mL). The resin was then returned to a round bottom flask and stirred slowly for 5 h at 50°C in a solution of di-tert-butyl dicarbonate (Boc_2O, 5 equiv.), N-methyl morpholine (5 equiv.) in THF (final conc. 0.1 M). The resin was again transferred to an SPPS tubed and washed with THF (5 x 3 mL), DCM (5 x 3), and DMF (5 x 3 mL).

Procedure for split-and-pool synthesis After the first deprotection step, the resin was washed as described above and dried on vacuum after the last DCM wash. The dried resin was weighed and split into equivalent portions for amino acid coupling. Coupling for each portion was performed as described above. After coupling and washing, the resin portions were recombined for the deprotection step. This strategy was employed for each variable position in the library design.

Procedure for FITC labeling of peptides After synthesis and purification, CyClick cyclized peptides with a single Lys residue were incubated at a 5mM concentration with 1.5 equivalents of fluorescein isothiocyanate and 5 equivalents of diisopropylethylamine in DMF for 2 hours at room temperature.

Procedure for Peptide Cleavage Peptides were cleaved in a cocktail containing 2.5% triisopropylsilane, 2.5% water, and 95% trifluoroacetic acid and allowed to shake for 1.5 hours. After filtering the solid phase resin, the peptide TFA solution was dried under a stream of air. The crude peptide was then precipitated in cold ether, centrifuged, and the ether decanted three times before the peptide was placed in the dessicator to dry for one hour.

IV. CyClick PEPTIC Workflow

Hydrazide Resin-based Peptide Aldehyde Purification Crude model peptide aldehyde or peptide aldehyde libraries were dissolved in either ACN or ACN:DMF cosolvent containing 2% acetic acid. Hydrazide resin slurry was transferred to a solid phase synthesis tube and storage buffer was filtered off. The resin was then washed 2x with MeOH, 2x with DCM, and allowed to dry over vacuum. The resin was then transferred to either a glass scintillation vial (for heating in an incubator shaker) or a round-bottomed flask with a magnetic stir bar (for heating in an oil bath) and the peptide aldehyde solution was added. For both heating strategies the temperature was set to 60° C. If using the incubator shaker, shaking was set to 250 rpm. If using an oil bath on a heated stir-plate, stirring was set to the lowest setting of 60 rpm. Functional group loading of the Hydrazide Ultralink Resin is not provided by the manufacturer, but good yields were observed when utilizing 2 mL of hydrazide resin slurry for every 100 mg of Rink Resin used in peptide synthesis. The peptide/resin slurry was allowed to shake/stir for 4 hours before being transferred back to the solid phase synthesis tube. The eluate was collected into a 15 mL centrifuge tube and the resin was washed 2x with DMF, MeOH, and DCM. After washing, the resin was dried over vacuum and added to a new reaction vessel. The resin was then incubated with a solution of 50:50 ACN:H_2O with 2% AcOH for another 4 hours and 60°C. After incubation, the resin was again transferred to a solid phase synthesis tube and the eluate collected in a 15 mL centrifuge tube. The eluate was subjected to centrifugation and the supernatant was frozen and lyophilized. If excess peptide was detected in the scavenging eluate, the procedure could be repeated with the same hydrazide resin used in the initial purification.

CyClick Chemistry. CyClick reaction was performed by dissolving the purified linear peptide aldehyde or peptide aldehyde library in 1% DIEA in DMF at a 5mM concentration. The solution was added to a round-bottom flask with a stir bar. The reaction was allowed to proceed for 12-16 hours at 60°C with fast stirring. For peptide libraries, total mmoles were estimated by first dividing the total mass of enriched peptide (m) by the number of theoretical sequences in the library (s) to get an "individual" peptide mass (i). This incorrectly assumes each peptide contributes equally to the total mass but provides a straightforward estimation strategy. The molecular weight of each theoretical sequence is calculated (w_n) and the mmoles determined by dividing the "individual" peptide mass by the molecular weight. The calculated mmoles for all peptides are summed (t) and this is used to estimate concentration.

$$i = \frac{m}{s}$$

$$t = \sum_{n=1}^{s} \frac{i}{w_n}$$

Thr-Gly Resin-based Macrocycle Purification To the CyClick cyclization mixture, 5 equivalents sodium sulfate and 5 equivalents of rink resin functionalized with a TG dipeptide (utilizing a Fmoc-Thr-OH residue) were added. The stirring was slowed to 60 rpm and the solution was incubated at a maintained 60°C for 8 hours. Afterwards, the slurry was transferred to a solid phase synthesis tube and the eluate along with two washes in DMF were collected in a 15 mL centrifuge tube. The final solution was evaporated on speed vacuum concentrator and stored at -80°C until further use.

One-pot Linearization and Derivatization Peptide linearization and derivatization was performed with 2 equivalents (relative to peptide) of the H_2N-O-GGRG tetrapeptide probe in either 50:50 ACN:H_2O with 2% formic acid or PBS buffer at pH 3. The reaction was performed in an incubator shaker at 60°C for 8-10 hours. In the context of the peptide libraries, mmoles were estimated using the same method described above in the CyClick cyclization section.

V. Hydrazone PEPTIC Workflow

Hydrazine Peptide Synthesis The hydrazone libraries were generated on resin pre-loaded with Fmoc-Ala-CHO using standard SPPS protocol described above. After the desired peptide sequences were generated, the N-terminus capped with 10 equivalents of bromoacetic acid and 9.3 equivalents of DIC in DMF. The solution was allowed to shake for one hour before washing 3x with DMF, 3x with DCM, and 3x with DMF. The subsequent displacement reaction is performed with 20 equivalents of methylhydrazine in DMF and allowed to shake for one hour. After displacement, the resin was washed twice with DMF, MeOH, and DCM. Once dried, the peptides were cleaved from the resin as described above

Library Purification The crude hydrazone library was subjected to preparatory HPLC purification using 0.1% formic acid in water as solvent A and 0.1% formic acid in acetonitrile as solvent B. For libraries that readily dissolved in water/acetonitrile cosolvent, a gradient of 2-50% B was utilized. For more hydrophobic libraries, a gradient of 15-70% was used. Fractions were collected in one minute increments and those containing predicted library members were combined.

One-pot Linearization and Derivatization Peptide linearization and derivatization was performed with 2 equivalents (relative to peptide) of the H_2N-O-GGRG tetrapeptide probe in PBS buffer at pH 3. The reaction was allowed to shake for 4 hours and was immediately frozen. In the context of the peptide libraries, mmoles were estimated using the same method described above in the CyClick cyclization section.

VI. Affinity Selections

Magnetic Bead Strategy 100 μL portions of MyOne Streptavidin T1 Dynabeads (10 mg/mL; 1 mg; 0.13 nmol IgG binding capacity) were transferred to 1.7 mL plastic centrifuge tubes, and placed in a magnetic separation rack (New England Biolabs, cat# S1506S). The beads were washed

three times with blocking buffer (1 mg/mL BSA, 0.02% Tween 20, 1M PBS), and subsequently incubated with Anti-HA-Biotin. The tubes were transferred to a rocking shaker for 1 hour at 4 °C. Afterwards, the beads were returned to the separating rack and the
supernatant was removed. The beads were washed again with blocking buffer and incubated with 1 mL of peptide library (~200 pM per member concentration) or positive control antigen sequence (200 pM) in blocking buffer with 2.5% DMF for 1 hour at 4 °C on a rocking shaker. After incubation the tubes were again transferred to a magnetic separation rack, the supernatant removed, and the beads washed 3x with 1M PBS. Beads were then washed 2x with 150 uL of 200 mM PBS with 6M guanidinium hydrocholoride. All 300 uL were kept and subjected to peptide linearization and derivatization conditions.

Size Exclusion Strategy 24 mg of the peptide library was dissolved in 5 mL of 5% DMSO in PBS at pH 7.5 to achieve a ~400 nM per library member concentration. 0.13 nmol of 12ca5 was dissolved in 100 µL of PBS pH 7.4 and added to the peptide library and incubated at room temperature for 30 mins. Size Exclusion Chromatography was done with the incubate mixture using a flow rate of 1 mL/min with a 3µm Agilent SEC Column with dimension 7.8 x 150mm. 100 µL of the peptide library with the target protein was injected into the HPLC with an isocratic mobile phase using PBS Buffer pH 7.5. The HPLC run was for 15min. The target protein-binder complexes eluted at 4.155 min. The affinity selection experiment was monitored by UV (214 nm). After the run, the size exclusion column was cleaned with deionized water.

VII. Microscale Thermophoresis

All microscale thermophoresis experiments were performed on a Nanotemper Monolith NT.115 Pico. Each sample was prepared in Nanotemper Monolith Premium Capillaries and measurements of fluorescence intensity were performed using the BLUE filter set at a set temperature of 25°C . Peptides were dissolved in DMSO and diluted in analysis buffer (1M PBS with 0.1% pluronic F-127) to 80 nM concentrations. The anti-HA antibody was dissolved in the same analysis buffer to a 6 ųm concentration. Peptide only traces were prepared by mixing 25 ųL of diluted peptide solution with 25 ųL of analysis buffer. Peptide/antibody traces were prepared by mixing 25 ųL of diluted peptide solution with 25 ųL of antibody solution. Laser power was set using the instrument's auto-detect feature.

VIII. Peptide Stability Experiments

Peptide stability studies were conducted using the macrocyclized sequence AVGAFEYA. For each condition, 100ug (0.000126 mmole) of peptide was incubated in either affinity selection conditions, MST conditions, or affinity selection conditions in the presence of a nucleophilic small molecule. Nucleophiles studied included Lys, Cys, glutathione, and O-benzyl hydroxylamine. Ten equivalents of each nucleophile was used relative to the cyclic peptide and four equivalents of TCEP was used relative to the thiol in the case of Cys and glutathione. The mixtures were analyzed at the start of the incubation, 1 hour, and 3 hour time points.

IX. HIV Capsid Experimental Procedures

Expression and Purification of HIV-1 Capsid (CA) HIV-1 capsid protein monomers (CA) was cloned in a pET11a expression plasmid, provided by Dr. Chun Tang (Peking University). *E. coli* BL21(DE3)RIL was used for protein expression and CA was purified by ammonium sulfate precipitation followed by anion exchange chromatography as previously described.[5]

Cross-linked CA hexamers, containing A14C/E45C/W184A/M185A mutations for disulfide stabilization, (CA121 or CA_{HEX}) were cloned in a pET11a expression plasmid, provided by Dr. Owen Pornillos (University of Virginia).[11] Subsequently, a 6xHIS tag was added to the C-terminal end of CA_{HEX} to create the $CA_{HEX:6HIS}$ construct in pET11a vector (Genscript). *E. coli* BL21(DE3)RIL was used for protein expression, and both CA_{HEX} and $CA_{HEX:6HIS}$ were purified as previously described,[11] with additional size-exclusion chromatography step for added protein purity to remove non-crosslinked CA using HiLoad™ 26/600 Superdex 200 pg in storage buffer (20 mM Tris pH 8.2 and 40 mM NaCl).

CA Assembly Assay

The CA assembly assay was modified from a previously described method.[12] Briefly, a 2X solution was made of 100 μM of CA monomer, diluted from frozen aliquots in 50 mM Tris (pH 8.0), and treated with equimolar (100 μM) of LEN, cyFG-3, or a DMSO vehicle control (0.4 %) for approximately 30 minutes on ice. These 2X Solutions were dispensed into a 96-well plate and mixed 1:1 with 2 M NaCl in 50 mM Tris (pH 8.0) to initiate assembly. Absorbance at 350 nm (A_{350}) was measured every 25 seconds for 60 minutes at room temperature with a Synergy Neo 2 (BioTek) plate reader. Samples containing the 1X solution of CA, compound and 2 M NaCl were background subtracted from a blank well that lacked NaCl. In the LEN-treated background, we note CA assembly occurs in the absence of NaCl (A_{350} = 0.480 ± 0.091; time = 60 minutes), thus leading to an apparent lower A_{350} reading of the sample compared to the DMSO and cyFG-3, once the available CA multimerizes in the NaCl-treated condition (Raw Data: A_{350} = 0.741 ± 0.042; Subtracted Data: A_{350} = 0.261 ± 0.116; time = 60 minutes). The data are transformed by background subtraction, and the rate of A_{350} increase remains higher in LEN than the DMSO-treated control initially, however, soon after NaCl is added, CA polymerization rapidly completes, and the LEN-treated samples plateau (Figure 6G).

Biolayer Interferometry (BLI)

The BLI protocol was modified from the default parameters in the Octet® BLI Discovery program (version 13.0.0.17, Sartorius). LEN conditions adapted from reported Surface Plasmon Resonance experiments for a biotinylated CA_{HEX}.[1] Frozen aliquots of $CA_{HEX:6HIS}$ were diluted to 100 μg/mL in BLI buffer [20 mM Tris (pH 8.2) with 40 mM NaCl, 20 mM imidazole, 1% Bovine Serum Albumin (BSA), 600 mM sucrose; modified from Dubrow et al. (2022)[14]. Anti-penta-HIS (HIS1K) Dip and Read™ Biosensors (FortéBio #18-5120) were first hydrated in 200 μL of buffer for 10-30 minutes before sample loading. All experiments were performed in 96-well microplates (Greiner, 655209), agitated at 1000 rpm, at 25 °C, and at a volume of 200 μL per well.

Experiments were initiated with a 120 second baseline step, followed by loading of CA_{HEX} at 100 μg/mL in BLI buffer for 600 seconds. The CA_{HEX}-loaded probe was washed twice in BLI buffer for 60 seconds. For the LEN experiments, the protein-loaded probes were dipped into a 200 μL solution of BLI buffer containing 7.5, 5.0, or 2.5 μM LEN for 200 seconds of association time, then 1,000 seconds of dissociation time in a BLI buffer. For the cyFG-3 experiments, the protein-loaded probes were prepared as described above; the concentrations of cyFG-3 tested were 100, 75, or 50 μM with an association time of 50 seconds and a dissociation time of 100 seconds. The Octet Analysis Studio (version 13.0.0.32, Sartorius) was used to perform double background subtraction for both LEN and cyFG-3. The first subtraction is the protein-loaded biosensor from the parallel, protein-absent biosensor. The second data transformation is done by subtracting an acquired measurement of protein and an equivalent volume of DMSO. Then, data were corrected using the "Average of Baseline Step"

from time = 115.0–119.8 and "Baseline Inter-step Correct" at time = 0. Association and Dissociation were fit with a continuous 1:1 protein:ligand binding model. The resulting K_D, k_{on}, and k_{off} values were determined in triplicate for each concentration of drug (except 50 μM cyFG-3, which was performed in duplicate), and these were reported as an average and error of globally fit values.

Thermal Shift Assay (TSA)

Prior to TSA, 20 μM $CA121_{HEX}$ was incubated with 0.08 mg/mL of the library of cyclic peptides (≤1% DMSO) in 50 mM Tris (pH 8.0). Samples were then mixed with 1X SYPRO™ Orange dye in a qPCR plate and samples were heated from 25–95°C QuantStudio 3 Real-Time PCR Systems (Thermo Fisher Scientific) as previously described.[15] Thermal profiles were analyzed with Protein Thermal Shift Software v1.3 (Applied Biosystems) and visualized with TSAR.[16] Statistical significance was determined by comparing the treated condition to the DMSO vehicle with a two-sided unpaired t-test.

X. Supplementary Tables and Figures

Supplementary Table 1. Optimization table for a model linear peptide H_2N-AVGPFEYA-CHO capture with aldehyde scavenging resins.

Functionalized Resin	Conditions	Temp. (°C)	Time (hours)	% Capture
Hydrazide	2% AcOH in DMF	RT	4	20%
Hydrazide	2% AcOH in DMF	60	4	83%
Hydrazide	2% AcOH in ACN	60	4	100%
Sulfonyl Hydrazine	2% FA in ACN	60	4	0%
Rink-GT	1% DIEA in DMF	60	4	55%
Rink-GC	1% DIEA in DMF	60	4	28%
Merrifield-GT	1% DIEA in MeOH	60	4	3%
Merrifield-GC	1% DIEA in MeOH	60	4	0%
Merrifield-GT	1% DIEA in DMF	60	16	13%
Merrifield-GC	1% DIEA in DMF	60	16	65%

Supplementary Table 2. Optimization table for a model cyclic peptide H_2N-AVGPFEYA-CHO purification with aldehyde scavenging resins.

Functionalized Resin	**Conditions**	**Temp. (°C)**	**Time (hours)**	**Purity of CyClick Peptide**
Hydrazide	2% AcOH in ACN	60	4	Blank Chromatogram
Hydrazide	2% AcOH in ACN	RT	4	Mixed Results
Hydrazide	2% AcOH in ACN	0	4	65%
Rink-GT	1% DIEA in DMF, Na_2SO_4	60	Overnight	100%
Rink-GT	1% DIEA in DMF, Na_2SO_4	60	4	100%

Supplementary Figure 1. Model peptide N_2H-AVGPFEYA-CHO cyclization scheme and stacked chromatograms (DAD) of cyclization mixture and TG resin purification analysis

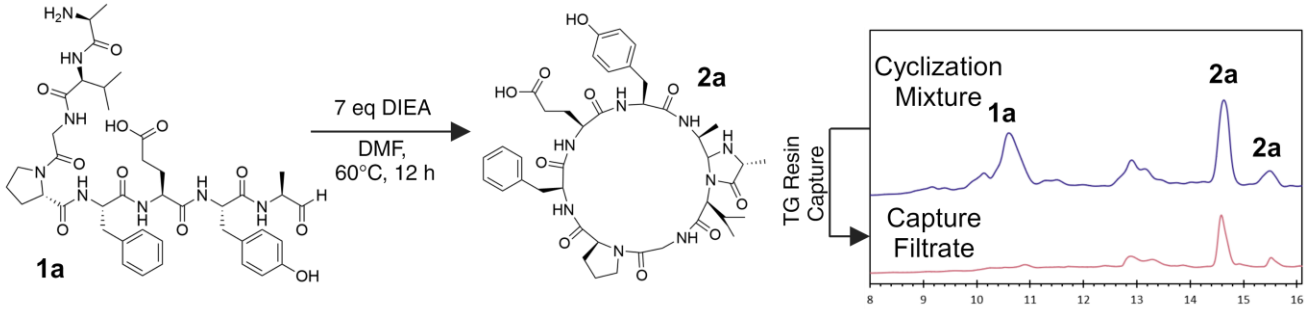

Supplementary Figure 2. Extracted ion chromatograms from LC/MS analysis of linear (blue) and CyClick (pink) peptide small-scale library mixtures after cyclization (left column) and after two round of TG resin scavenging (right column). The percent linear peptide is calculated as the percentage of total ion intensities of both the linear and CyClick species.

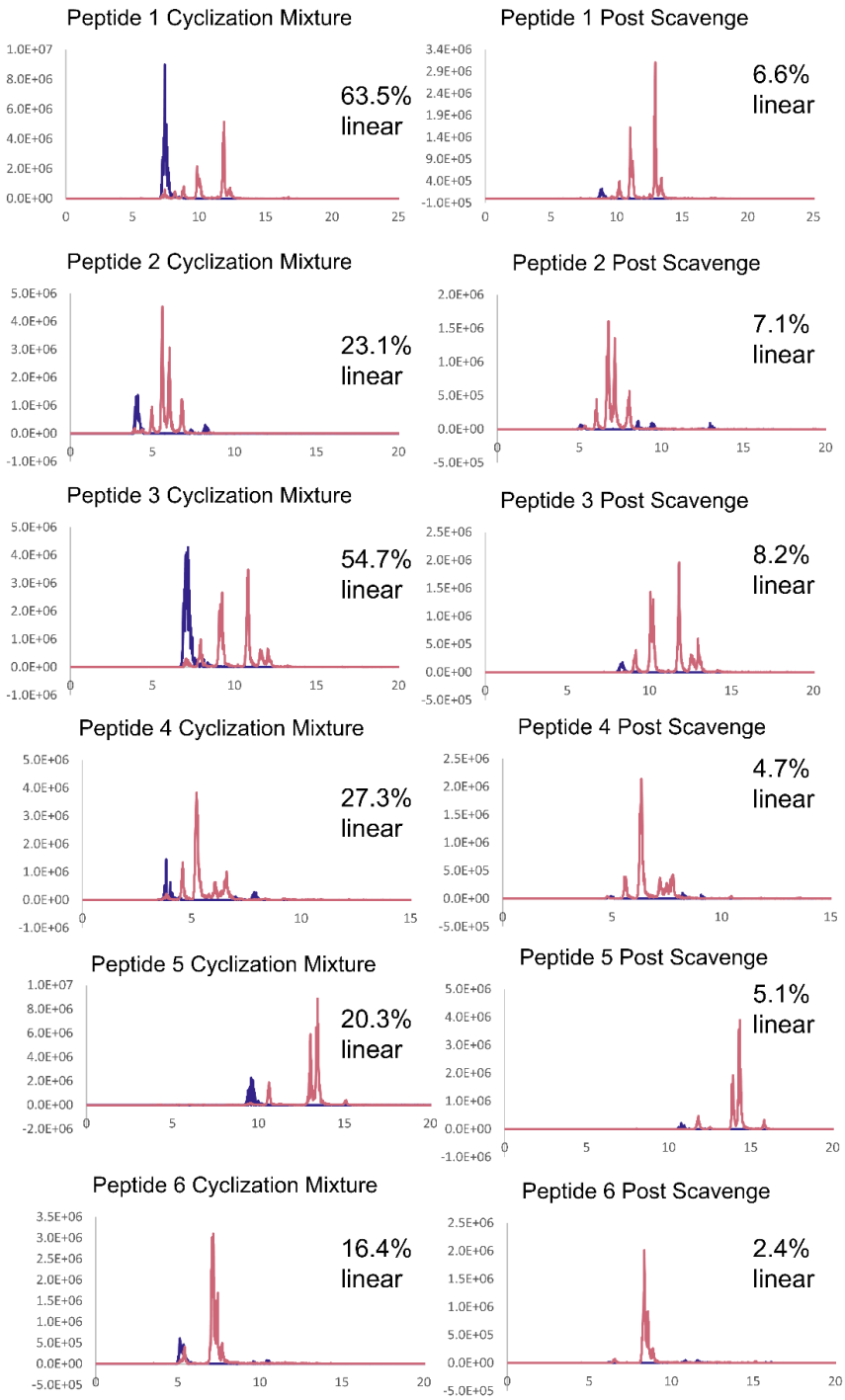

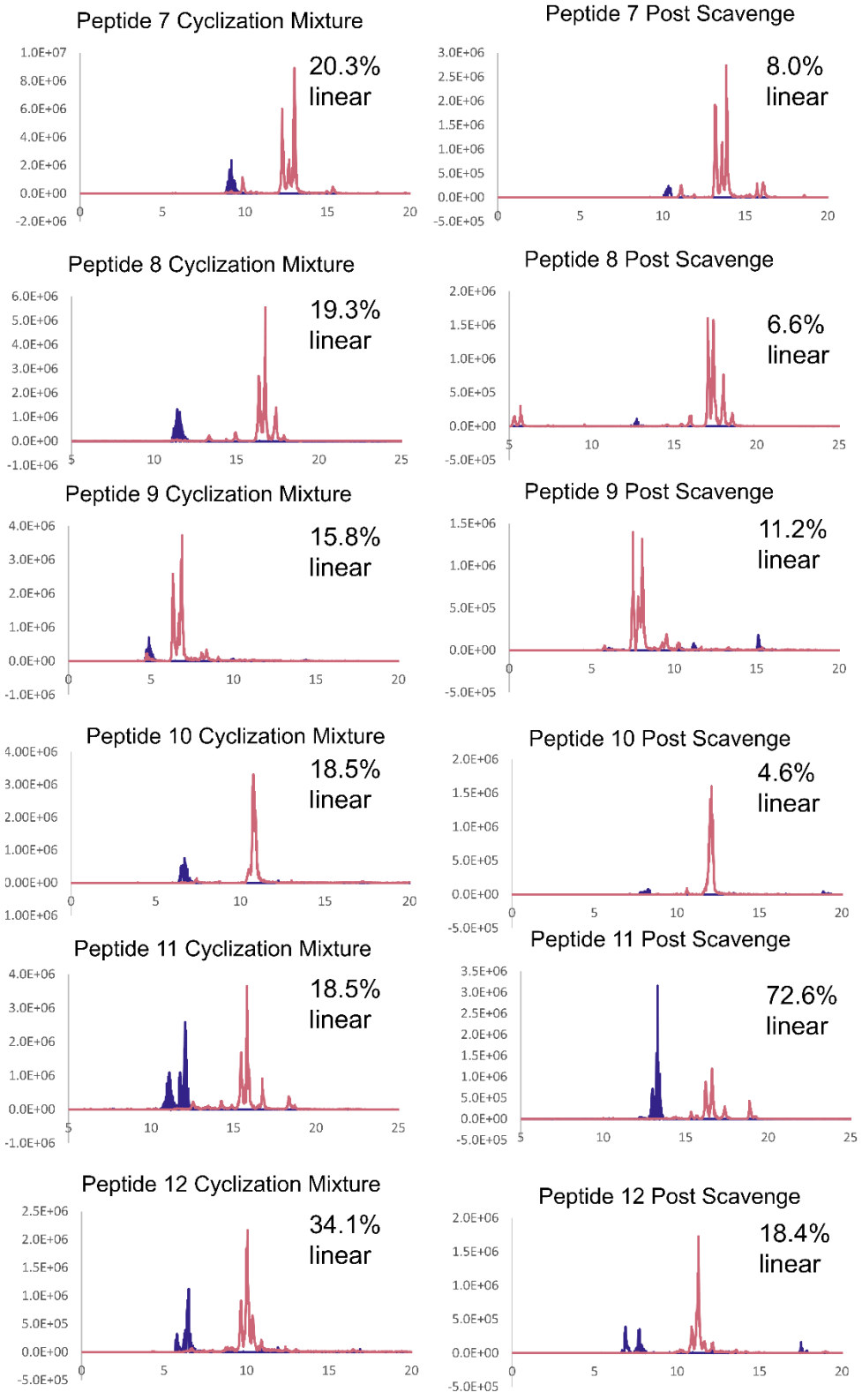
Peptide 7 Cyclization Mixture
20.3%
linear
Peptide 7 Post Scavenge
8.0%
linear
Peptide 8 Cyclization Mixture
19.3%
linear
Peptide 8 Post Scavenge
6.6%
linear
Peptide 9 Cyclization Mixture
15.8%
linear
Peptide 9 Post Scavenge
11.2%
linear
Peptide 10 Cyclization Mixture
18.5%
linear
Peptide 10 Post Scavenge
4.6%
linear
Peptide 11 Cyclization Mixture
18.5%
linear
Peptide 11 Post Scavenge
72.6%
linear
Peptide 12 Cyclization Mixture
34.1%
linear
Peptide 12 Post Scavenge
18.4%
linear

Peptide 13 Cyclization Mixture

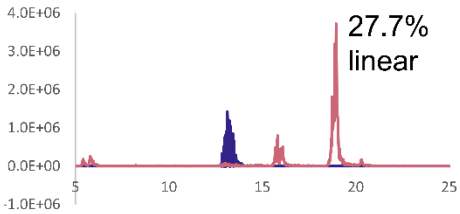

Peptide 13 Post Scavenge

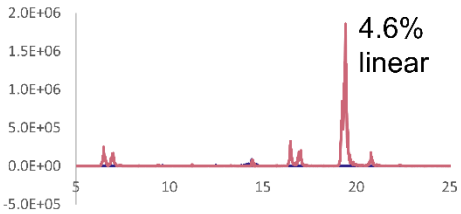

Peptide 14 Cyclization Mixture

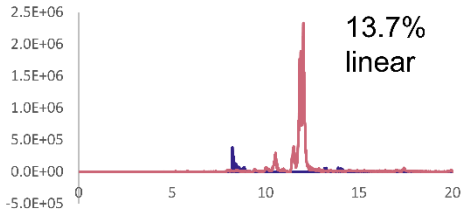

Peptide 14 Post Scavenge

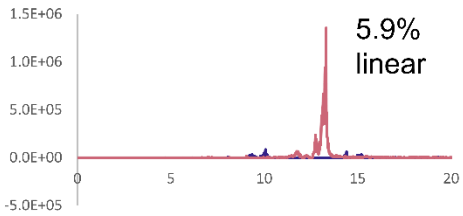

Peptide 15 Cyclization Mixture

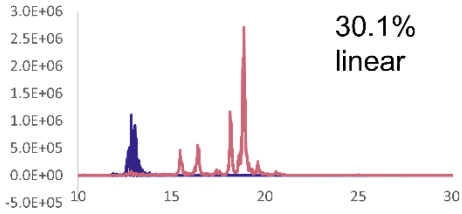

Peptide 15 Post Scavenge

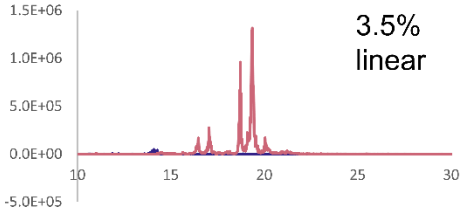

Peptide 16 Cyclization Mixture

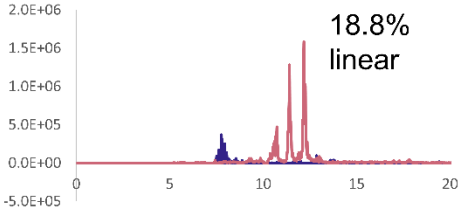

Peptide 16 Post Scavenge

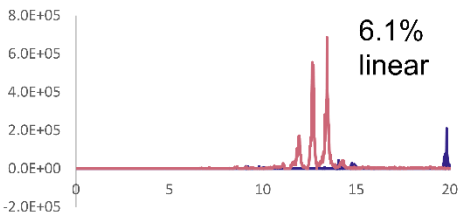

Supplementary Figure 3. Stacked chromatograms (DAD) for time point analysis of model CyClick peptide **2a** linearization.

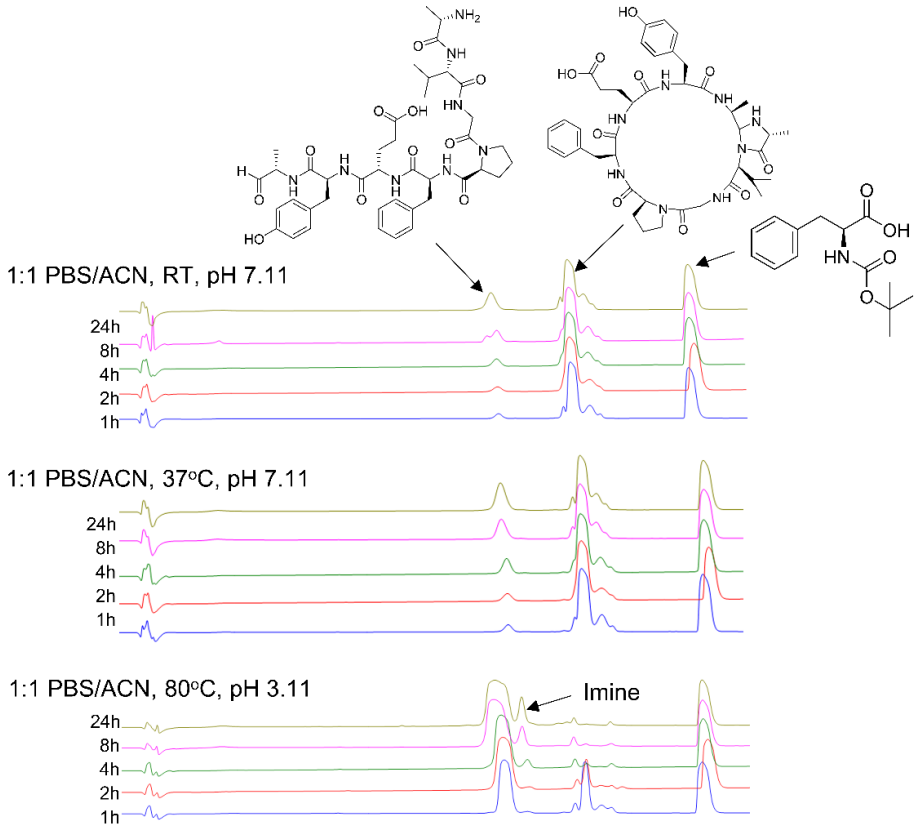

Supplementary Figure 4. Limit of detection experiments with derivatized model peptide **3a**. MS2 spectra of highest and lowest sample loading for model peptide.

B ions	Y ions
72.04444	1179.59
171.1129	1108.553
228.1343	1009.485
325.1871	952.4635
472.2555	855.4107
601.2981	708.3423
764.3614	579.2997
1161.58	416.2364

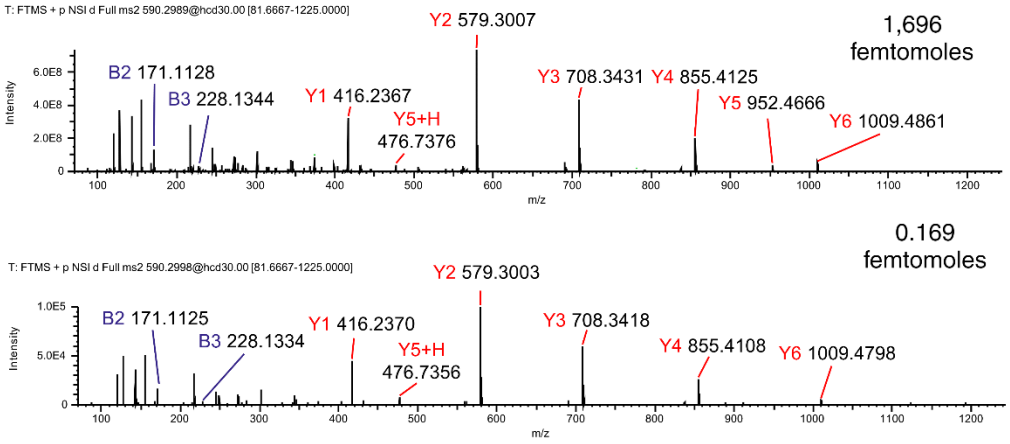

Supplementary Figure 5. MS2 spectra of the CyClick peptide small-scale library after linearization and derivatization with mass ionization tag.

B ions	Y ions
58.0287	1268.6705
129.0659	1211.6491
230.1135	1140.612
329.1819	1039.5643
400.219	940.4958
515.2460	869.4587
612.2988	754.4318
669.3202	657.3790
782.4043	600.3575
853.4414	487.2735
1250.6599	416.2364

L1

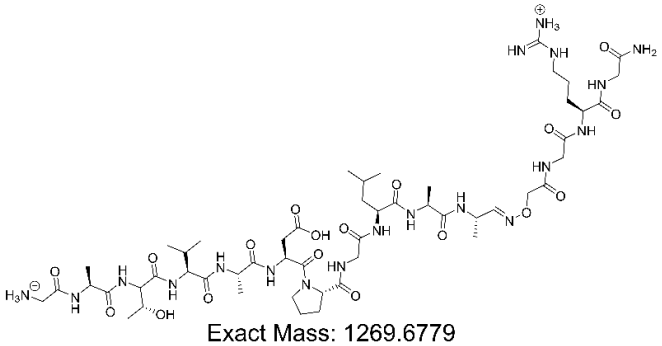

Exact Mass: 1269.6779
m/z: 634.8389

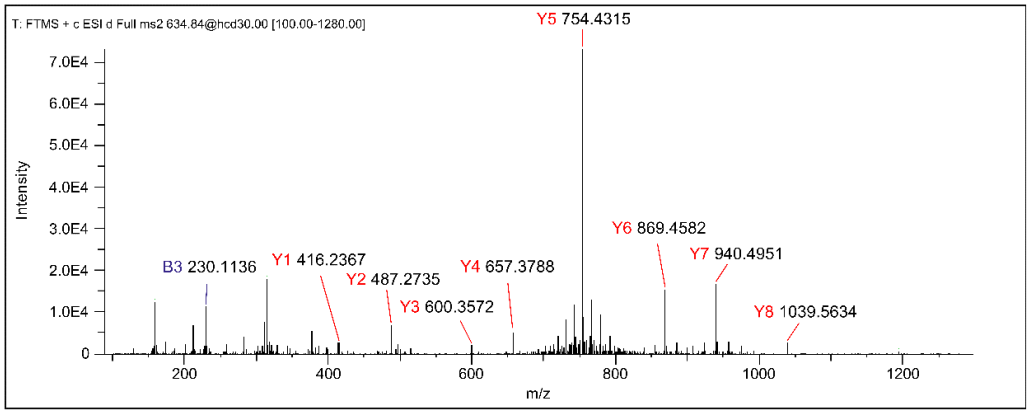

B ions	Y ions
58.0287	1283.6814
129.0659	1226.6599
230.1135	1155.6228
329.1819	1054.5751
400.2191	955.5067
515.2460	884.4696
612.2988	769.4427
669.3202	672.3899
797.4152	615.3684
868.4523	487.2735
1265.6708	416.2364

L2

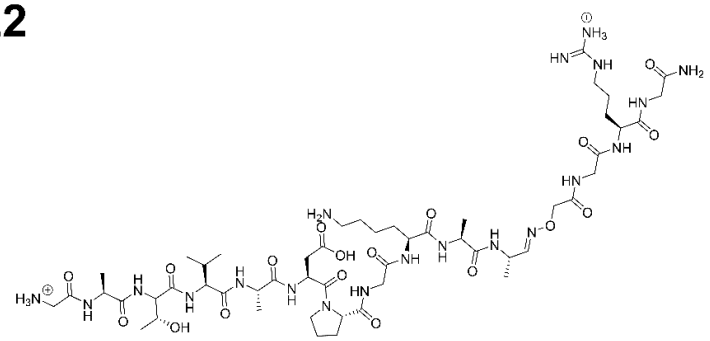

Exact Mass: 1284.6887
m/z: 642.3444

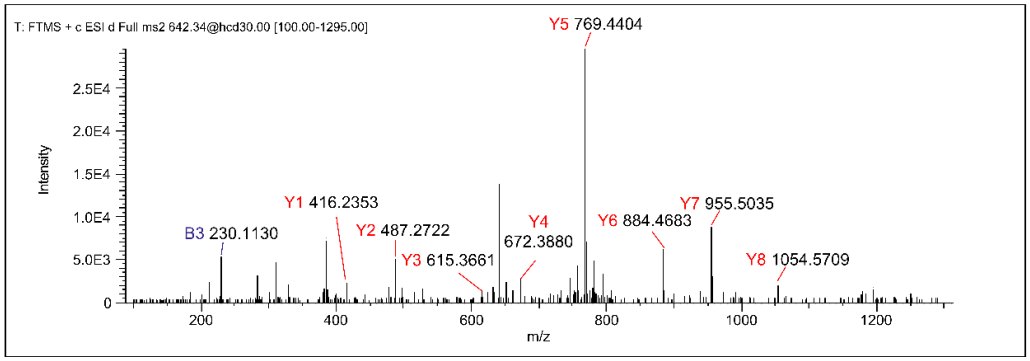

B ions	Y ions
58.0287	1284.6654
129.0659	1227.6439
230.1135	1156.6068
329.1819	1055.5591
416.2140	956.4907
531.2409	869.4587
628.2937	754.4318
685.3151	657.3790
798.3992	600.3575
869.4363	487.27351
1266.6548	416.2364

L3

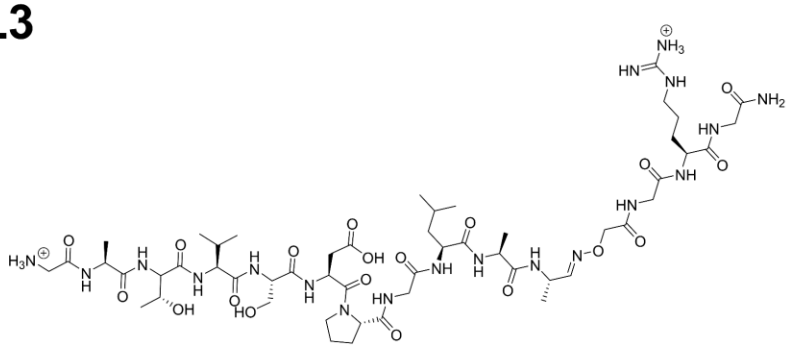

Exact Mass: 1285.6728
m/z: 642.8364

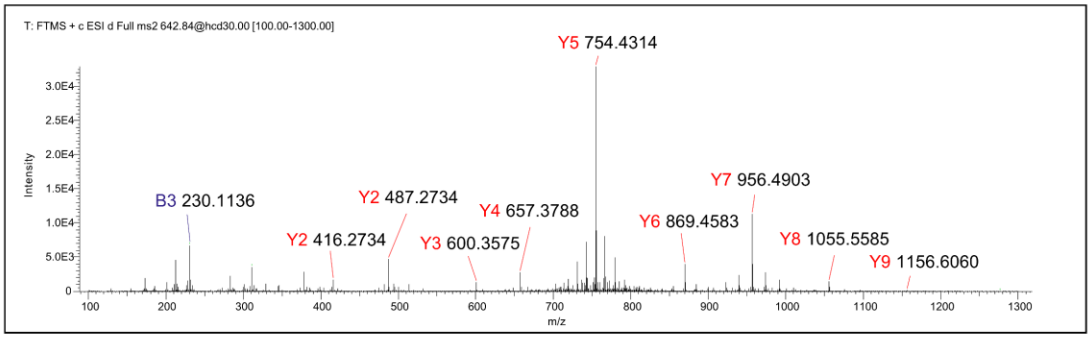

B ions	Y ions
58.02879	1299.676
129.0659	1242.655
230.1136	1171.618
329.182	1070.57
416.214	971.5017
531.241	884.4697
628.2937	769.4427
685.3152	672.3899
813.4102	615.3685
884.4473	487.2735
1281.666	416.2364

L4

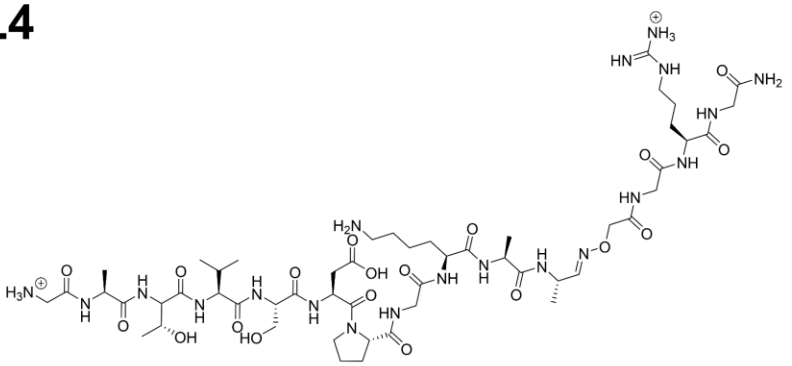

Exact Mass: 1300.6837
m/z: 650.3419

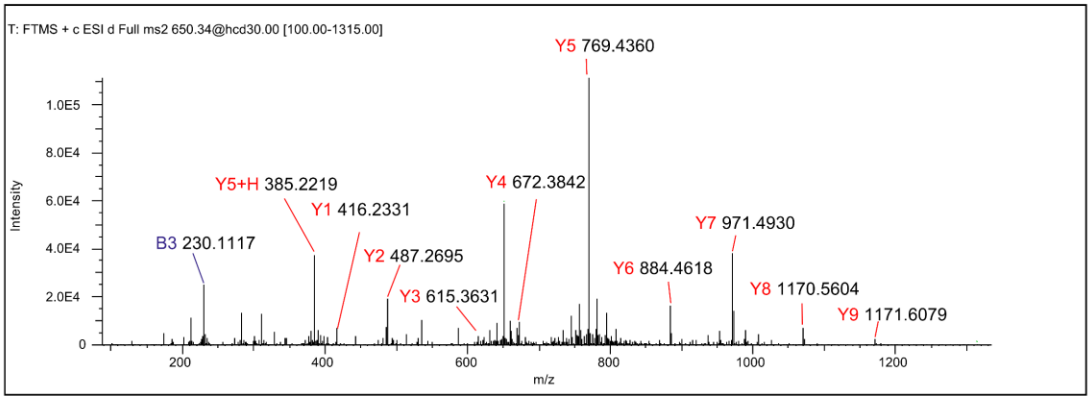

B ions	Y ions
58.02879	1334.681
129.0659	1277.66
230.1136	1206.623
329.182	1105.575
400.2191	1006.506
515.2461	935.4693
678.3094	820.4424
735.3308	657.379
848.4149	600.3576
919.452	487.2735
1316.671	416.2364

L5

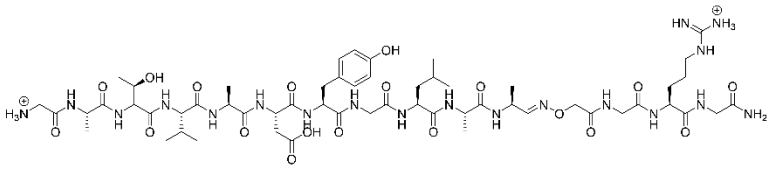

Exact Mass: 1335.6884
m/z: 667.8442

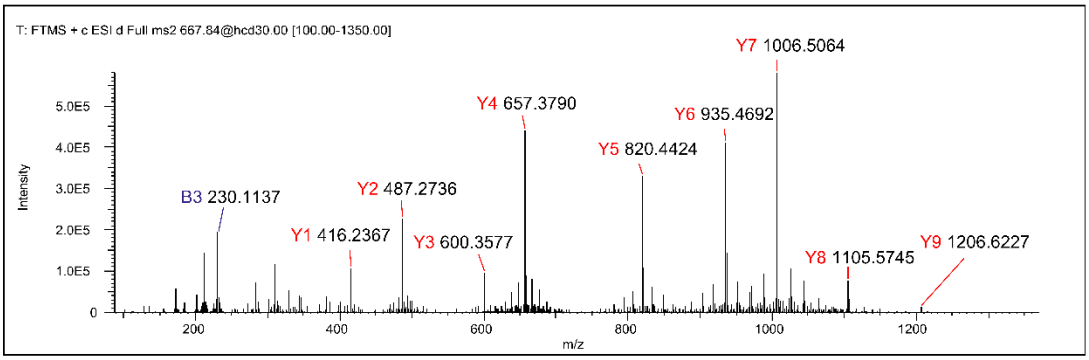

B ions	Y ions
58.0287	1349.6919
129.0659	1292.6705
230.1135	1221.6334
329.1819	1120.5857
400.2191	1021.5173
515.2460	950.4802
678.3093	835.4532
735.3308	672.3899
863.4258	615.3684
934.4629	487.2735
1331.6814	416.2364

L6

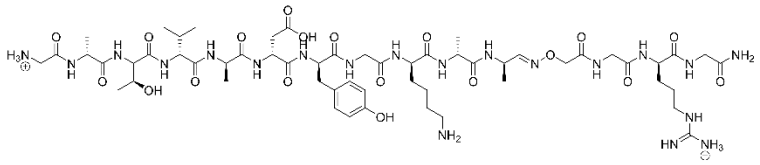

Exact Mass: 1350.6993
m/z: 675.3497

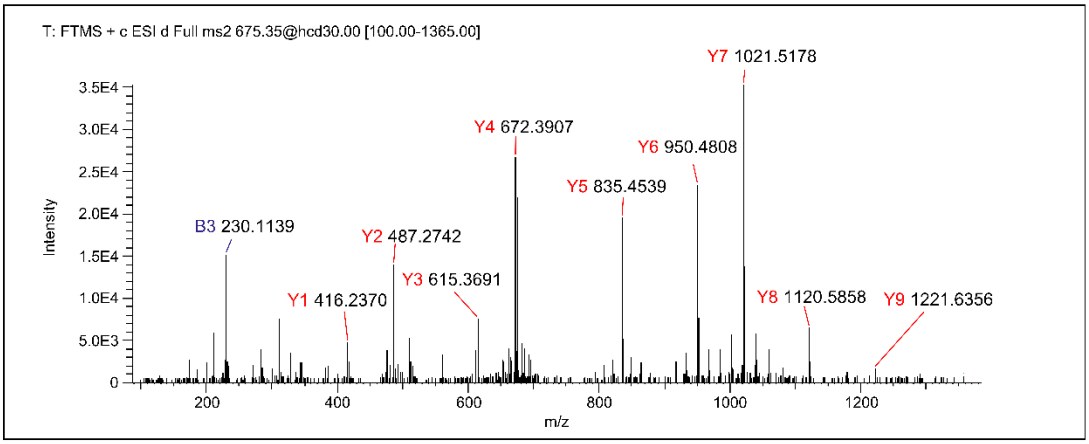

B ions	Y ions
58.02879	1350.67601
129.0659	1293.65455
230.11358	1222.61743
329.18199	1121.56975
416.21402	1022.50134
531.24096	935.46931
694.30429	820.44237
751.32575	657.37904
864.40982	600.35758
935.44693	487.27351
1332.66544	416.2364

L7

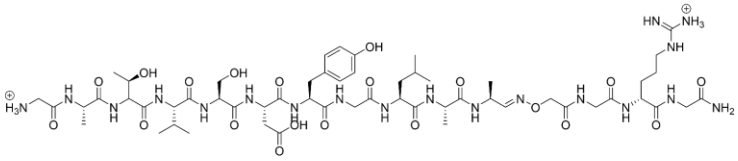

Exact Mass: 1351.6833
m/z: 675.8417

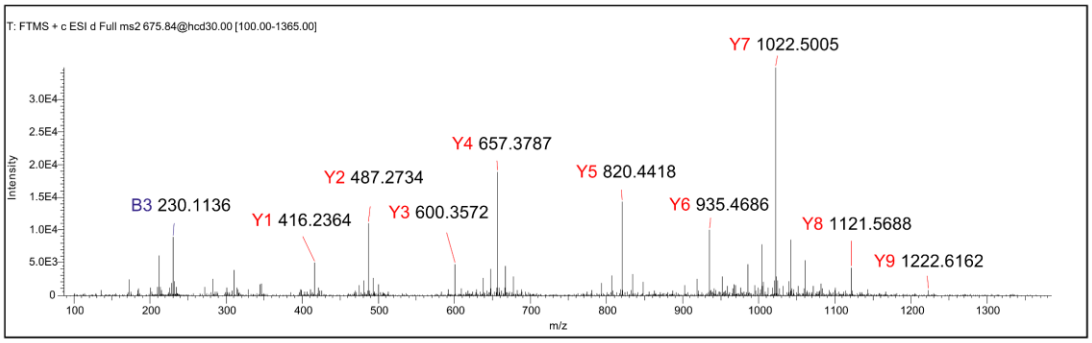

B ions	Y ions
58.0287	1353.7021
129.0659	1296.6807
315.1452	1225.6435
414.2136	1039.5642
485.2507	940.49586
600.2776	869.4587
697.3304	754.431
754.3519	657.3790
867.4359	600.3575
938.4730	487.2735
1335.6916	416.2364

L8

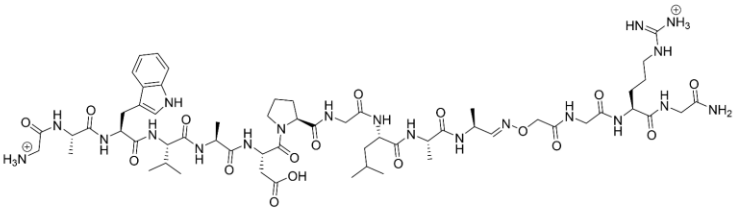

Exact Mass: 1354.7095
m/z: 677.3548

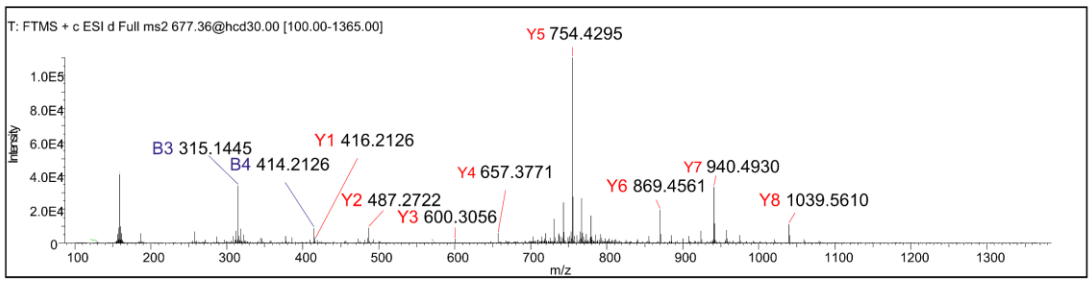

B ions	Y ions
58.0287	1365.6869
129.0659	1308.6654
230.1135	1237.6283
329.1819	1136.5806
416.2140	1037.5122
531.2409	950.4802
694.3042	835.4532
751.3257	672.3899
879.4207	615.3684
950.4578	487.2735
1347.6763	416.2364

L9

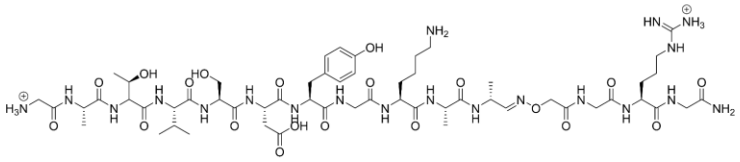

Exact Mass: 1366.6942
m/z: 683.3471

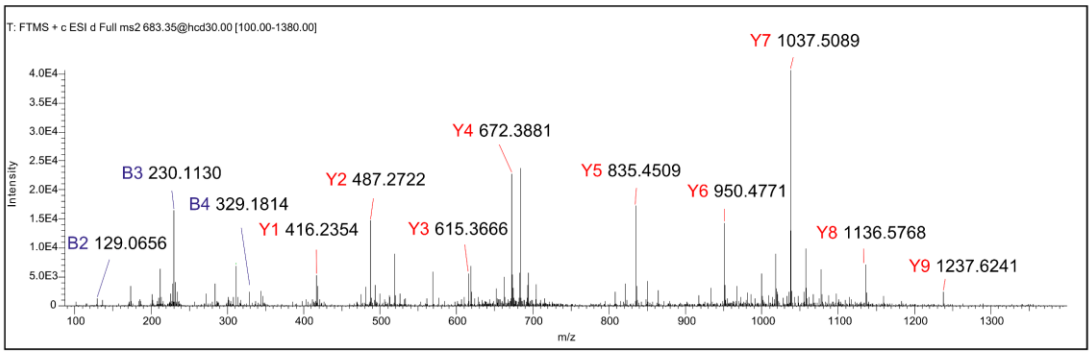

B ions	Y ions
58.0287	1368.7130
129.0659	1311.6916
315.1452	1240.6544
414.2136	1054.5751
485.2507	955.5067
600.2776	884.4696
697.3304	769.4427
754.3519	672.3899
882.4468	615.3684
953.4839	487.2735
1350.7025	416.2364

L10

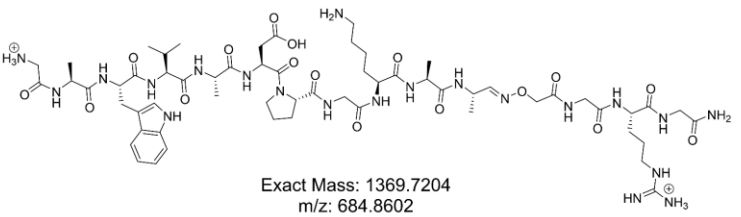

Exact Mass: 1369.7204
m/z: 684.8602

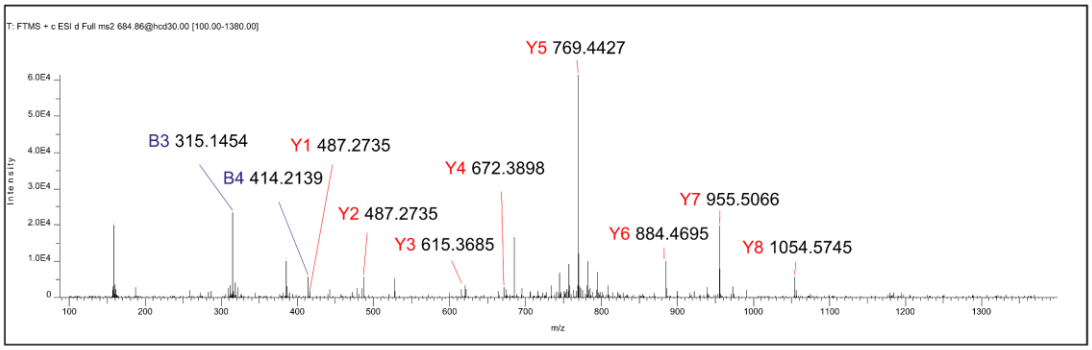

B ions	Y ions
58.0287	1369.6970
129.0659	1312.6756
315.1452	1241.6385
414.2136	1055.5591
501.2456	956.4907
616.2726	869.4587
713.3253	754.4318
770.3468	657.3790
883.4308	600.3575
954.468	487.2735
1351.6865	416.2364

L11

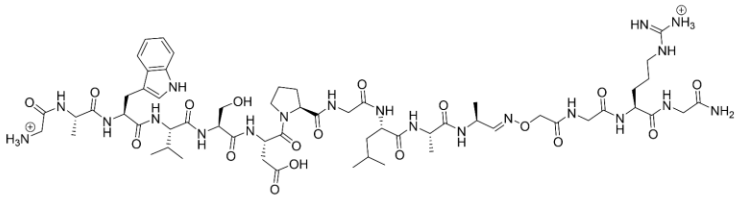

Exact Mass: 1370.7044
m/z: 685.3522

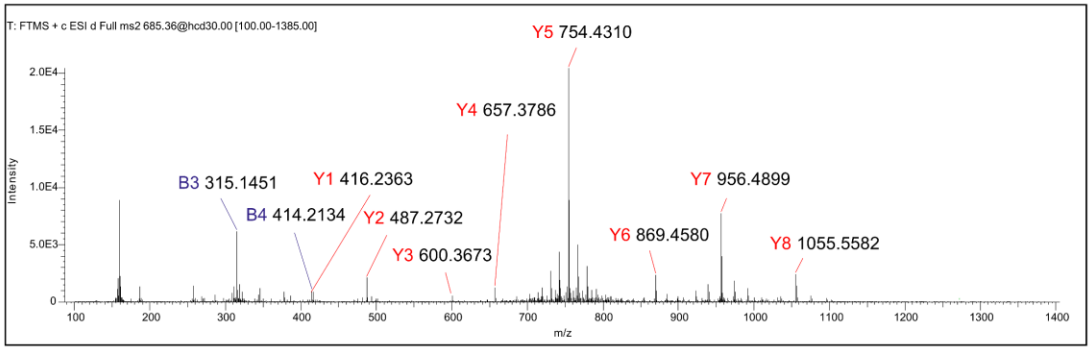

B ions	Y ions
58.0287	1384.7079
129.0659	1327.6865
315.1452	1256.6494
414.2136	1070.5700
501.2456	971.5016
616.2726	884.4696
713.3253	769.4427
770.3468	672.3899
898.4417	615.3684
969.4789	487.2735
1366.6974	416.2364

L12

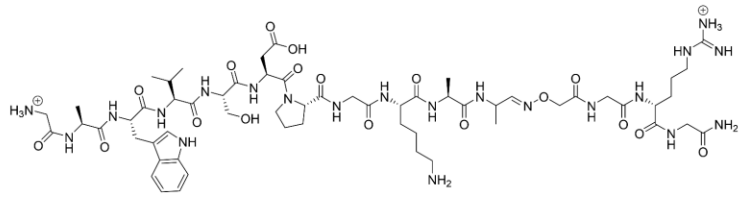

Exact Mass: 1385.7153
m/z: 692.8577

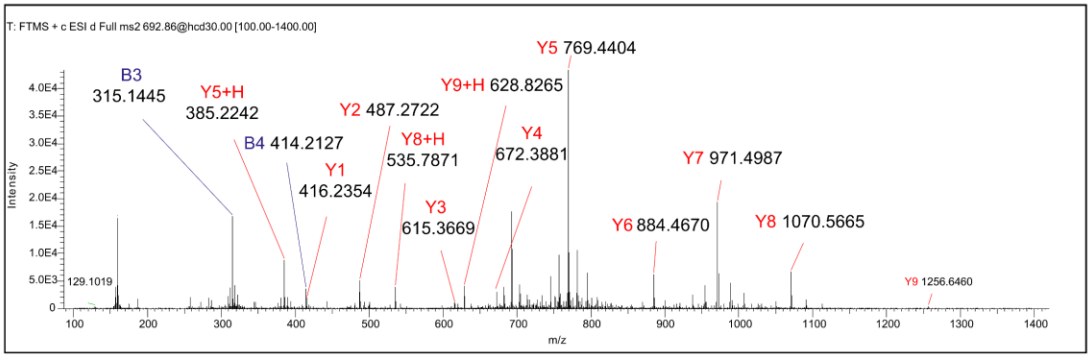

B ions	Y ions
58.0287	1419.7127
129.0659	1362.6912
315.1452	1291.6541
414.2136	1105.5748
485.2507	1006.5064
600.2776	935.4693
763.3410	820.4423
820.3624	657.3790
933.4465	600.3575
1004.4836	487.2735
1401.7021	416.2364

L13

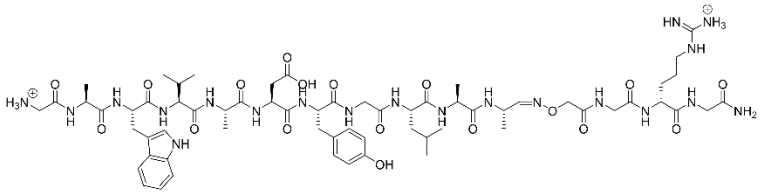

Exact Mass: 1420.7200
m/z: 710.3600

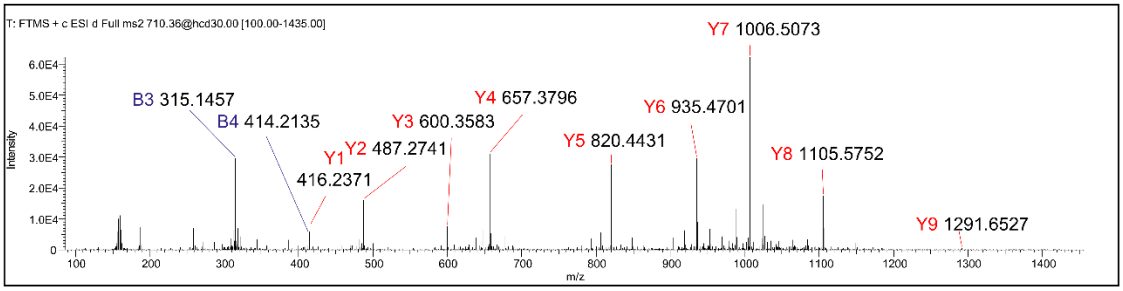

B ions	Y ions
58.02879	1434.7236
129.0659	1377.7021
315.1452	1306.6650
414.2136	1120.5857
485.2507	1021.5173
600.2776	950.4802
763.3410	835.4532
820.3624	672.3899
948.4574	615.3684
1019.4945	487.2735
1416.7130	416.2364

L14

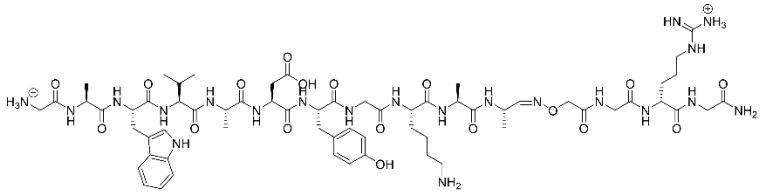

Exact Mass: 1435.7309
m/z: 717.8655

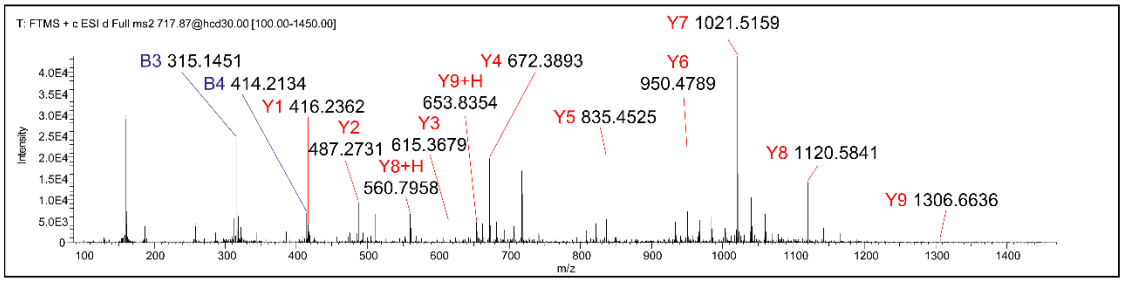

B ions	Y ions
58.0287	1435.7076
129.0659	1378.6861
315.1452	1307.6490
414.2136	1121.5697
501.2456	1022.5013
616.2726	935.4693
779.3359	820.4423
836.3573	657.3790
949.4414	600.3575
1020.4785	487.2735
1417.6970	416.2364

L15

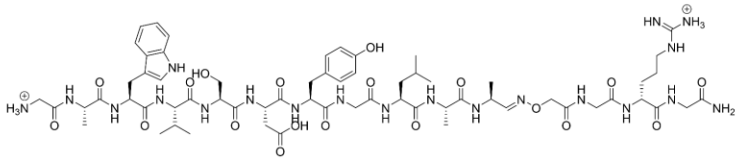

Exact Mass: 1436.7150
m/z: 718.3575

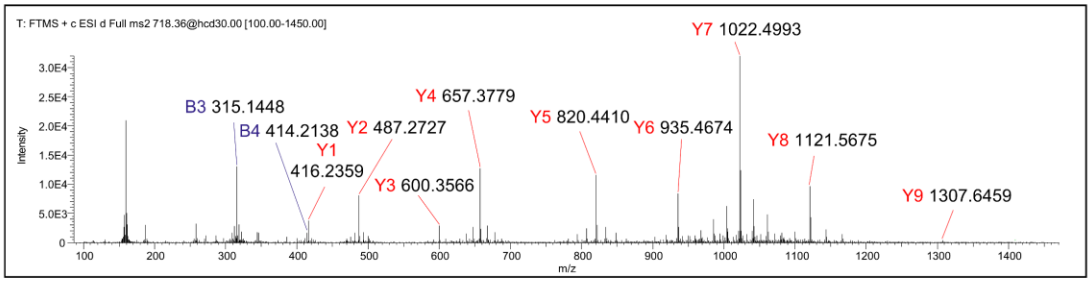

B ions	Y ions
58.0287	1450.7185
129.0659	1393.6970
315.1452	1322.6599
414.2136	1136.5806
501.2456	1037.5122
616.2726	950.4802
779.3359	835.4532
836.3573	672.3899
964.4523	615.3684
1035.4894	487.2735
1432.7079	416.2364

L16

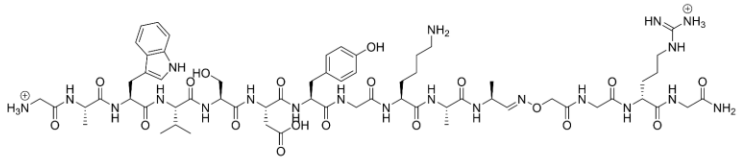

Exact Mass: 1451.7259
m/z: 725.8630

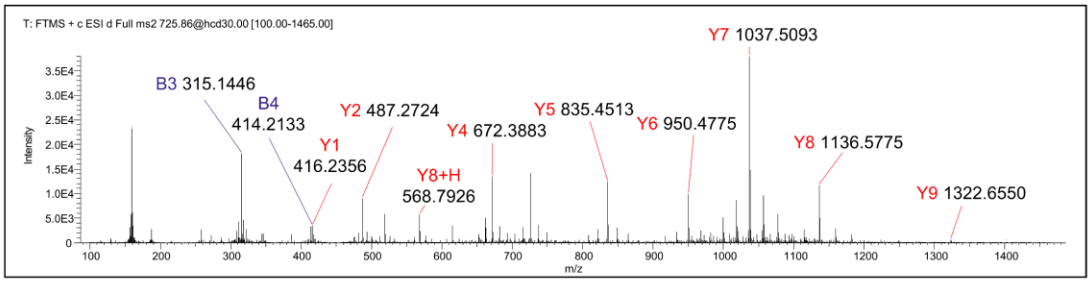

Supplementary Table 3. Database matched sequences from Comet search of size exclusion chromatography-based affinity selection with 12ca5.

Expect	Number of ions	Sequences	Mass Error (ppm)
0.0389	14/20	GDAGPYDADYA	-1.9714
0.000771	16/20	GDVVVLDADYA	-1.6994
4.01E-06	15/20	GDVGPDYYDYA	-1.676
0.00326	12/20	GDDPPYDASYA	-1.0611
0.0103	14/20	GDAGPLDASYA	-0.6074
0.000244	16/20	GDVVVLDYDYA	-0.3212
0.00443	13/20	GDVGALAYDLA	-0.2857
3.30E-05	13/20	GDVGADDASYA	-0.093
0.0225	13/20	GDAPPYDYSLA	-0.0763
0.00041	12/20	GDAGPYDASYA	0.0085
0.00098	15/20	GDVVALDADLA	0.2826
6.95E-05	13/20	GDAPDDAYSYA	0.3491
2.62E-05	12/20	GDAPDDAYSYA	0.4321
2.94E-05	15/20	GDVGPDAYDYA	0.4443
0.000242	14/20	GDAGVLAADYA	0.6671
6.12E-05	15/20	GDAPPYDASLA	0.8547
0.000113	16/20	GDVGPLDYDYA	0.8677
0.000786	14/20	GDDGPYDASYA	0.8739
5.80E-06	15/20	GDAGVLAADYA	1.0292
1.04E-07	16/20	GDVGPDAASYA	1.0352
0.000156	13/20	GDAGALDASYA	1.2279
0.0225	11/20	GDVGADDADYA	1.8061
0.000232	16/20	GDVPADDASYA	1.9579
0.000328	14/20	GDVGPDAYDYA	2.1081
0.015	14/20	GDVGPLDADYA	2.2805
0.00901	14/20	GDVGPDAYDLA	3.1411

Supplementary Figure 6. MS2 spectra of two cyclic peptide binders after affinity selection, linearization and derivatization with mass ionization tag.

B ions	Y ions
58.0288	1468.65
173.056	1411.62
272.124	1296.6
329.146	1197.53
426.198	1140.51
541.225	1043.45
612.262	928.427
775.326	857.39
890.353	694.327
1053.42	579.2997
1450.63	416.236

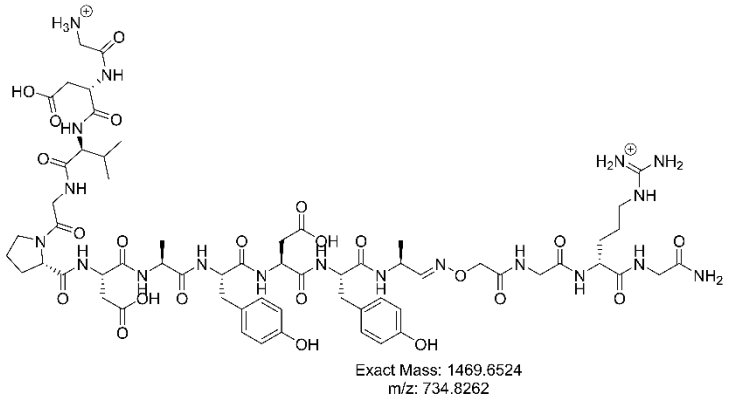

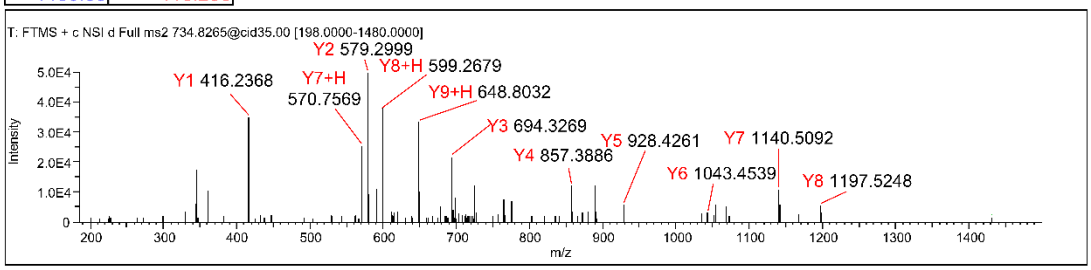

B ions	Y ions
58.0287	1440.614
173.0557	1383.592
244.0928	1268.565
301.1143	1197.528
398.1671	1140.507
561.2304	1043.454
676.2573	880.3907
747.2945	765.3638
862.3214	694.3267
1025.385	579.2997
1422.603	416.2364

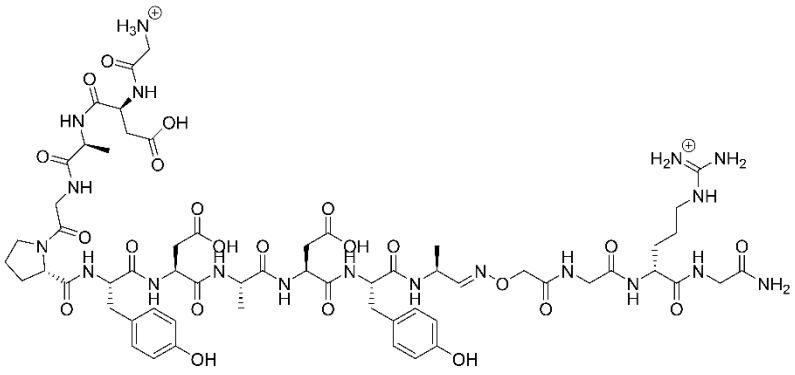

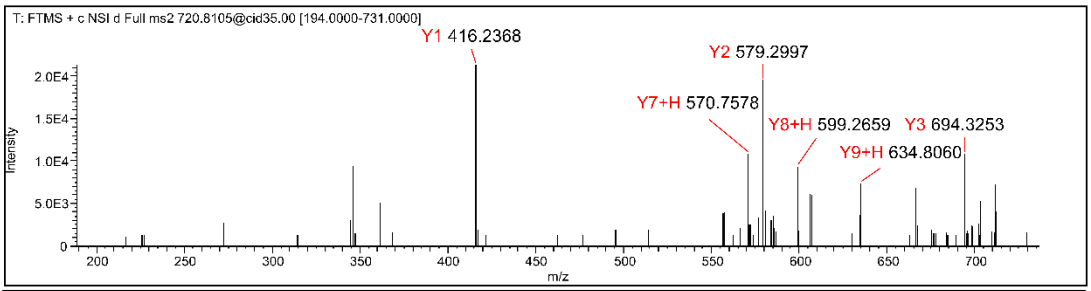

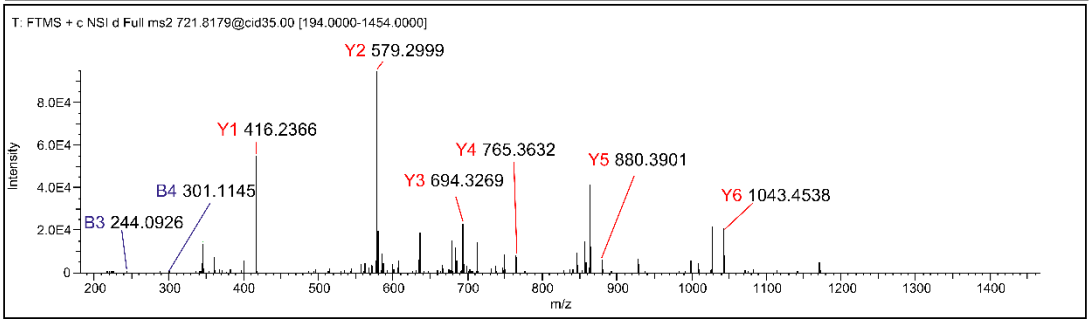

Supplementary Figure 7. Structure and HRMS of FITC labeled cyclic peptide binders utilized for MST binding studies.

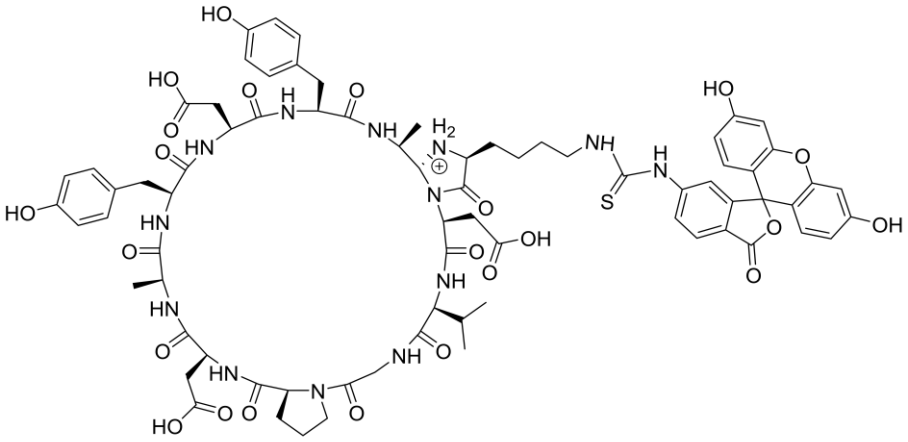

Exact Mass: 1568.5675

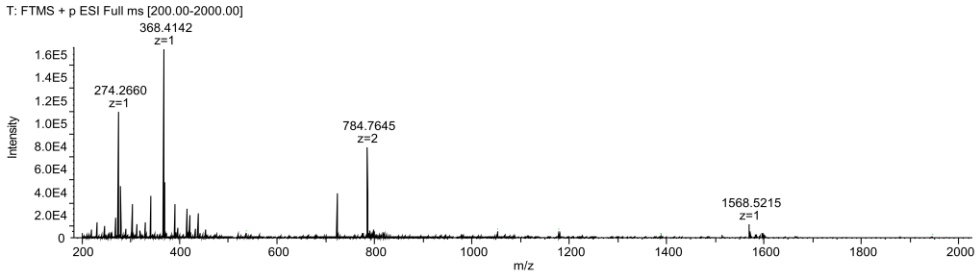

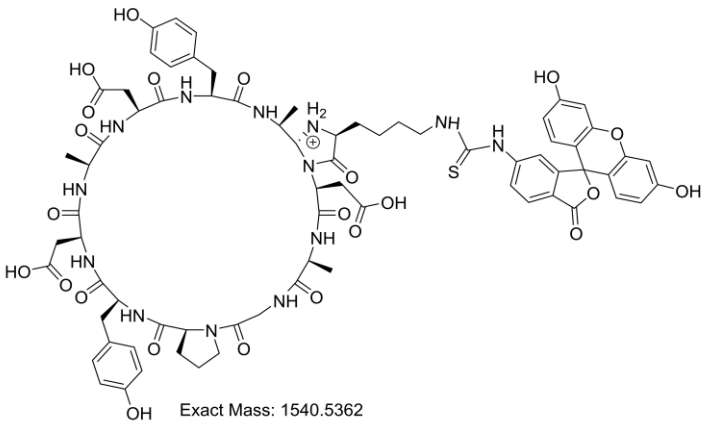

Exact Mass: 1540.5362

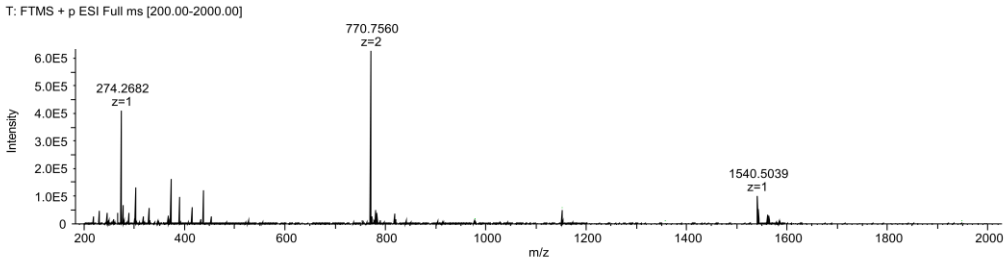

Supplementary Figure 8. Thermal Shift Assay data for FG CyClick peptides with point mutated HIV capsid protein (CAN74D and CAM66I).

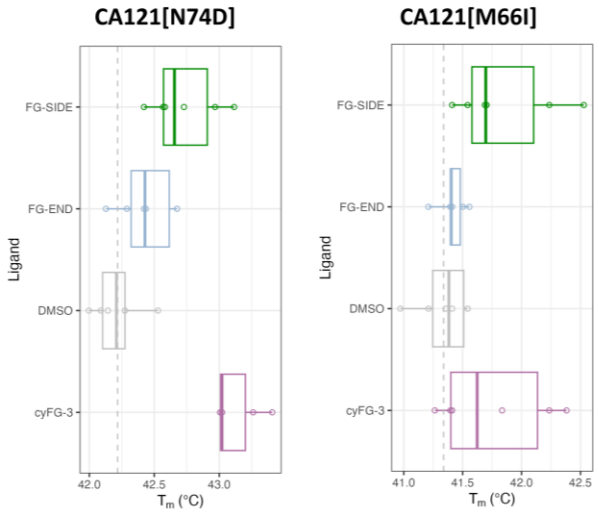

Supplementary Figure 9. Lenacapavir (LEN) small molecule inhibitor (a) Structure (b) Representative Biolayer Interferometry (BLI) sensograms of double background subtracted data and modeled fit for CA Hexamers with LEN at 5 μM (c) Kinetics of CA assembly in the presence of DMSO or 5 μM LEN (d) Kinetics of CA assembly in the presence of DMSO, 5 μM LEN, or 75 μM cyFG-3

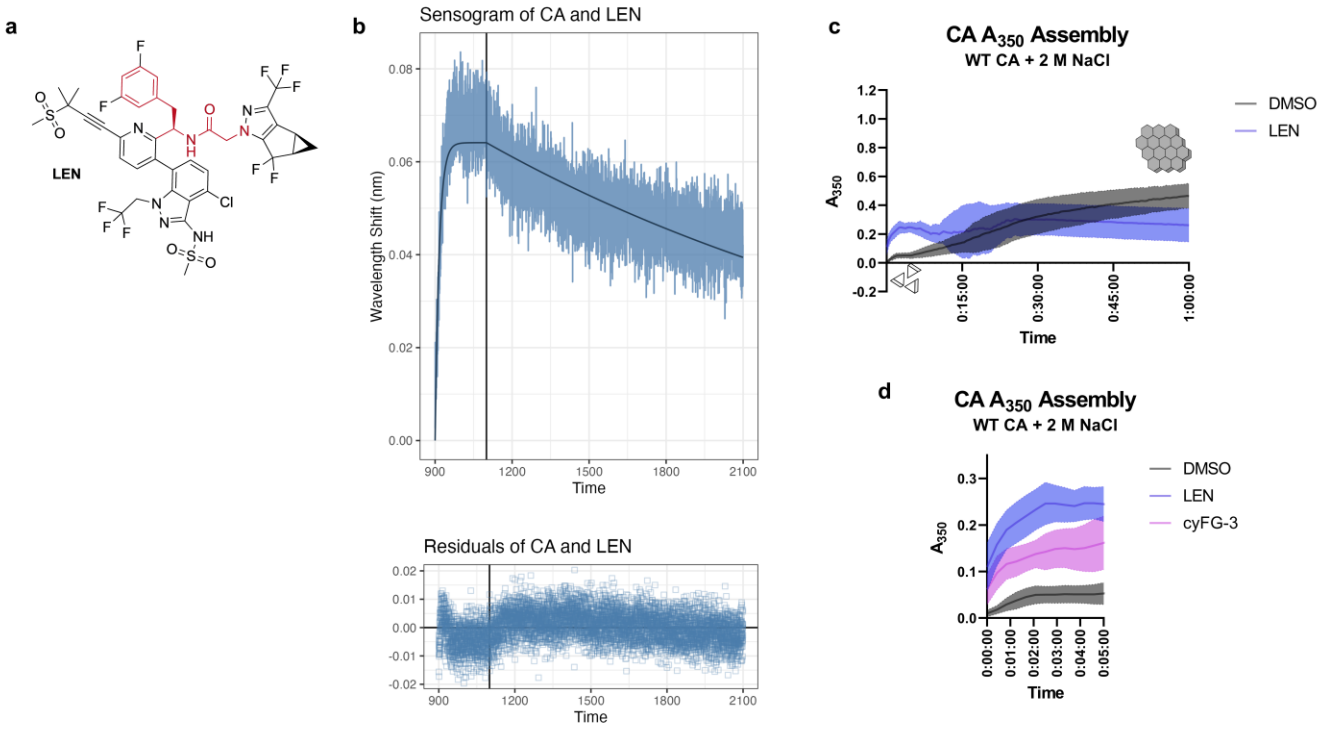

Supplmentary Table 4. timsTOF Acquisition method parameter optimization with library C for application in the analysis of CyClick and Hydrazone peptide libraries

Parameter	Method 1	Method 2	Method 3	Method 4	Method 5	Method 6
Injection amount	200 ng	200 ng	100 ng	100 ng	100 ng	150 ng
TIMS accumulation time	100 ms	100 ms	100 ms	200 ms	200 ms	200 ms
Polygon	Normal	Custom	Normal	Normal	Normal	Normal
Targeted intensity	10'000	10'000	10'000	10'000	25'000	25'000
Fragmentation energy	20 eV at 0.6 1/K0 - 59 eV at 1.60 1/K0	20 eV at 0.6 1/K0 - 59 eV at 1.60 1/K0	20 eV at 0.6 1/K0 - 59 eV at 1.60 1/K0	10 eV at 0.6 1/K0 - 55 eV at 1.60 1/K0	10 eV at 0.6 1/K0 - 55 eV at 1.60 1/K0	10 eV at 0.6 1/K0 - 55 eV at 1.60 1/K0
Cycle time	1.17 s	1.17 s	1.17 s	1.17 s	1.17 s	1.17 s
Isolation window	2 Da	2 Da	2 Da	2 Da	2 Da	2 Da

Supplementary Figure 10. Peptides identified and quantified from library C1 across differing method parameters

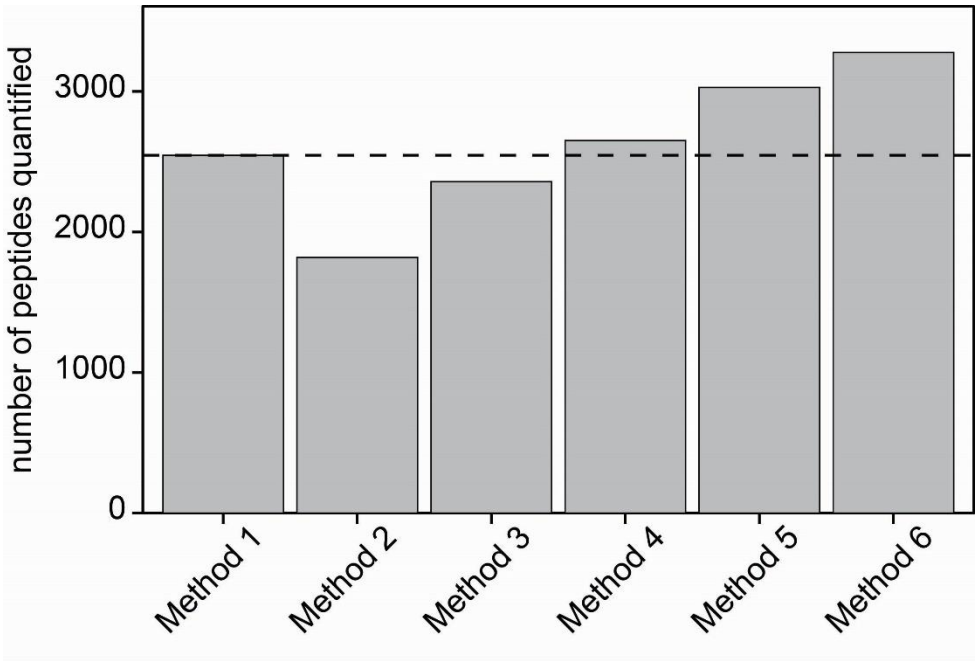

Supplementary Figure 11. Extracted ion chromatograms for LC-HRMS analysis of model peptides **5-9** (pink) and linear peptide (blue)

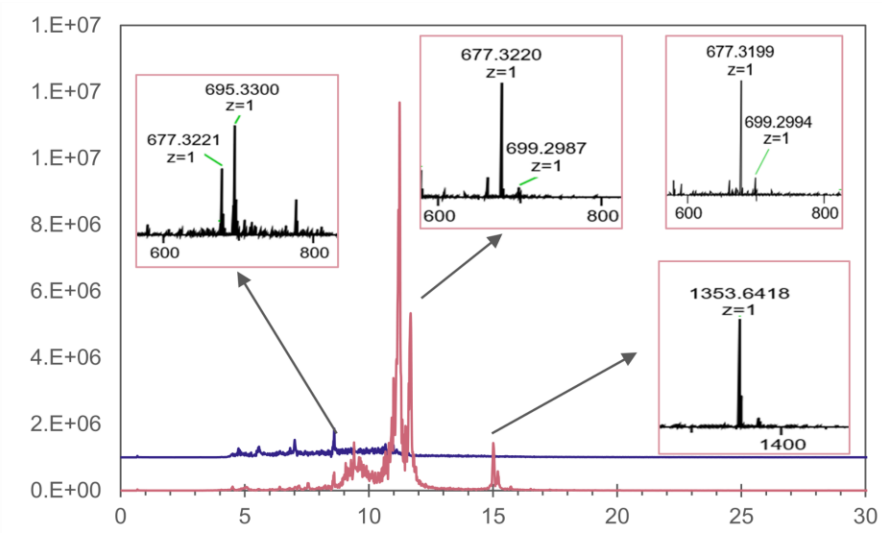
695.3300
z=1
677.3221
z=1
600
800
677.3220
z=1
699.2987
z=1
600
800
677.3199
z=1
699.2994
z=1
600
800
1353.6418
z=1
1400
1.E+07
1.E+07
1.E+07
8.E+06
6.E+06
4.E+06
2.E+06
0.E+00
0
5
10
15
20
25
30

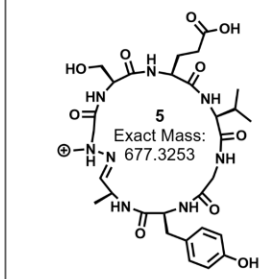
5
Exact Mass:
677.3253

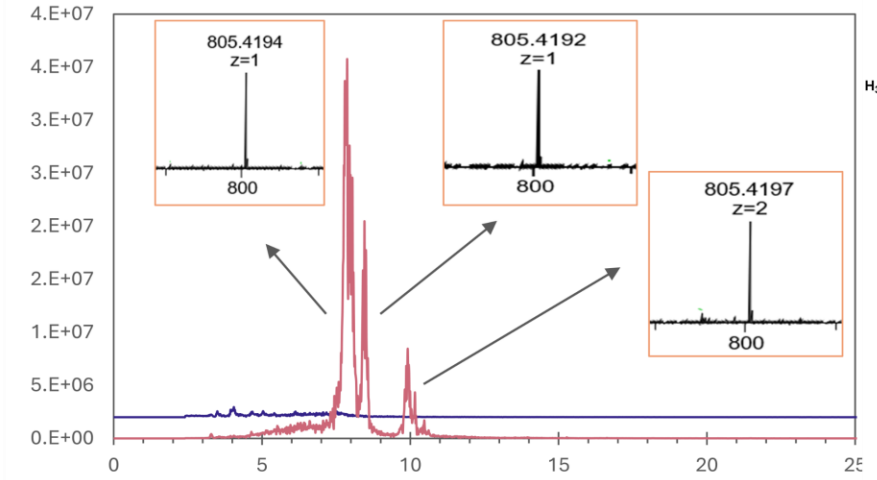
805.4194
z=1
800
805.4192
z=1
800
805.4197
z=2
800
4.E+07
4.E+07
3.E+07
3.E+07
2.E+07
2.E+07
1.E+07
5.E+06
0.E+00
0
5
10
15
20
25

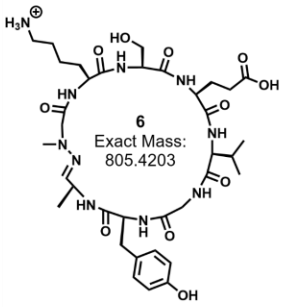
6
Exact Mass:
805.4203

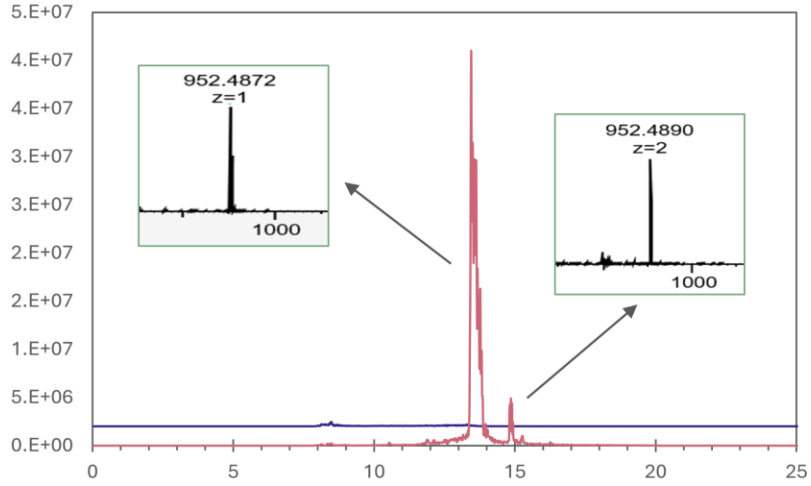
952.4872
z=1
1000
952.4890
z=2
1000
5.E+07
4.E+07
4.E+07
3.E+07
3.E+07
2.E+07
2.E+07
1.E+07
5.E+06
0.E+00
0
5
10
15
20
25

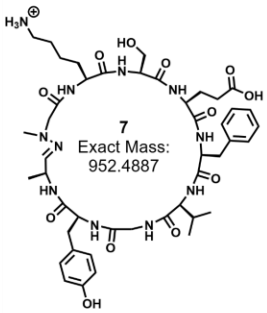
7
Exact Mass:
952.4887

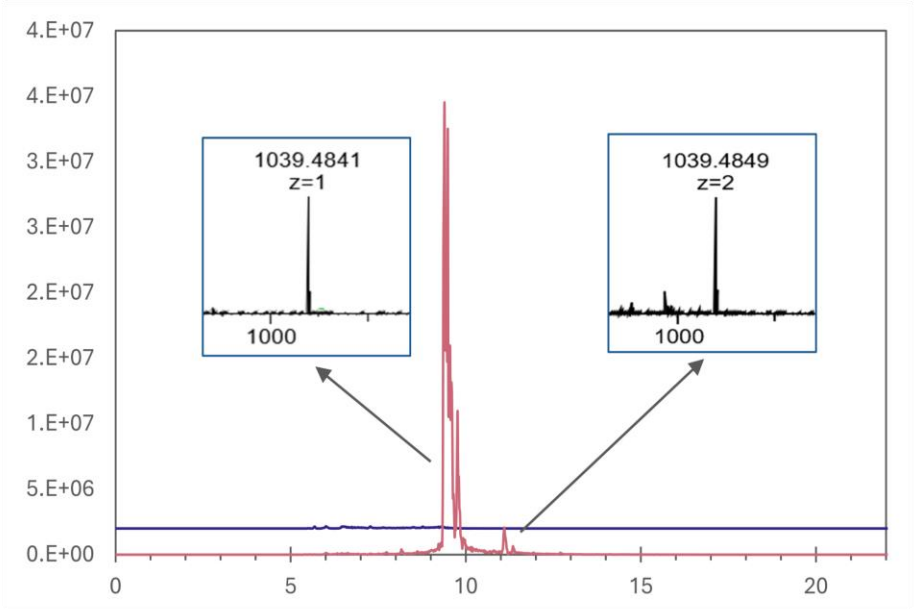
4.E+07
4.E+07
3.E+07
3.E+07
2.E+07
2.E+07
1.E+07
5.E+06
0.E+00
0
5
10
15
20
1039.4841
z=1
1000
1039.4849
z=2
1000

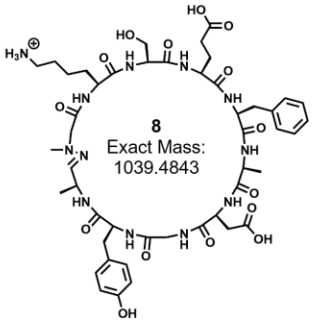
8
Exact Mass:
1039.4843

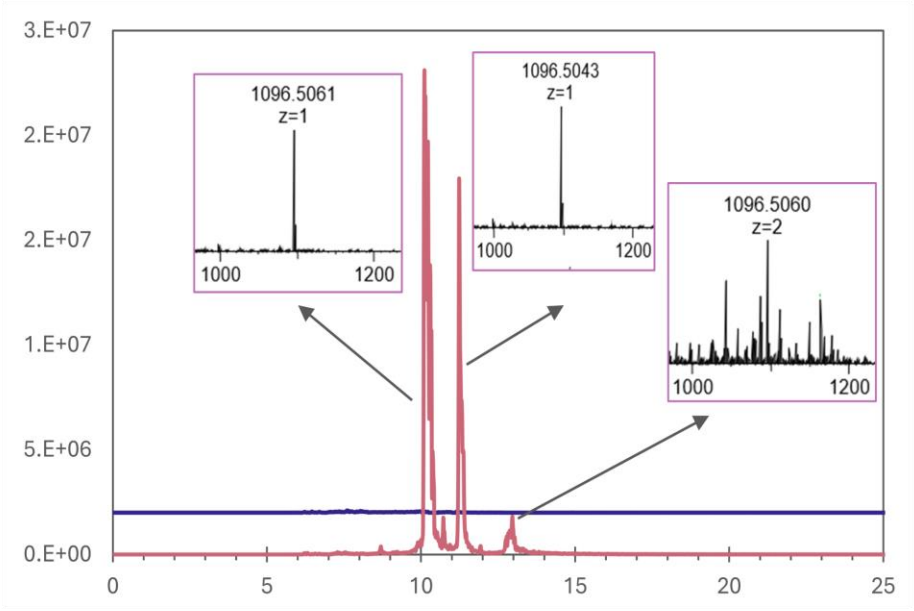
3.E+07
2.E+07
2.E+07
1.E+07
5.E+06
0.E+00
0
5
10
15
20
25
1096.5061
z=1
1000
1200
1096.5043
z=1
1000
1200
1096.5060
z=2
1000
1200

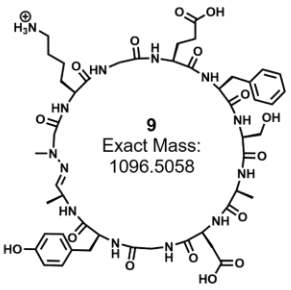
9
Exact Mass:
1096.5058

Supplementary Figure 12. Suspected side product from base promoted cleavage of model peptide **5**

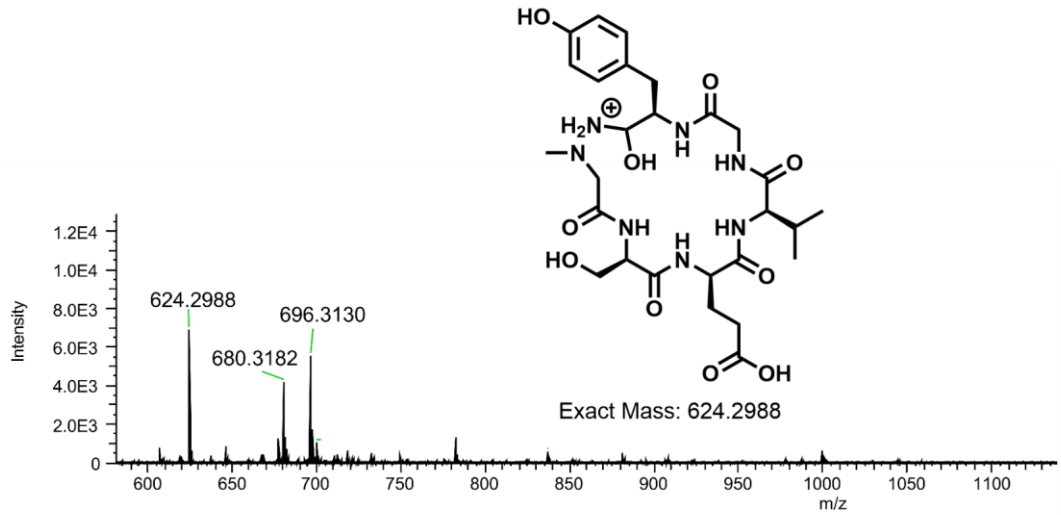

Supplementary Figure 13. Preparatory HPLC traces of individual model hydrazone peptides

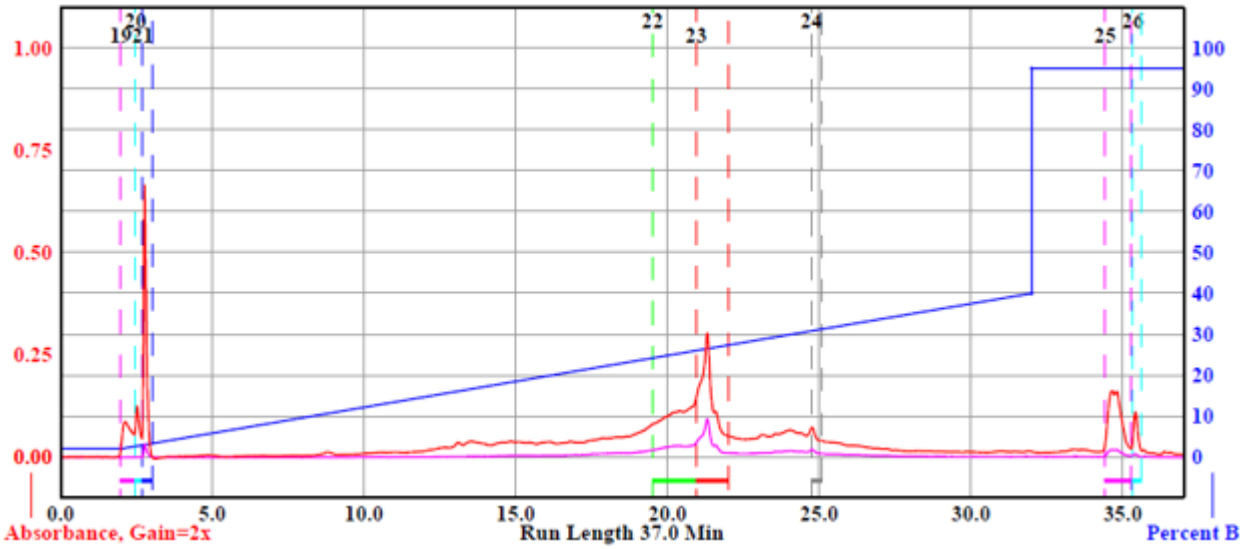

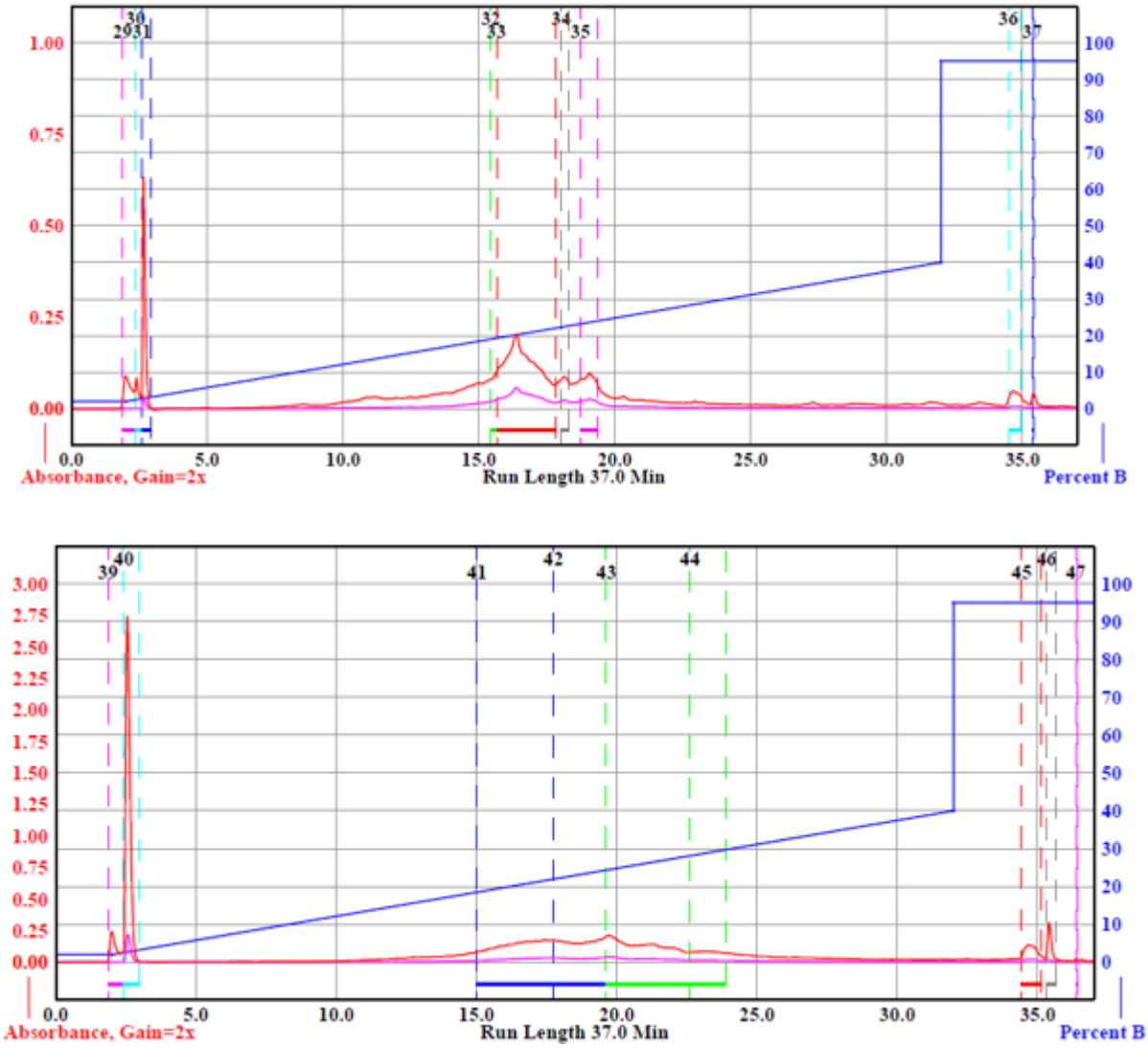

Supplementary Figure 14. Structures of HL 1-16 hydrazones macrocycles from small-scale library design

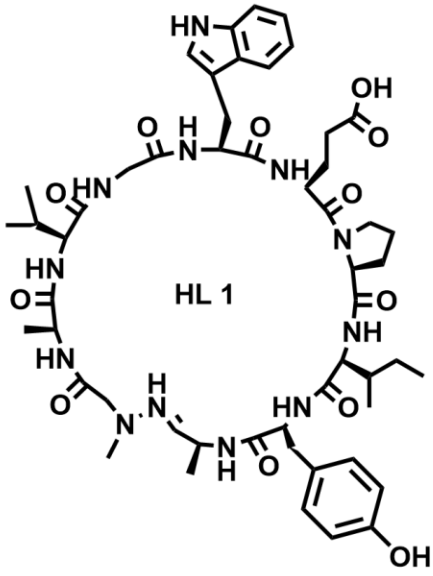
HL 1

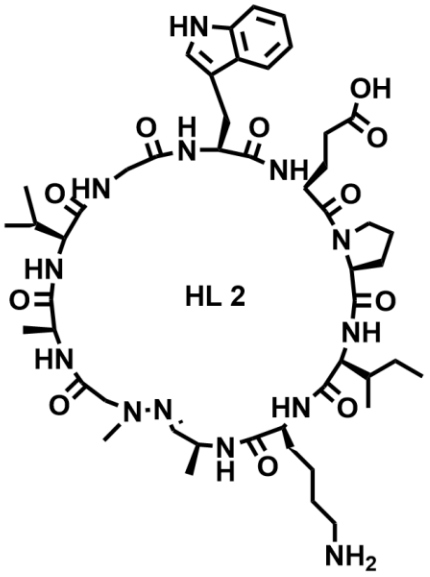
HL 2

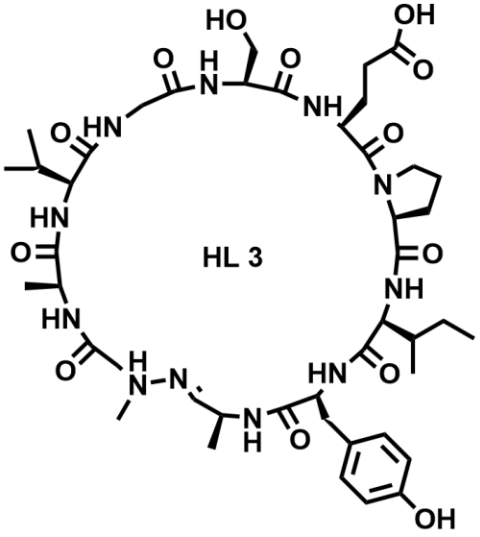
HL 3

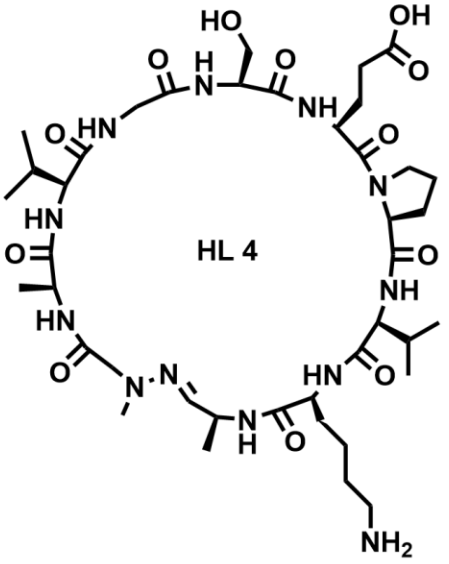
HL 4

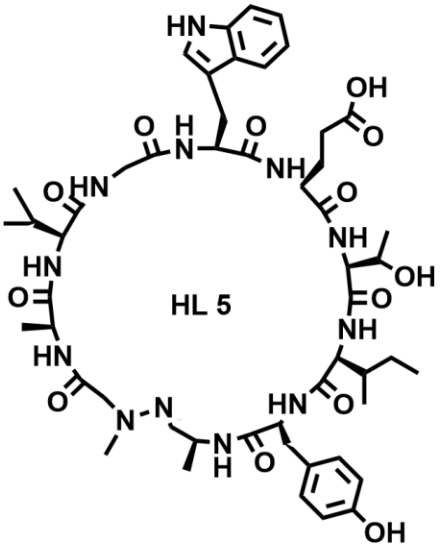
HL 5

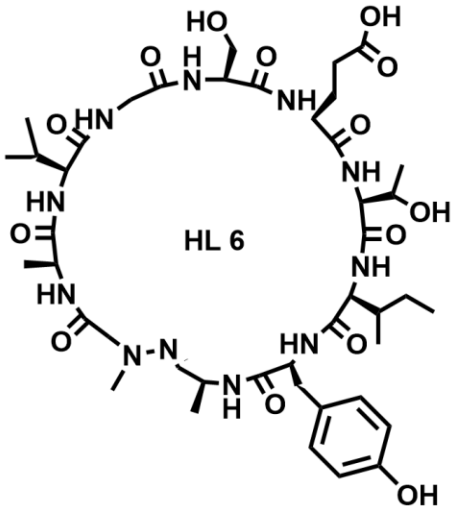
HL 6

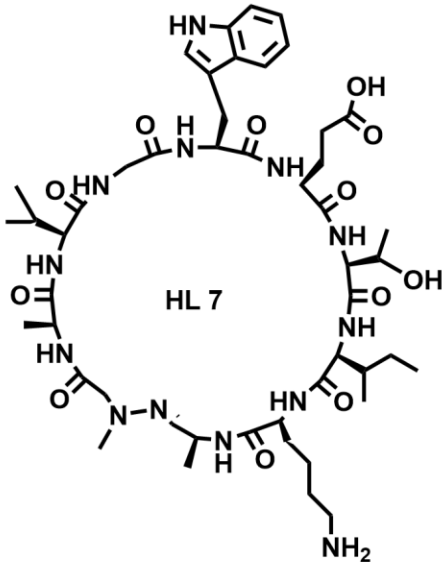
HL 7

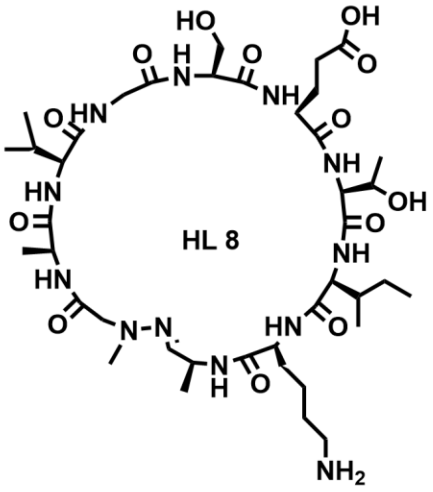
HL 8

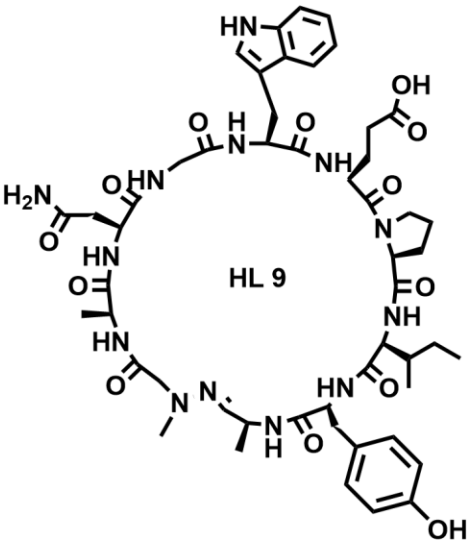
HL 9

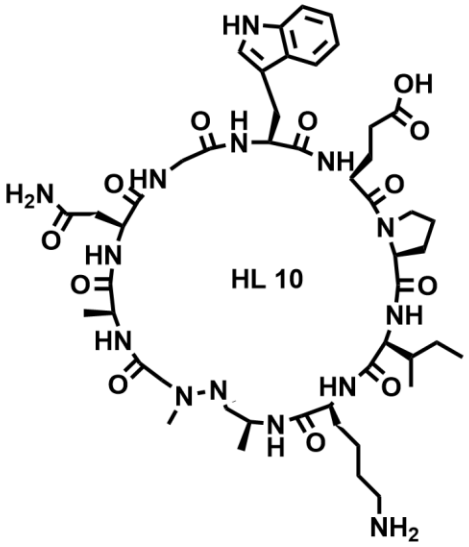
HL 10

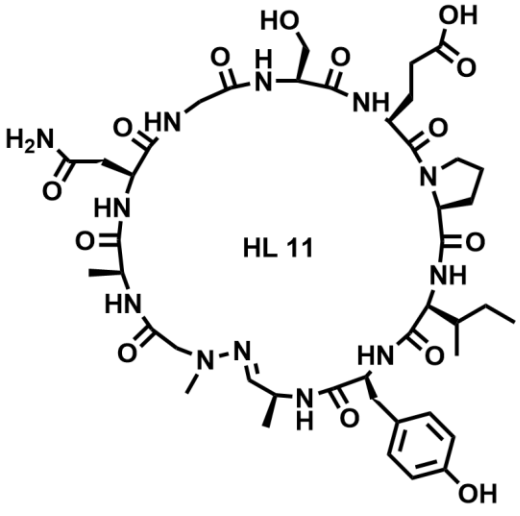
HL 11

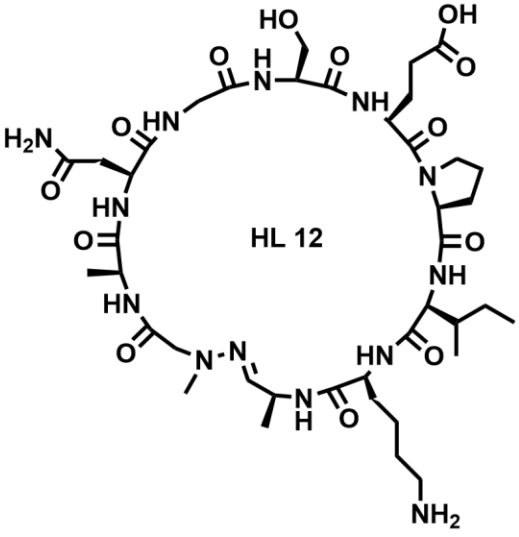
HL 12

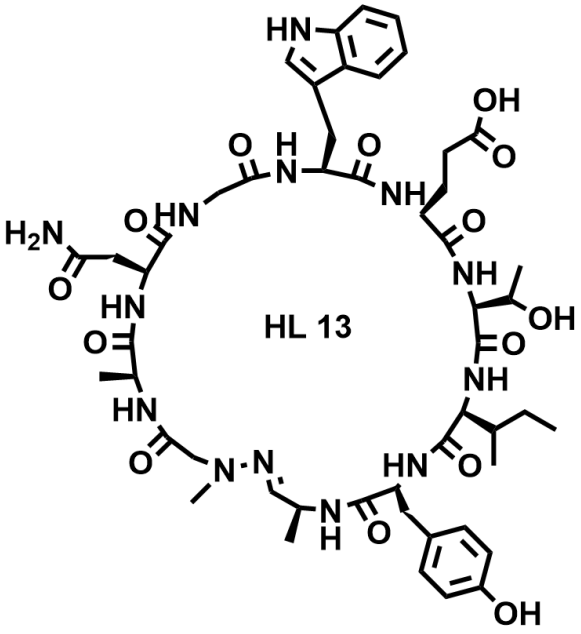
HL 13

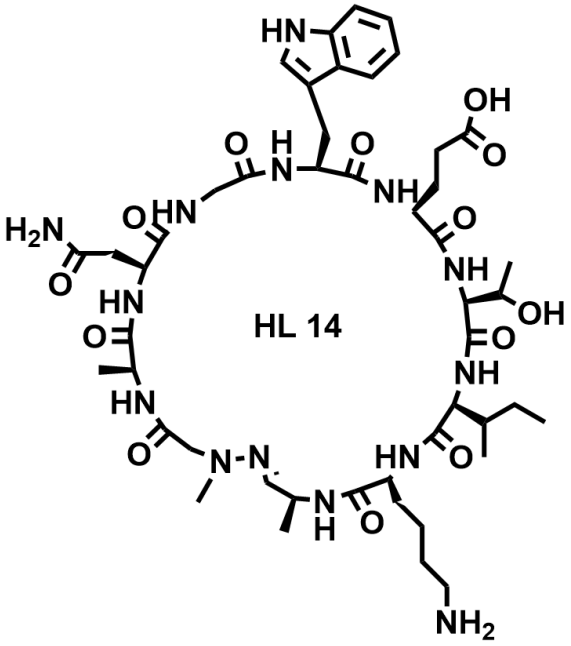
HL 14

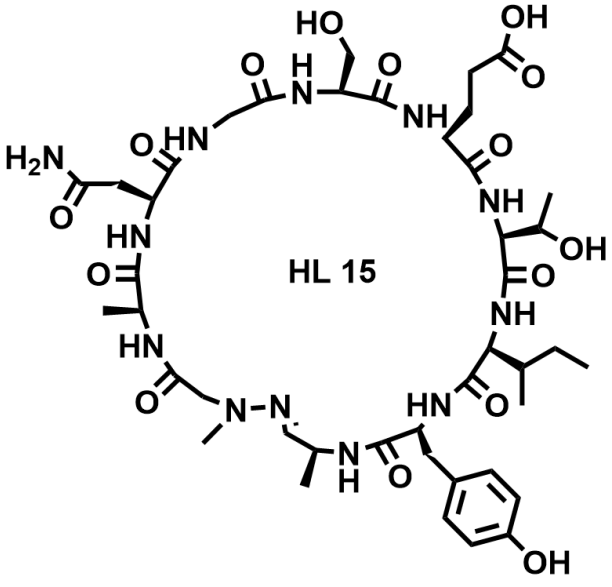
HL 15

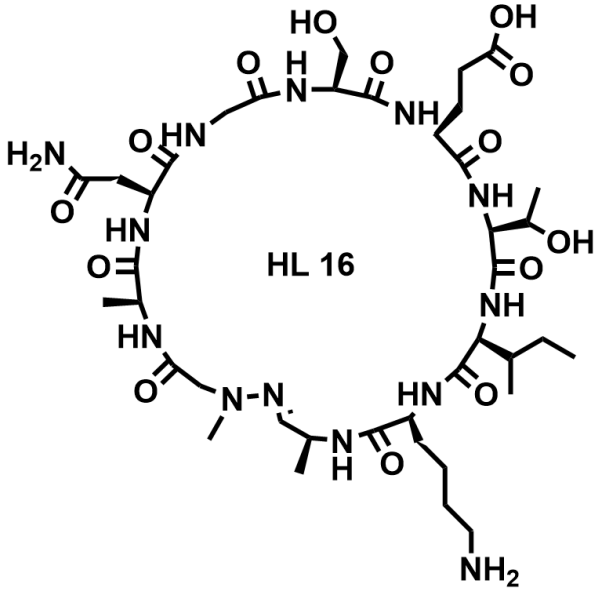
HL 16

Supplementary Figure 15. LC-HRMS analysis of crude small-scale hydrazone library mixture without acidic modifier in the mobile phase.

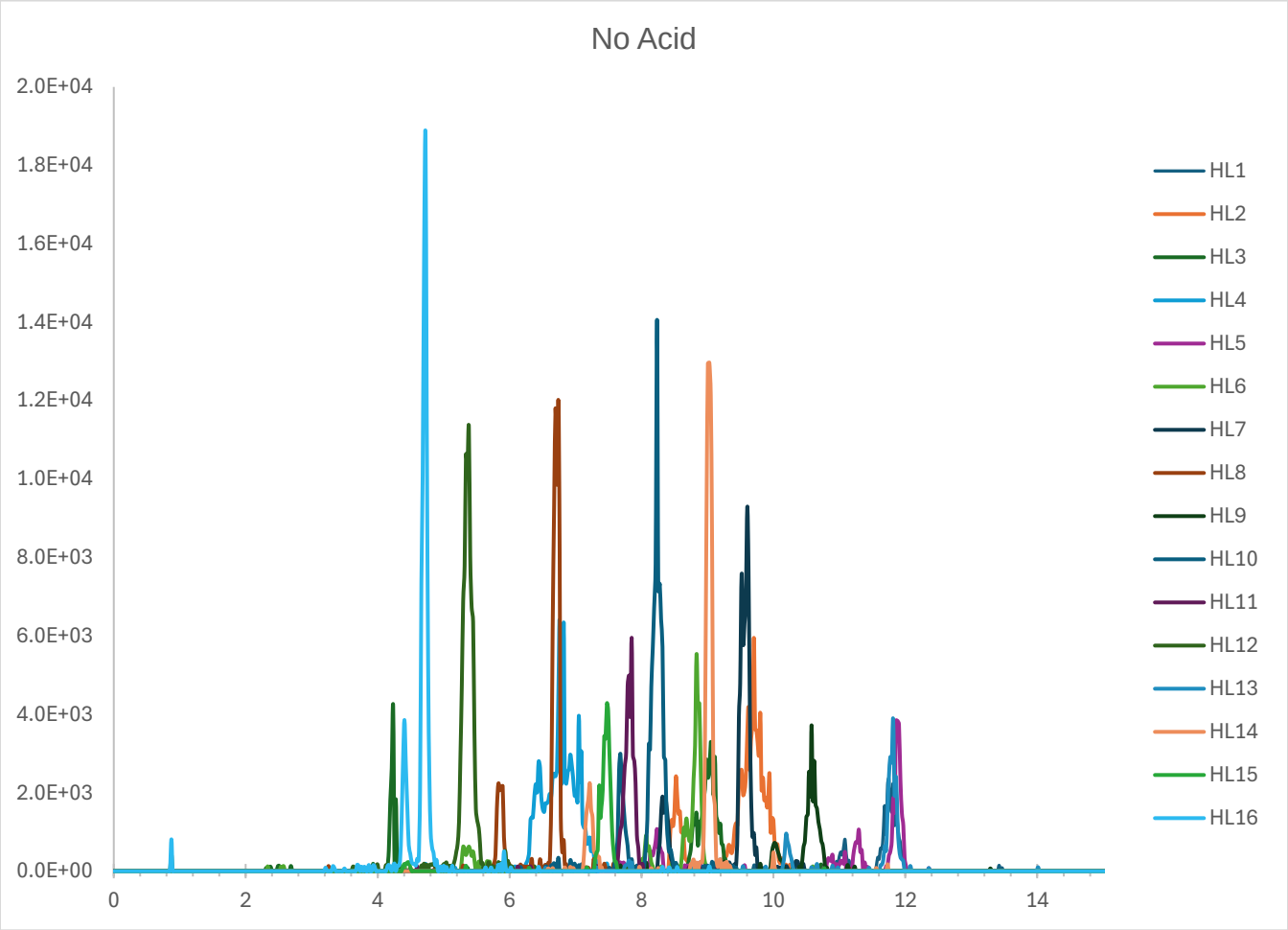

Supplementary Figure 16. MS2 spectra of the hydrazone peptide small-scale library after linearization and derivatization with mass ionization tag.

B ions	Y ions
91.0625	1421.741
162.0997	1331.685
261.1681	1260.648
318.1896	1161.58
504.2689	1104.558
633.3115	918.4792
730.3642	789.4366
843.4483	692.3838
1006.512	579.2997
1403.73	416.2364

HL 1

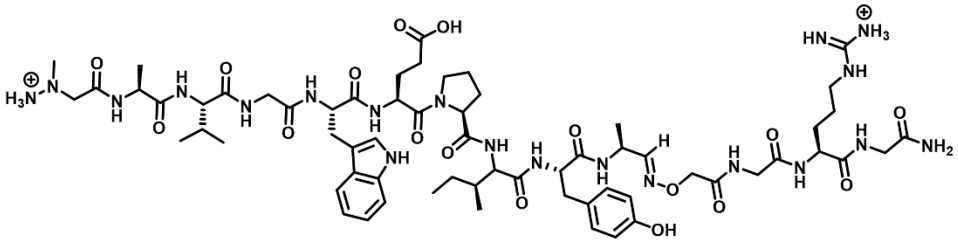

m/z: 709.3704

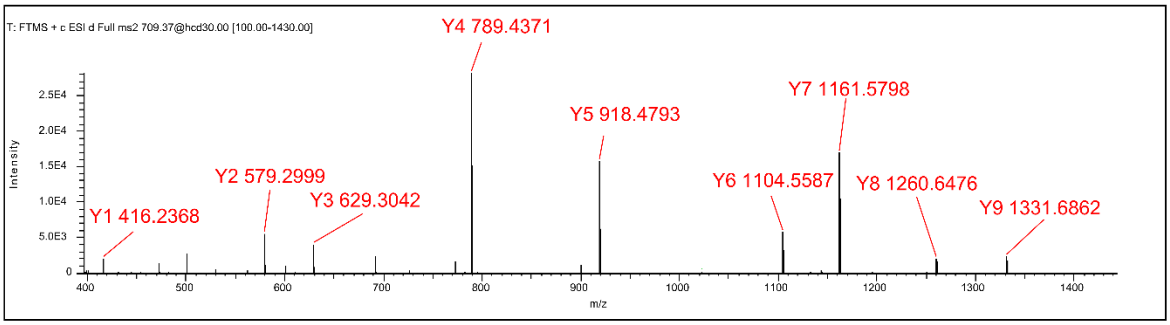

B ions	Y ions
91.06259	1386.772
162.0997	1296.717
261.1681	1225.68
318.1896	1126.612
504.2689	1069.59
633.3115	883.5108
730.3642	754.4682
843.4483	657.4154
971.5433	544.3314
1368.762	416.2364

HL 2

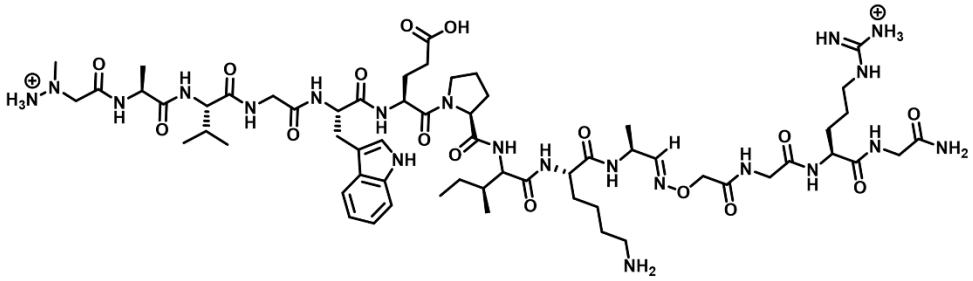

m/z: 691.8862

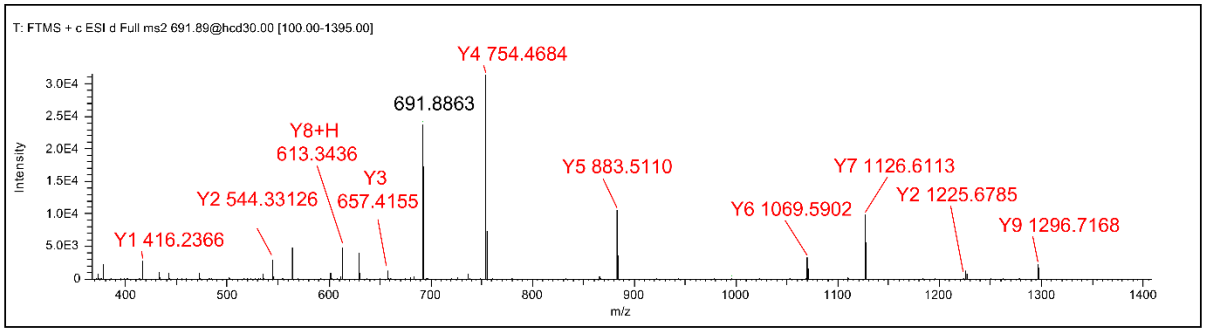

B ions	Y ions
91.06259	1322.693
162.0997	1232.638
261.1681	1161.601
318.1896	1062.533
405.2216	1005.511
534.2642	918.4792
631.317	789.4366
744.401	692.3838
907.4644	579.2997
1304.683	416.2364

HL 3

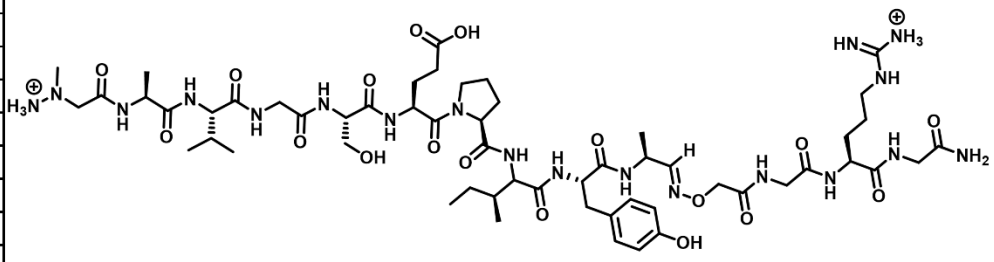

m/z: 659.8468

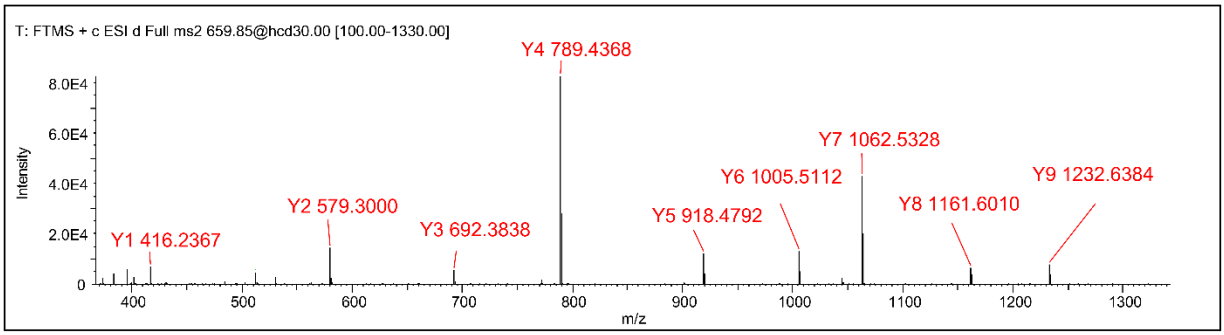

B ions	Y ions
91.06259	1287.725
162.0997	1197.67
261.1681	1126.633
318.1896	1027.564
405.2216	970.5428
534.2642	883.5108
631.317	754.4682
744.401	657.4154
872.496	544.3314
1269.715	416.2364

HL 4

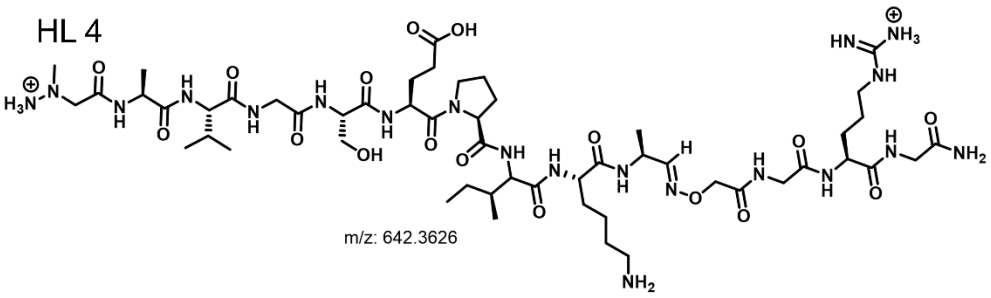

m/z: 642.3626

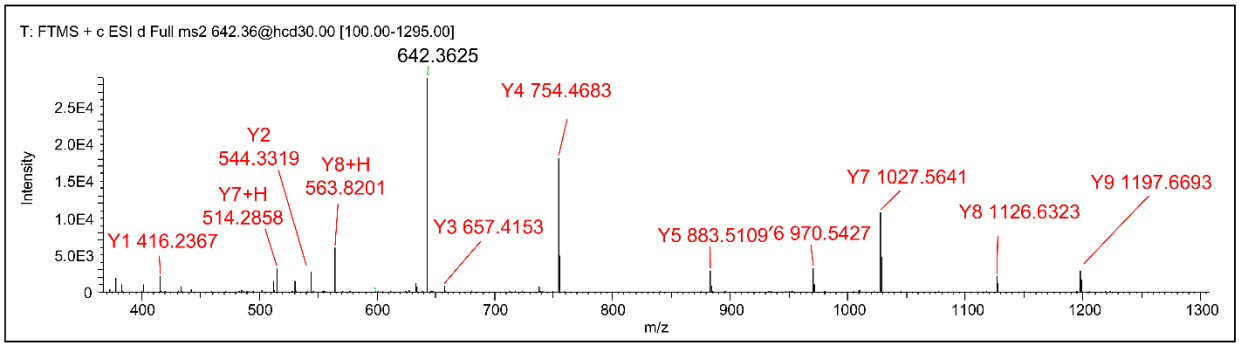

B ions	Y ions
91.06259	1425.736
162.0997	1335.68
261.1681	1264.643
318.1896	1165.575
504.2689	1108.553
633.3115	922.4741
734.3592	793.4315
847.4432	692.3838
1010.507	579.2997
1407.725	416.2364

HL 5

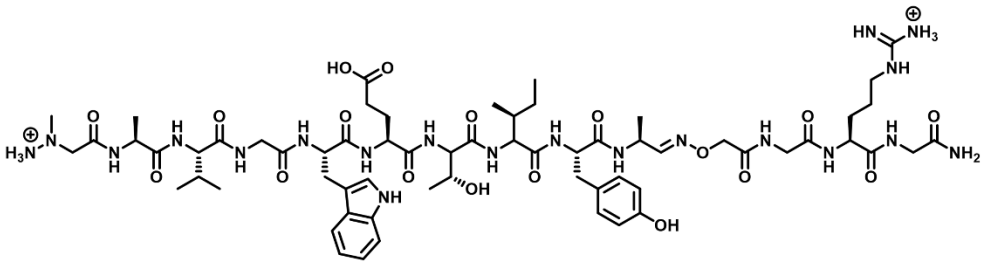

m/z: 711.3679

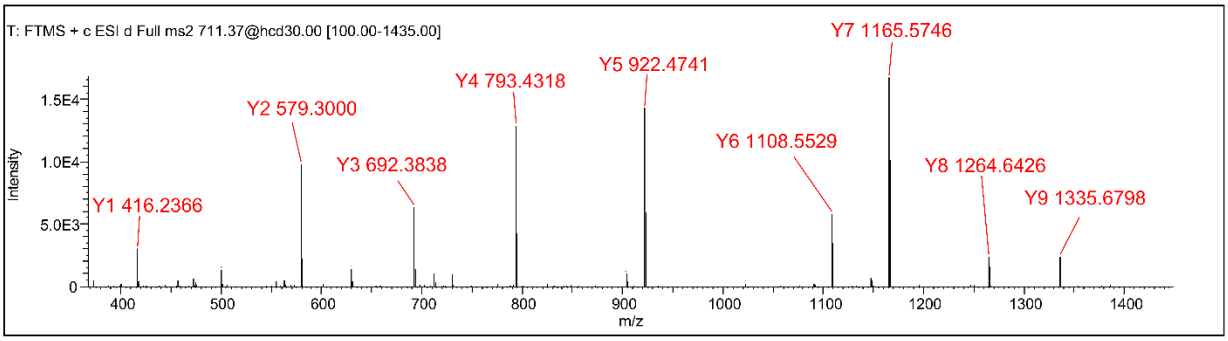

B ions	Y ions
91.06259	1326.688
162.0997	1236.633
261.1681	1165.596
318.1896	1066.528
405.2216	1009.506
534.2642	922.4741
635.3119	793.4315
748.3959	692.3838
911.4593	579.2997
1308.678	416.2364

HL 6

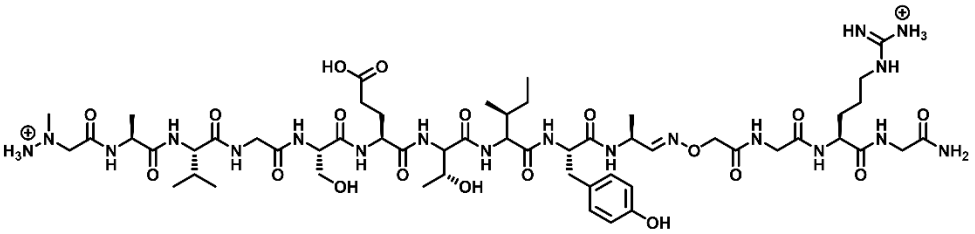

m/z: 661.8442

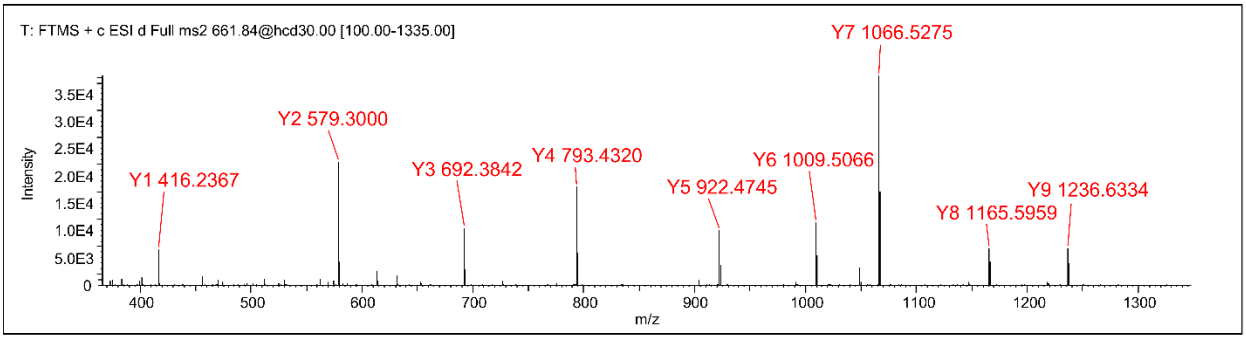

B ions	Y ions
91.06259	1390.767
162.0997	1300.712
261.1681	1229.675
318.1896	1130.606
504.2689	1073.585
633.3115	887.5057
734.3592	758.4631
847.4432	657.4154
975.5382	544.3314
1372.757	416.2364

HL 7

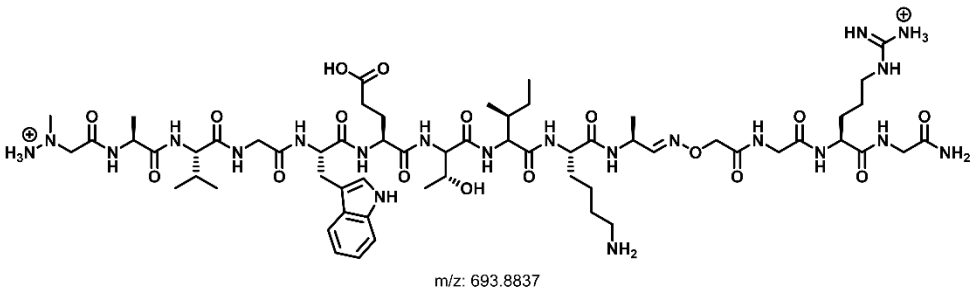

m/z: 693.8837

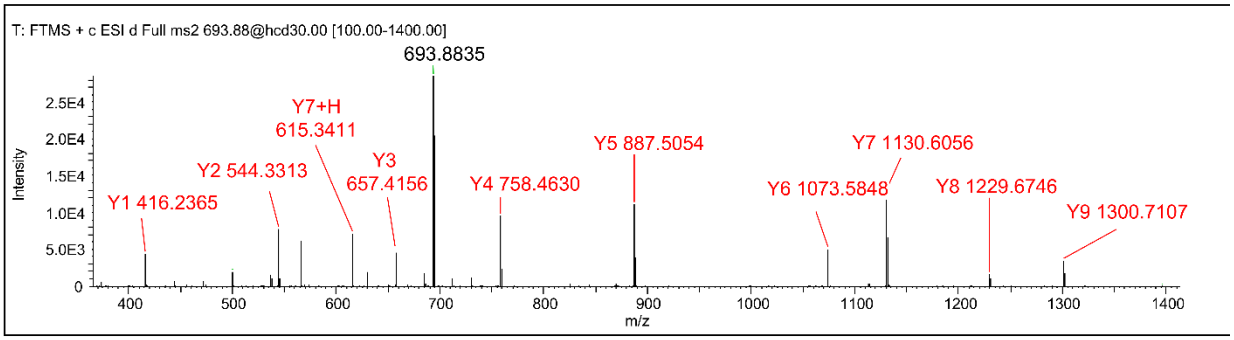

B ions	Y ions
91.06259	1291.72
162.0997	1201.665
261.1681	1130.628
318.1896	1031.559
405.2216	974.5377
534.2642	887.5057
635.3119	758.4631
748.3959	657.4154
876.4909	544.3314
1273.709	416.2364

HL 8

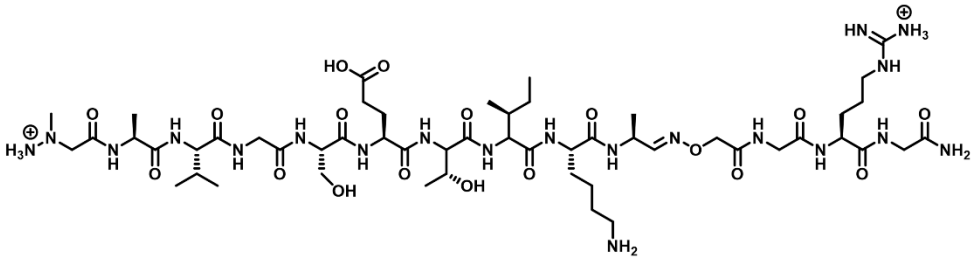

m/z: 644.3600

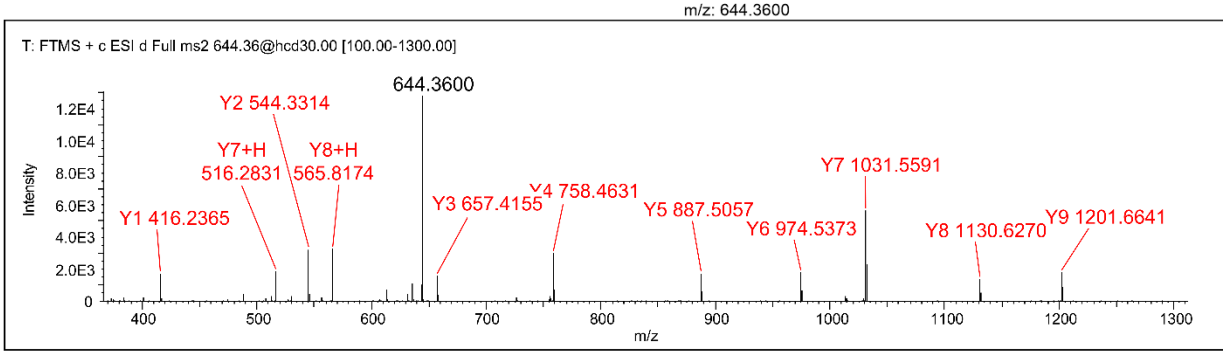

B ions	Y ions
91.06259	1436.715
162.0997	1346.66
276.1426	1275.623
333.1641	1161.58
519.2434	1104.558
648.286	918.4792
745.3388	789.4366
858.4228	692.3838
1021.486	579.2997
1418.705	416.2364

HL 9

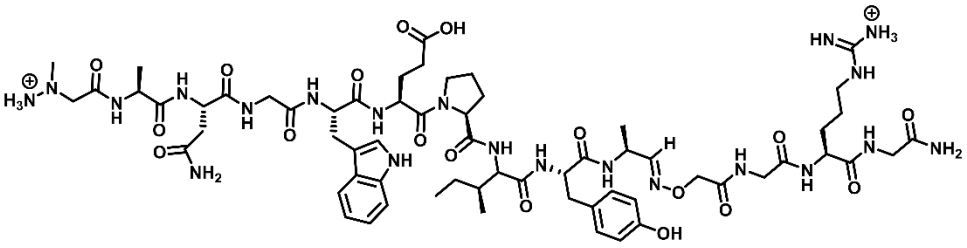

m/z: 716.8577

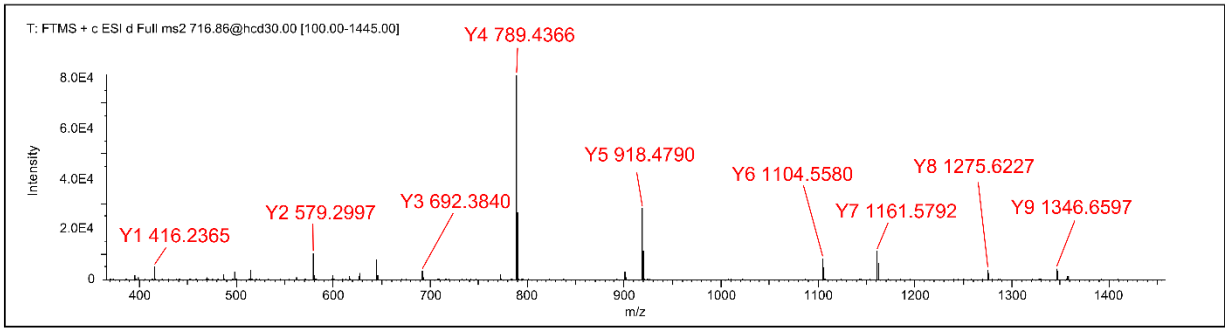

B ions	Y ions
91.06259	1401.747
162.0997	1311.692
276.1426	1240.654
333.1641	1126.612
519.2434	1069.59
648.286	883.5108
745.3388	754.4682
858.4228	657.4154
986.5178	544.3314
1383.736	416.2364

HL 10

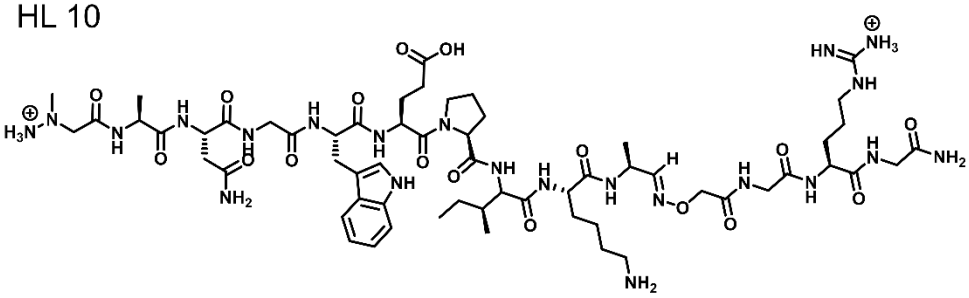

m/z: 699.3735

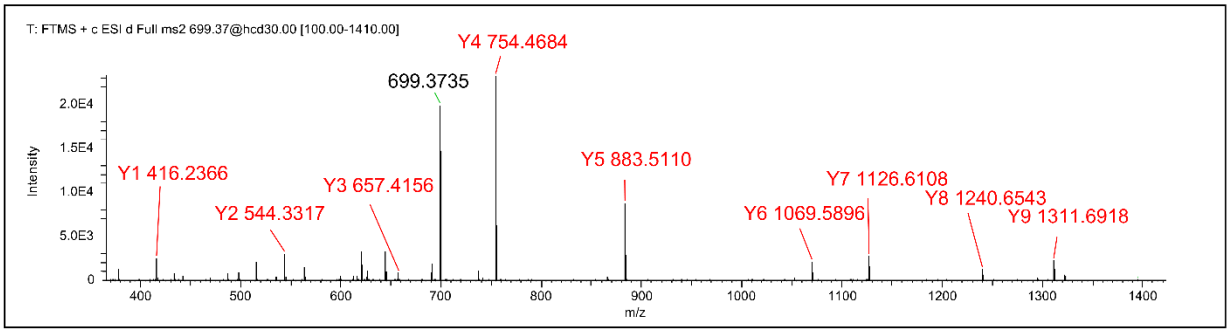

B ions	Y ions
91.06259	1337.668
162.0997	1247.613
276.1426	1176.576
333.1641	1062.533
420.1961	1005.511
549.2387	918.4792
646.2915	789.4366
759.3755	692.3838
922.4389	579.2997
1319.657	416.2364

HL 11

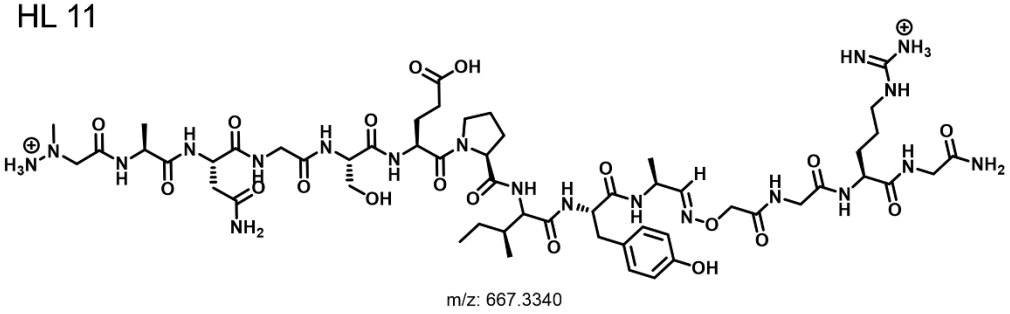

m/z: 667.3340

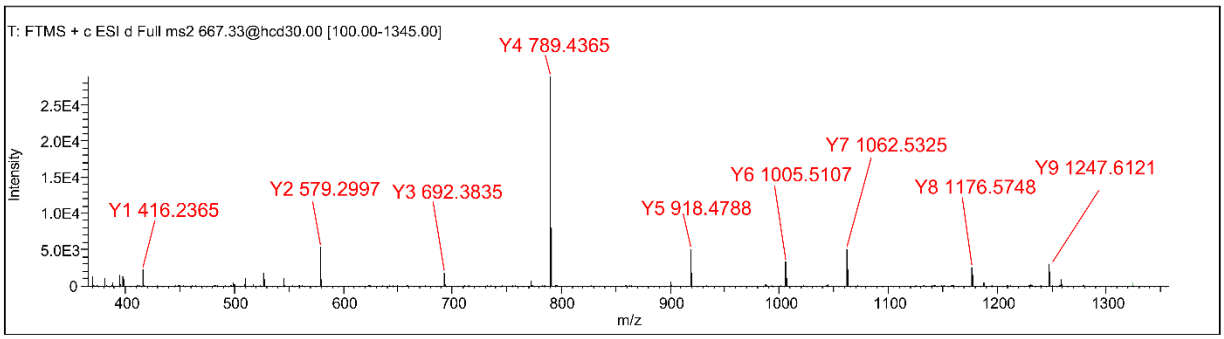

B ions	Y ions
91.06259	1302.7
162.0997	1212.644
276.1426	1141.607
333.1641	1027.564
420.1961	970.5428
549.2387	883.5108
646.2915	754.4682
759.3755	657.4154
887.4705	544.3314
1284.689	416.2364

HL 12

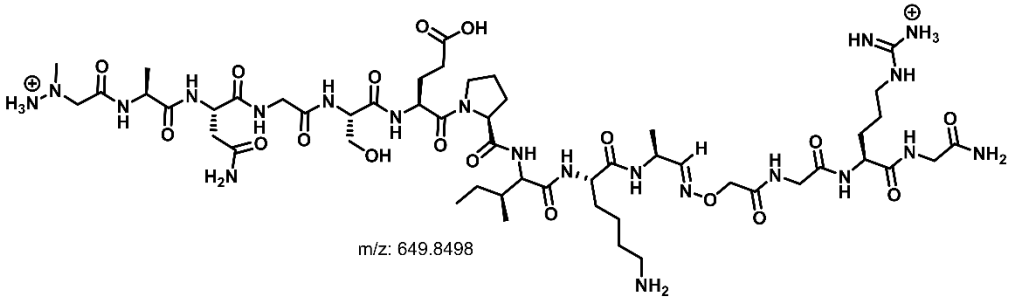

m/z: 649.8498

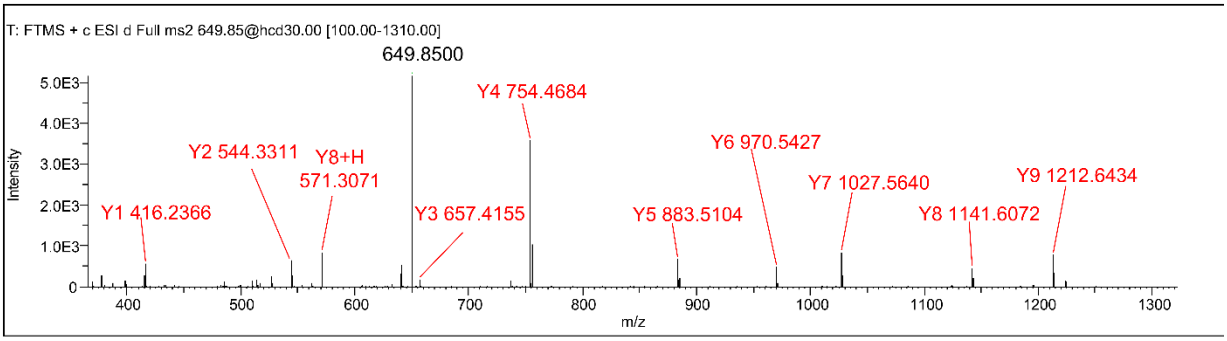

B ions	Y ions
91.06259	1440.71
162.0997	1350.655
276.1426	1279.618
333.1641	1165.575
519.2434	1108.553
648.286	922.4741
749.3337	793.4315
862.4177	692.3838
1025.481	579.2997
1422.7	416.2364

HL 13

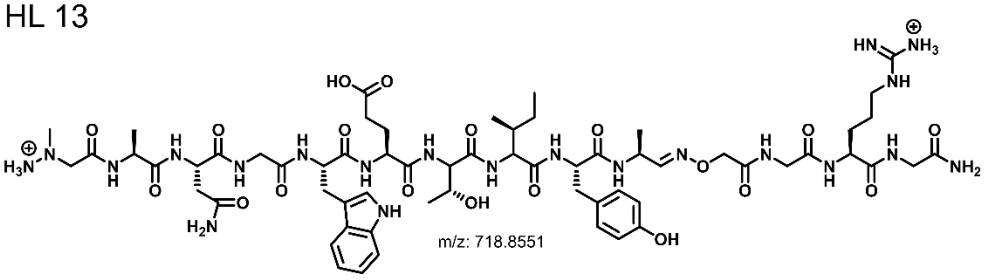

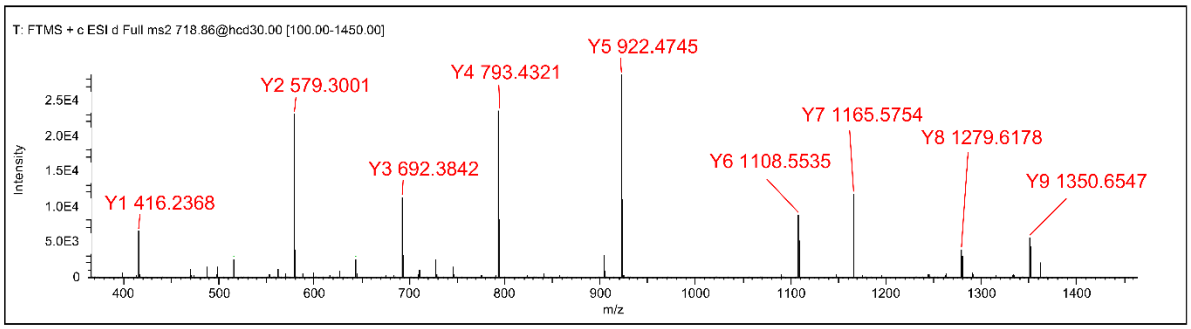

B ions	Y ions
91.06259	1405.742
162.0997	1315.687
276.1426	1244.649
333.1641	1130.606
519.2434	1073.585
648.286	887.5057
749.3337	758.4631
862.4177	657.4154
990.5127	544.3314
1387.731	416.2364

HL 14

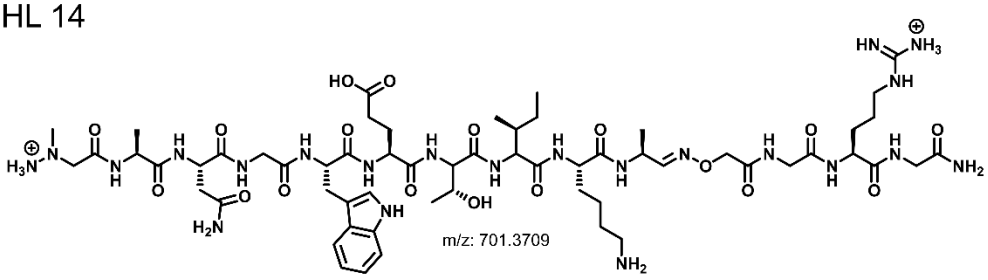

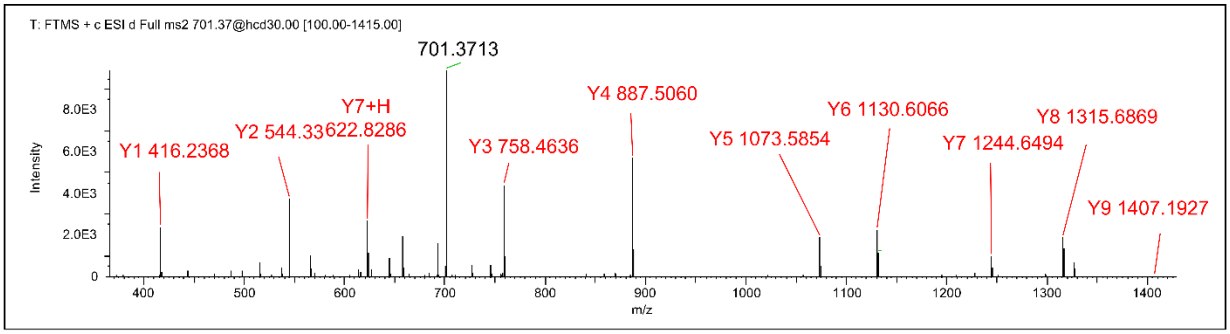

B ions	Y ions
91.06259	1341.663
162.0997	1251.608
276.1426	1180.57
333.1641	1066.528
420.1961	1009.506
549.2387	922.4741
650.2864	793.4315
763.3705	692.3838
926.4338	579.2997
1323.652	416.2364

HL 15

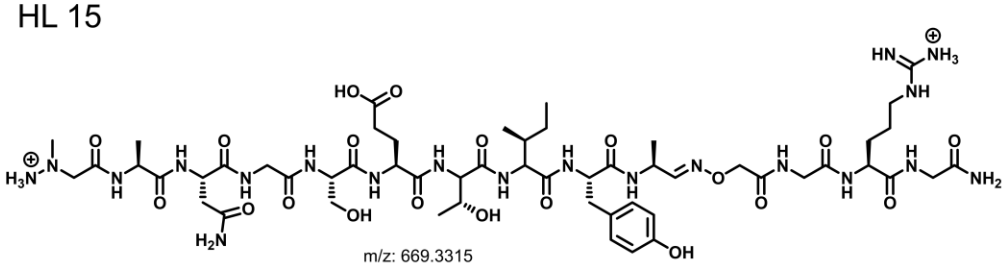

m/z: 669.3315

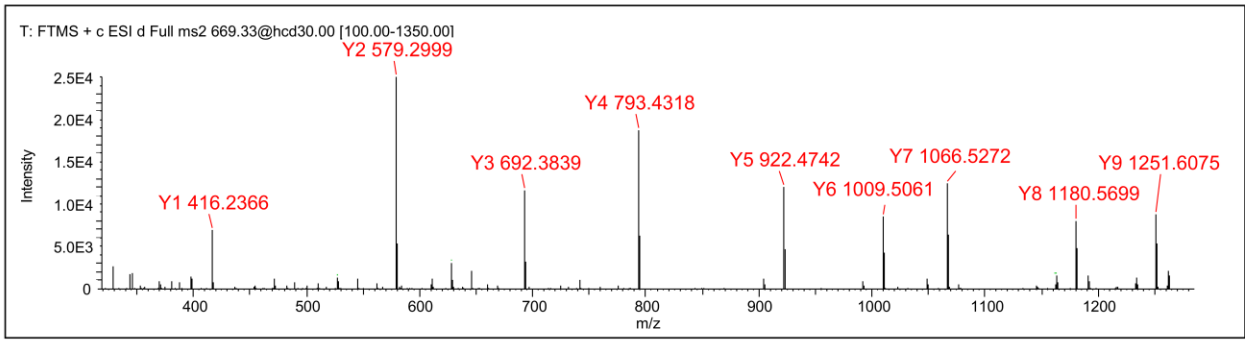

B ions	Y ions
91.06259	1306.694
162.0997	1216.639
276.1426	1145.602
333.1641	1031.559
420.1961	974.5377
549.2387	887.5057
650.2864	758.4631
763.3705	657.4154
891.4654	544.3314
1288.684	416.2364

HL 16

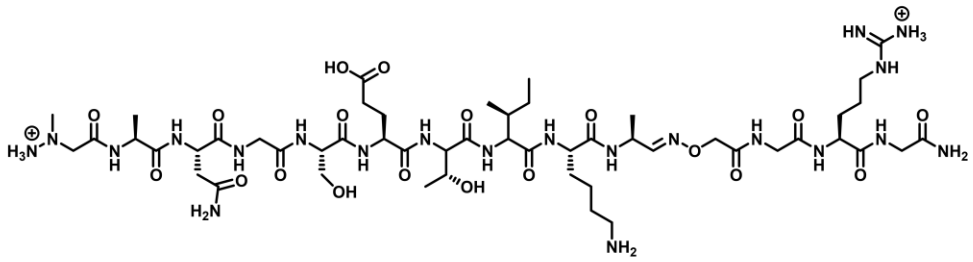

m/z: 651.8473

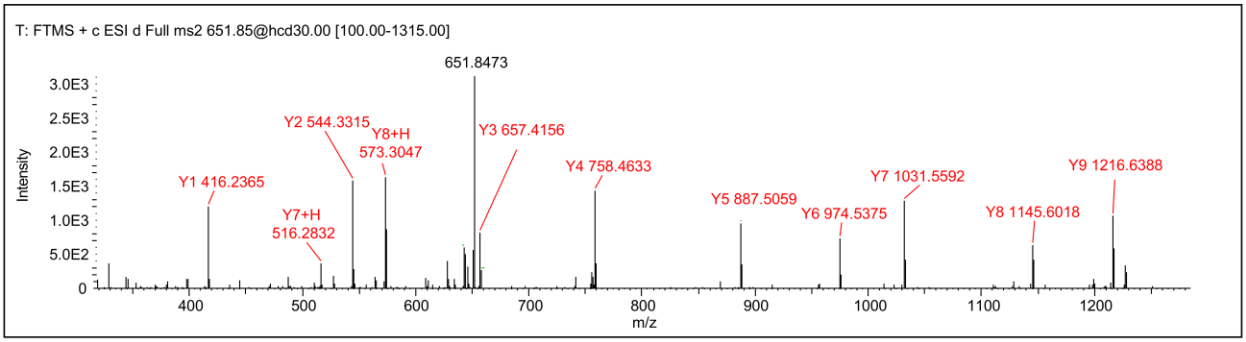

References

(1) Beck, H.; Härter, M.; Haß, B.; Schmeck, C.; Baerfacker, L. Small Molecules and Their Impact in Drug Discovery: A Perspective on the Occasion of the 125th Anniversary of the Bayer Chemical Research Laboratory. *Drug Discovery Today* **2022**, *27* (6), 1560–1574

(2) Hopkins, A. L.; Groom, C. R. The Druggable Genome. *Nat Rev Drug Discov* **2002**, *1* (9), 727–730

(3) Senior, M. Fresh from the Biotech Pipeline: Fewer Approvals, but Biologics Gain Share. *Nat Biotechnol* **2023**, *41* (2), 174–182

(4)Lu, R.-M.; Hwang, Y.-C.; Liu, I.-J.; Lee, C.-C.; Tsai, H.-Z.; Li, H.-J.; Wu, H.-C. Development of Therapeutic Antibodies for the Treatment of Diseases. *J Biomed Sci* **2020**, *27* (1), 1

(5) Bhat, A.; Roberts, L. R.; Dwyer, J. J. Lead Discovery and Optimization Strategies for Peptide Macrocycles. *Eur. J. Med. Chem.,* **2015**, *94*, 471–479.

(6) Bruzzoni-Giovanelli, H.; Alezra, V.; Wolff, N.; Dong, C.-Z.; Tuffery, P.; Rebollo, A. Interfering Peptides Targeting Protein–Protein Interactions: The next Generation of Drugs? *Drug Discov. Today,* **2018**, *23* (2), 272–285

(7) Gentilucci, L.; De Marco, R.; Cerisoli, L. Chemical Modifications Designed to Improve Peptide Stability: Incorporation of Non-Natural Amino Acids, Pseudo-Peptide Bonds, and Cyclization. *CPD,* **2010**, *16* (28), 3185–3203

(8) Craik, D. J. Seamless Proteins Tie Up Their Loose Ends. *Science* **2006**, *311* (5767), 1563–1564.

(9) Zhang, L.; Tam, J. P. Synthesis and Application of Unprotected Cyclic Peptides as Building Blocks for Peptide Dendrimers. *J. Am. Chem. Soc.* **1997**, *119* (10), 2363–2370.

(10) Pattabiraman, V. R.; Ogunkoya, A. O.; Bode, J. W. Chemical Protein Synthesis by Chemoselective α-Ketoacid–Hydroxylamine (KAHA) Ligations with 5-Oxaproline. *Angew Chem Int Ed* **2012**, *51* (21), 5114–5118.

(11)Kleineweischede, R.; Hackenberger, C. P. Chemoselective Peptide Cyclization by Traceless Staudinger Ligation. Angew. Chem., Int. Ed. 2008, 47, 5984−5988

(12)Soellner, M. B.; Tam, A.; Raines, R. T. Staudinger Ligation of Peptides at Non-Glycyl Residues. J. Org. Chem. 2006, 71, 9824−9830.

(13) Nilsson, B. L.; Kiessling, L. L.; Raines, R. T. High-Yielding Staudinger Ligation of a Phosphinothioester and Azide to Form a Peptide. Org. Lett. 2001, 3, 9−12.

(14) Malins, L. R.; deGruyter, J. N.; Robbins, K. J.; Scola, P. M.; Eastgate, M. D.; Ghadiri, M. R.; Baran, P. S. Peptide Macrocyclization Inspired by Non-Ribosomal Imine Natural Products. *J. Am. Chem. Soc.* **2017**, *139* (14), 5233–5241.

(15) Li, B.; Tang, H.; Turlik, A.; Wan, Z.; Xue, X.; Li, L.; Yang, X.; Li, J.; He, G.; Houk, K. N.; Chen, G. Cooperative Stapling of Native Peptides at Lysine and Tyrosine or Arginine with Formaldehyde. *Angew Chem Int Ed* **2021**, *60* (12), 6646–6652.

(16) Almeida, A. M.; Li, R.; Gellman, S. H. Parallel β-Sheet Secondary Structure Is Stabilized and Terminated by Interstrand Disulfide Cross-Linking. *J. Am. Chem. Soc.* **2012**, *134* (1), 75–78.

(17) Tian, Y.; Li, J.; Zhao, H.; Zeng, X.; Wang, D.; Liu, Q.; Niu, X.; Huang, X.; Xu, N.; Li, Z. Stapling of Unprotected Helical Peptides via Photo-Induced Intramolecular Thiol–Yne Hydrothiolation. *Chem. Sci.* **2016**, *7* (5), 3325–3330.

(18) Goto, Y.; Ohta, A.; Sako, Y.; Yamagishi, Y.; Murakami, H.; Suga, H. Reprogramming the Translation Initiation for the Synthesis of Physiologically Stable Cyclic Peptides. *ACS Chem. Biol.* **2008**, *3* (2), 120–129.

(19) Timmerman, P.; Beld, J.; Puijk, W. C.; Meloen, R. H. Rapid and Quantitative Cyclization of Multiple Peptide Loops onto Synthetic Scaffolds for Structural Mimicry of Protein Surfaces. *ChemBioChem* **2005**, *6* (5), 821–824.

(20) Scott, L. T., Rebek, J., Ovsyanko, L. & Sims, C. Organic chemistry on the solid phase. Site-site interactions on functionalized polystyrene. *J. Am. Chem. Soc.* **99**, 626–627 (1977).

(21) Mazur, S. & Jayalekshmy, P. Chemistry of polymer-bound *o*-benzyne. Frequency of encounter between substituents on cross-linked polystyrenes. *J. Am. Chem. Soc.* **101**, 677–683 (1979).

(22) Kates, S. A. et al. A novel, convenient, three-dimensional orthogonal strategy for solid-phase synthesis of cyclic peptides. *Tetrahedron Lett.* **34**, 1549–1552 (1993).

(23) Garnes-Portolés, F.; Leyva-Pérez, A. Macrocyclization Reactions at High Concentration (≥0.2M): The Role of Catalysis. *ACS Catal.* **2023**, *13* (14), 9415–9426.

(24) Constable, D. J. C.; Curzons, A. D.; Cunningham, V. L. Metrics to 'Green' Chemistry—Which Are the Best? *Green Chem.* **2002**, *4* (6), 521–527.

(25) Vinogradov, A. A.; Yin, Y.; Suga, H. Macrocyclic Peptides as Drug Candidates: Recent Progress and Remaining Challenges. *J. Am. Chem. Soc.,* **2019**, *141* (10), 4167–4181.

(26) Zhang, H.; Chen, S. Cyclic Peptide Drugs Approved in the Last Two Decades (2001–2021). *RSC Chem. Biol.,* **2022**, *3* (1), 18–31

(27) You, S.; McIntyre, G.; Passioura, T. The Coming of Age of Cyclic Peptide Drugs: An Update on Discovery Technologies. *Expert Opinion on Drug Discovery* **2024**, *19* (8), 961–973.

(28) Macarron, R.; Banks, M. N.; Bojanic, D.; Burns, D. J.; Cirovic, D. A.; Garyantes, T.; Green, D. V. S.; Hertzberg, R. P.; Janzen, W. P.; Paslay, J. W.; Schopfer, U.; Sittampalam, G. S. Impact of High-Throughput Screening in Biomedical Research. *Nat Rev Drug Discov* **2011**, *10* (3), 188–195.

(29) Obexer, R.; Walport, L. J.; Suga, H. Exploring Sequence Space: Harnessing Chemical and Biological Diversity towards New Peptide Leads. *Current Opinion in Chemical Biology* **2017**, *38*, 52–61

(30) O'Neil, K. T.; Hoess, R. H.; Jackson, S. A.; Ramachandran, N. S.; Mousa, S. A.; Degrado, W. F. Identification of Novel Peptide Antagonists for GPIIb/IIIa from a Conformationally Constrained Phage Peptide Library. Proteins: Struct., Funct., Genet. 1992, 14, 509− 515.

(31) Owens, A. E.; Iannuzzelli, J. A.; Gu, Y.; Fasan, R. MOrPH-PhD: An Integrated Phage Display Platform for the Discovery of Functional Genetically Encoded Peptide Macrocycles. *ACS Cent. Sci.* **2020**, *6* (3), 368–381.

(32) Heinis, C.; Rutherford, T.; Freund, S.; Winter, G. Phage Encoded Combinatorial Chemical Libraries Based on Bicyclic Peptides. Nat. Chem. Biol. 2009, 5, 502−507.

(33) Hampton, J. T.; Liu, W. R. Diversification of Phage-Displayed Peptide Libraries with Noncanonical Amino Acid Mutagenesis and Chemical Modification. *Chem. Rev.* **2024**, *124* (9), 6051–6077.

(34) Lamboy, J. A.; Tam, P. Y.; Lee, L. S.; Jackson, P. J.; Avrantinis, S. K.; Lee, H. J.; Corn, R. M.; Weiss, G. A. Chemical and Genetic Wrappers for Improved Phage and RNA Display. *ChemBioChem* **2008**, *9* (17), 2846–2852.

(35) Roberts, R. W.; Szostak, J. W. RNA-Peptide Fusions for the *in Vitro* Selection of Peptides and Proteins. *Proc. Natl. Acad. Sci. U.S.A.* **1997**, *94* (23), 12297–12302.

(36) Goto, Y.; Suga, H. The RaPID Platform for the Discovery of Pseudo-Natural Macrocyclic Peptides. *Acc. Chem. Res.* **2021**, *54* (18), 3604–3617.

(37) Passioura, T.; Suga, H. Flexizyme-Mediated Genetic Reprogramming As a Tool for Noncanonical Peptide Synthesis and Drug Discovery. *Chemistry A European J* **2013**, *19* (21), 6530–6536.

(38) Newton, M. S.; Cabezas-Perusse, Y.; Tong, C. L.; Seelig, B. *In Vitro* Selection of Peptides and Proteins—Advantages of mRNA Display. *ACS Synth. Biol.* **2020**, *9* (2), 181–190.

(39) Melsen, P. R. A.; Yoshisada, R.; Jongkees, S. A. K. Opportunities for Expanding Encoded Chemical Diversification and Improving Hit Enrichment in mRNA-Displayed Peptide Libraries. *ChemBioChem* **2022**, *23* (12), e202100685.

(40) Tavassoli, A. SICLOPPS Cyclic Peptide Libraries in Drug Discovery. *Curr. Opin.Chem. Bio.* **2017**, *38*, 30–35.

(41) Lian, W.; Upadhyaya, P.; Rhodes, C. A.; Liu, Y.; Pei, D. Screening Bicyclic Peptide Libraries for Protein–Protein Interaction Inhibitors: Discovery of a Tumor Necrosis Factor-α Antagonist. *J. Am. Chem. Soc.,* **2013**, *135* (32), 11990–11995.

(42) Shi, Y.; Challa, S.; Sang, P.; She, F.; Li, C.; Gray, G. M.; Nimmagadda, A.; Teng, P.; Odom, T.; Wang, Y.; Van Der Vaart, A.; Li, Q.; Cai, J. One-Bead–Two-Compound Thioether Bridged Macrocyclic γ-AApeptide Screening Library against EphA2. *J. Med. Chem.* **2017**, *60* (22), 9290–9298.

(43) Thakkar, A.; Trinh, T. B.; Pei, D. Global Analysis of Peptide Cyclization Efficiency. *ACS Comb. Sci.,* **2013**, *15* (2), 120–129

(44) Plais, L.; Scheuermann, J. Macrocyclic DNA-Encoded Chemical Libraries: A Historical Perspective. *RSC Chem. Biol.,* **2022**, *3* (1), 7–17

(45) Adebomi, V.; Cohen, R. D.; Wills, R.; Chavers, H. A. H.; Martin, G. E.; Raj, M. CyClick Chemistry for the Synthesis of Cyclic Peptides. *Angew. Chem., Int. Ed.,* **2019**, *58* (52), 19073–19080.

(46) Davis, A. C.; Levy, A. L. 768. The Interaction of α-Amino-Nitriles and Aldehydes and Ketones. *J. Chem. Soc.* **1951**, *0* (0), 3479–3489.

(47) Bak, A.; Fich, M.; Larsen, B. D.; Frokjaer, S.; Friis, G. J. N-Terminal 4-Imidazolidinone Prodrugs of Leu-Enkephalin: Synthesis, Chemical and Enzymatic Stability Studies. *European Journal of Pharmaceutical Sciences* **1999**, *7* (4), 317–323.

(48) Larsen, S. W.; Sidenius, M.; Ankersen, M.; Larsen, C. Kinetics of Degradation of 4-Imidazolidinone Prodrug Types Obtained from Reacting Prilocaine with Formaldehyde and Acetaldehyde. *European Journal of Pharmaceutical Sciences* **2003**, *20* (2), 233–240.

(49) Shao, H.; Adebomi, V.; Bruce, A.; Raj, M.; Houk, K. N. Intramolecular Hydrogen Bonding Enables a Zwitterionic Mechanism for Macrocyclic Peptide Formation: Computational Mechanistic Studies of CyClick Chemistry. *Angew Chem Int Ed.,* **2023**, *62* (41), e202307210.

(50) Avrutina, O.; Schmoldt, H. U.; Gabrijelcic-Geiger, D.; Wentzel, A.; Frauendorf, H.; Sommerhoff, C. P.; Diederichsen, U.; Kolmar, H. Head-to-Tail Cyclized Cystine-Knot Peptides by a Combined Recombinant and Chemical Route of Synthesis. *ChemBioChem* **2008**, 9, 33−37.

(51) Nwajiobi, O.; Verma, A. K.; Raj, M. Rapid Arene Triazene Chemistry for Macrocyclization. *J. Am. Chem. Soc.* **2022**, *144* (10), 4633–4641.

(52) Johnson, A. M.; Anslyn, E. V. Reversible Macrocyclization of Peptides with a Conjugate Acceptor. *Org. Lett.* **2017**, *19* (7), 1654–1657.

(53) Lam, K. S.; Salmon, S. E.; Hersh, E. M.; Hruby, V. J.; Kazmierski, W. M.; Knapp, R. J. A New Type of Synthetic Peptide Library for Identifying Ligand-Binding Activity. *Nature* **1991**, *354* (6348), 82–84.

(54) Furukawa, J.; Shinohara, Y.; Kuramoto, H.; Miura, Y.; Shimaoka, H.; Kurogochi, M.; Nakano, M.; Nishimura, S.-I. Comprehensive Approach to Structural and Functional Glycomics Based on Chemoselective Glycoblotting and Sequential Tag Conversion. *Anal. Chem.,* **2008**, *80* (4), 1094–1101. DOI:

(55) Abe, M.; Shimaoka, H.; Fukushima, M.; Nishimura, S.-I. A Cross-Linked Polymer Possessing a High Density of Hydrazide Groups: High-Throughput Glycan Purification and Labeling for High-Performance Liquid Chromatography Analysis. *Polym. J.,* **2012**, *44* (3), 269–277.

(56) Wang, C.; Yuan, J.; Li, X.; Wang, Z.; Huang, L. Sulfonyl Hydrazine-Functionalized Polymer as a Specific Capturer of Reducing Glycans from Complex Samples for High-Throughput Analysis by Electrospray Ionization Mass Spectrometry. *Analyst* **2013**, *138* (18), 5344.

(57) Ede, N. J.; Bray, A. M. A Simple Linker for the Attachment of Aldehydes to the Solid Phase. Application to Solid Phase Synthesis by the Multipin™ Method. *Tetrahedron Lett.,* **1997**, *38* (40), 7119–7122.

(58) Townsend, C.; Furukawa, A.; Schwochert, J.; Pye, C. R.; Edmondson, Q.; Lokey, R. S. CycLS: Accurate, Whole-Library Sequencing of Cyclic Peptides Using Tandem Mass Spectrometry. *Bioorg, Med. Chem.,* **2018**, *26* (6), 1232–1238.

(59) Zhang, S.; De Leon Rodriguez, L. M.; Li, F. F.; Huang, R.; Leung, I. K. H.; Harris, P. W. R.; Brimble, M. A. A Novel Tyrosine Hyperoxidation Enables Selective Peptide Cleavage. *Chem. Sci.,* **2022**, *13* (9), 2753–2763.

(60) Liang, X.; Girard, A.; Biron, E. Practical Ring-Opening Strategy for the Sequence Determination of Cyclic Peptides from One-Bead-One-Compound Libraries. *ACS Comb. Sci.,* **2013**, *15* (10), 535–540.

(61) Simpson, L. S.; Kodadek, T. A Cleavable Scaffold Strategy for the Synthesis of One-Bead One-Compound Cyclic Peptoid Libraries That Can Be Sequenced by Tandem Mass Spectrometry. *Tetrahedron Lett.,* **2012**, *53* (18), 2341–2344.

(62) Elashal, H. E.; Cohen, R. D.; Elashal, H. E.; Raj, M. Oxazolidinone-Mediated Sequence Determination of One-Bead One-Compound Cyclic Peptide Libraries. *Org. Lett.,* **2018**, *20* (8), 2374–2377.

(63) Borges, A.; Nguyen, C.; Letendre, M.; Onasenko, I.; Kandler, R.; Nguyen, N. K.; Chen, J.; Allakhverdova, T.; Atkinson, E.; DiChiara, B.; Wang, C.; Petler, N.; Patel, H.; Nanavati, D.; Das, S.; Nag, A. Facile de Novo Sequencing of Tetrazine-Cyclized Peptides through UV-Induced Ring-Opening and Cleavage from the Solid Phase. *ChemBioChem.,* **2023**, *24* (4).

(64) Quartararo, A. J.; Gates, Z. P.; Somsen, B. A.; Hartrampf, N.; Ye, X.; Shimada, A.; Kajihara, Y.; Ottmann, C.; Pentelute, B. L. Ultra-Large Chemical Libraries for the Discovery of High-Affinity Peptide Binders. *Nat. Commun.,* **2020**, *11* (1), 3183.

(65) Zhang, G.; Li, C.; Quartararo, A. J.; Loas, A.; Pentelute, B. L. Automated Affinity Selection for Rapid Discovery of Peptide Binders. *Chem. Sci.,* **2021**, *12* (32), 10817–10824.

(66) Touti, F.; Gates, Z. P.; Bandyopadhyay, A.; Lautrette, G.; Pentelute, B. L. In-Solution Enrichment Identifies Peptide Inhibitors of Protein–Protein Interactions. *Nat. Chem. Biol.,* **2019**, *15* (4), 410–418.

(67) Link, J.O., Rhee, M.S., Tse, W.C., Zheng, J., Somoza, J.R., Rowe, W., Begley, R., Chiu, A., Mulato, A., Hansen, D., et al. Clinical targeting of HIV capsid protein with a long-acting small molecule. *Nature,* **2020**, *584*, 614-618.

(68) Selyutina, A., Hu, P., Miller, S., Simons, L.M., Yu, H.J., Hultquist, J.F., Lee, K., KewalRamani, V.N., and Diaz-Griffero, F. GS-CA1 and lenacapavir stabilize the HIV-1 core and modulate the core interaction with cellular factors. iScience, **2022,** *25*.

(69) Zhuang, S., and Torbett, B.E. Interactions of HIV-1 Capsid with Host Factors and Their Implications for Developing Novel Therapeutics. *Viruses,* **2021**, *13*, 417.

(70) Gres, A.T., Kirby, K.A., McFadden, W.M., Du, H., Liu, D., Xu, C., Bryer, A.J., Perilla, J.R., Shi, J., Aiken, C., et al. Multidisciplinary studies with mutated HIV-1 capsid proteins reveal structural mechanisms of lattice stabilization. *Nat Commun,* **2023**, *14*, 5614.

(71) Matreyek, K.A., Yücel, S.S., Li, X., and Engelman, A. Nucleoporin NUP153 phenylalanine-glycine motifs engage a common binding pocket within the HIV-1 capsid protein to mediate lentiviral infectivity. *PLoS Pathog,* **2013,** *9*, e1003693.

(72) Price, A.J., Jacques, D.A., McEwan, W.A., Fletcher, A.J., Essig, S., Chin, J.W., Halambage, U.D., Aiken, C., and James, L.C. Host Cofactors and Pharmacologic Ligands Share an Essential Interface in HIV-1 Capsid That Is Lost upon Disassembly. *PLOS Pathogens,* **2014**, *10*, e1004459.

(73) Pornillos, O., Ganser-Pornillos, B.K., Banumathi, S., Hua, Y., and Yeager, M. Disulfide bond stabilization of the hexameric capsomer of human immunodeficiency virus. *J Mol Biol*, **2010**, *401*, 985-995.

(74) McFadden, W.M., and Sarafianos, S.G. Targeting the HIV-1 and HBV Capsids, an EnCore. *Viruses*, **2023,** *15*, 896.

(75) U.S. Food and Drug Administration (2022). FDA Approves New HIV Drug for Adults with Limited Treatment Options.

(76) Lanman, J., Sexton, J., Sakalian, M., and Prevelige, P.E., Jr. Kinetic analysis of the role of intersubunit interactions in human immunodeficiency virus type 1 capsid protein assembly in vitro. *J Virol*, **2002**, *76*, 6900-6908.

(77) Rihn, S.J., Wilson, S.J., Loman, N.J., Alim, M., Bakker, S.E., Bhella, D., Gifford, R.J., Rixon, F.J., and Bieniasz, P.D. Extreme Genetic Fragility of the HIV-1 Capsid. *PLOS Pathogens*, **2013**, *9*, e1003461.

(78) Kansy, M.; Senner, F.; Gubernator, K. Physicochemical High Throughput Screening: Parallel Artificial Membrane Permeation Assay in the Description of Passive Absorption Processes. *J. Med. Chem.* **1998**, *41* (7), 1007–1010.

(79) Hewitt, W. M.; Leung, S. S. F.; Pye, C. R.; Ponkey, A. R.; Bednarek, M.; Jacobson, M. P.; Lokey, R. S. Cell-Permeable Cyclic Peptides from Synthetic Libraries Inspired by Natural Products. *J. Am. Chem. Soc.* **2015**, *137* (2), 715–721.

(80) Michelmann, K.; Silveira, J. A.; Ridgeway, M. E.; Park, M. A. Fundamentals of Trapped Ion Mobility Spectrometry. *J. Am. Soc. Mass Spectrom.* **2015**, *26* (1), 14–24.

(81) Sharma, V. R.; Mehmood, A.; Janesko, B. G.; Simanek, E. E. Efficient Syntheses of Macrocycles Ranging from 22–28 Atoms through Spontaneous Dimerization to Yield Bis-Hydrazones. *RSC Adv.* **2020**, *10* (6), 3217–3220.

(82) Davies, L. J.; Shuttleworth, L. M.; Zhang, X.; Peng, S.; Nitsche, C. Bioorthogonal Peptide Macrocyclization Using Oxime Ligation. *Org. Lett.* **2023**, *25* (16), 2806–2809.

(83) Kalia, J.; Raines, R. T. Hydrolytic Stability of Hydrazones and Oximes. *Angew Chem Int Ed* **2008**, *47* (39), 7523–7526.

(84) Pettazzoni, L.; Ximenis, M.; Leonelli, F.; Vozzolo, G.; Bodo, E.; Elizalde, F.; Sardon, H. Oxime Metathesis: Tuneable and Versatile Chemistry for Dynamic Networks. *Chem. Sci.* **2024**, *15* (7), 2359–2364.

(85) Yu, J.; Qi, D.; Li, J. Design, Synthesis and Applications of Responsive Macrocycles. *Commun Chem* **2020**, *3* (1), 189.

(86) Szalai, P.; Hagen, L. K.; Sætre, F.; Luhr, M.; Sponheim, M.; Øverbye, A.; Mills, I. G.; Seglen, P. O.; Engedal, N. Autophagic Bulk Sequestration of Cytosolic Cargo Is Independent of LC3, but Requires GABARAPs. *Experimental Cell Research* **2015**, *333* (1), 21–38.

(87) Brown, H.; Chung, M.; Üffing, A.; Batistatou, N.; Tsang, T.; Doskocil, S.; Mao, W.; Willbold, D.; Bast, R. C.; Lu, Z.; Weiergräber, O. H.; Kritzer, J. A. Structure-Based Design of Stapled Peptides That Bind GABARAP and Inhibit Autophagy. *J. Am. Chem. Soc.* **2022**, *144* (32), 14687–14697.

(88) Rettie, S. A.; Juergens, D.; Adebomi, V.; Bueso, Y. F.; Zhao, Q.; Leveille, A. N.; Liu, A.; Bera, A. K.; Wilms, J. A.; Üffing, A.; Kang, A.; Brackenbrough, E.; Lamb, M.; Gerben, S. R.; Murray, A.; Levine, P. M.; Schneider, M.; Vasireddy, V.; Ovchinnikov, S.; Weiergräber, O. H.; Willbold, D.; Kritzer, J. A.; Mougous, J. D.; Baker, D.; DiMaio, F.; Bhardwaj, G. Accurate *de Novo* Design of High-Affinity Protein Binding Macrocycles Using Deep Learning. *bioRxiv*, **2024,** 10.1101/2024.11.18.622547

(89) Waliczek, M.; Kijewska, M.; Rudowska, M.; Setner, B.; Stefanowicz, P.; Szewczuk, Z. Peptides Labeled with Pyridinium Salts for Sensitive Detection and Sequencing by Electrospray Tandem Mass Spectrometry. *Sci Rep* **2016**, *6* (1), 37720.

(90) Singudas, R.; Reddy, N. C.; Rai, V. Sensitivity Booster for Mass Detection Enables Unambiguous Analysis of Peptides, Proteins, Antibodies, and Protein Bioconjugates. *Chem. Commun.* **2019**, *55* (67), 9979–9982

(91) Huh, S.; Batistatou, N.; Wang, J.; Saunders, G. J.; Kritzer, J. A.; Yudin, A. K. Cell Penetration of Oxadiazole-Containing Macrocycles. *RSC Chem. Biol.* **2024**, *5* (4), 328–334.